Democratic and Popular Algerian Republic

Ministry of Higher Education and Scientific Research

Ecole Nationale Polytechnique

Mechanical Engineering Department

This Memoire is submitted in partial fulfilment of the requirements for the Engineer Degree

Presented by:

Abdelhakim LAKEHAL

Title:

Characteristics and Performance Analysis of the SPP1 Solar Power Plant Hassi R'mel

Air-Cooled Condensers Role

Jury Members

-	Supervisor: Mohand Améziane AIT ALI	Professor	ENP
-	President: Belkacem KEBLI	Professor	ENP
-	Reviewer: Hocine BENNOUR	Master Professor	ENP

Promotion June 2014

تلخيص

العمل المقدم في هذا المشروع هو دراسة أداء المحطة الشمسية الهجينة للطاقة التي تقع في حاسي الرمل. الهدف من هذه الدراسة هو تحديد المكاسب التي تحققت في كل من طاقة المحطة، والكفاءة الحرارية؛ عن طريق خفض درجة حرارة التكثيف لتوربينات البخارية، وتحليل آثارها على الدورة المركبة، مسترد الحرارة ومولد البخار، مجال الطاقة الشمسية واستهلاك الغاز الطبيعي. كما يتم عرض مقارنة و تقييمات اقتصادية في نهاية المشروع.

الكلمات المفتاحية: محطة الطاقة الشمسية واحد، درجة حرارة التكثيف، الدمج للطاقة الشمسية بنظام الدورة المركبة.

Abstract

The work presented in this memoire is a performance study of the hybrid solar power plant one (SPP1) located in Hassi R'mel. The aim of this study is to quantify the gains in both power output and thermal efficiency by lowering the temperature of condensation of the steam turbine, and analyze its impacts on the combined-cycle, the heat recovery steam generator also the solar field and the natural gas consumption. A comparison and economics evaluations are presented at the end of this paper.

Keywords: SPP1, Condensation temperature, Integrated Solar Combined-Cycle.

Résumé

Le travail présenté dans cette mémoire est l'étude de performance de la centrale solaire hybride (SPP1) située dans Hassi R'mel. L'objectif de cette étude est de quantifier les gains de la puissance nette et le rendement thermique en abaissant la température de condensation de la turbine à vapeur et analyser ses impacts sur le cycle combiné, la chaudière de récupération, le champ solaire et la consommation de gaz naturel. Une comparaison et des évaluations économiques sont présentées à la fin de ce mémoire.

Mot clés: SPP1, Température de condensation, Cycle combiné solaire intégré.

قال الله تعالى:

﴿ إقرأ باسم ربك الذي خلق ۝١ خلق اللإنسان من علق ۝٢ اقرأ و ربك الأكرم ۝٣ الذي علم بالقلم ۝٤ علم اللإنسان ما لم يعلم ۝٥ ﴾

صدق الله العظيم

Acknowledgments

I thank Allah for giving me the strength to keep on going through all my educational years and to do this humble memoire.

I thank all my family especially my dearest mother and dear father for giving all they can and more in the sake of my success and encouraging me to pursuit my passion in Mechanical Engineering.

I thank Prof. Mohand Améziane AIT ALI for his dedication in teaching us, and for his continuous guidance through all the period of this work.

I thank the Jury members, Hocine BENNOUR and Belkacem KEBLI for taking the time to read and evaluate this modest memoire.

I thank the Ecole Nationale Polytechnique family for letting me become one of their graduates.

I thank the Mechanical Engineering Department family and all my teachers who contributed to my engineering education.

Finally I thank all my friends and all the promotion of Mechanical Engineering 2011-2014 for making the road easier even in the toughest times.

Table of Contents

General Introduction 1

Chapter I Introduction to Power Plants

I.1. Introduction 2
I.2. Solar Thermal Power Plants 3
I.2.1. Concentrating solar power plants (CSP) 3
I.2.1.1. Solar tower system 3
I.2.1.2. Parabolic dish-engine 4
I.2.1.3. Linear Fresnel system 5
I.2.1.4. Parabolic trough system 6
I.3. Parabolic Trough Solar Power Plants 6
I.3.1. The sun tracking control system 6
I.3.2. Parabolic trough plant configurations 7
I.3.2.1. Solar only mode 8
I.3.2.2. Hybrid systems 9
I.3.2.3. Direct steam generation 9
I.3.2.4. Integrated solar combined-cycle (ISCC) 10
I.4. Combined-Cycle Power Plant 11
I.5. Thermal Energy Storage 13
I.6. Solar Power Plant One 15
I.6.1. Presentation of SPP1 15
I.6.2. Components 16
I.6.2.1. Gas turbine 16
I.6.2.2. Heat recovery steam generator 17
I.6.2.3. Steam turbine 17
I.6.2.5. Solar field 17
I.7 Aim of This Study 18

Chapter II Thermodynamics of Power Plants

II.1. Gas Turbine 19
II.1.1. Simple Brayton cycle 20

II.1.2. Inefficiencies and actual Brayton cycle 22
II.2. Steam Turbine 25
II.2.1. Rankine cycle 25
II.2.1.1 The simple Rankine cycle 26
II.2.1.2 Rankine cycle with vapor superheating 27
II.2.2 Working fluid 29
II.3. Heat Recovery Steam Generator (HRSG) 30
II.3.1. Types of heat recovery steam generators 31
II.3.1.1. Natural circulation HRSG 31
II.3.1.2. Forced circulation HRSG 31
II.3.1.2. Once through HRSG 31
II.3.2. Heat recovery steam generator components 32
II.3.2.1. The evaporator 32
II.3.2.2. The economizer 32
II.3.2.3. The superheater 32
II.3.3. HRSG temperature profiles and steam generation 33
II.3.4. Heat transfer diagram and heat balances 35
II.3.4.1. Pinch point temperature difference 35
II.3.4.2. Heat balances in the HRSG 36
II.4. The Combined-Cycle 37
II.5. The Solar Field 40
II.5.1. Heat transfer fluid 40
II.5.2. Solar energy conversion 42
II.5.2.1. The Carnot cycle 42
II.5.2.2. The solar heat flux and balance in the HRSG 44
III.6. Conclusion 44

Chapter III Performance Analysis of the SPPI

III.1. Operating of SPP1 Solar Hybrid Power Plant 45
III.2. Objectives 47
III.3. Calculations 48
III.3.1. Gas turbine calculations 48
III.3.2. Cycle 01: Condensation at $\mathbf{25}\ \boldsymbol{kPa}$ (saturation temperature $\mathbf{64,97°C}$) 53

III.3.2.1 The steam turbine calculations 53
III.3.2.2 The heat recovery steam generator calculations 58
III.3.2.3 The Combined-cycle calculations 63
III.3.2.4 The Solar field calculations 64
III.3.3. Cycle 02: Condensation at $\mathbf{20}\ \boldsymbol{kPa}$ (saturation temperature $\mathbf{60,06}$°C) 67
III.3.3.1. The steam cycle calculations 67
III.3.3.2 The heat recovery steam generator calculations 69
III.3.3.3 The Combined-cycle calculations 71
III.3.3.4. The Solar field calculations 71
III.3.4. Cycle 03: Condensation at $\mathbf{15}\ \boldsymbol{kPa}$ (saturation temperature $\mathbf{53,97}$°C) 73
III.3.4.1. The steam cycle calculations 73
III.3.4.2 The heat recovery steam generator calculations 75
III.3.4.3 The Combined-Cycle calculations 76
III.3.4.4 The solar field calculations 77
III.3.5. Cycle 04: Condensation at $\mathbf{10}\ \boldsymbol{kPa}$ (saturation temperature $\mathbf{45,81}$°C) 78
III.3.5.1. The steam cycle calculations 78
III.3.5.2 The heat recovery steam generator calculations 80
III.3.5.3 The Combined-Cycle calculations 81
III.3.5.4 The Solar field calculations 81
III.4 Results and Discussion 82
III.4.1 Gas turbine analysis 82
III.4.2 Steam turbine analysis 83
III.4.2.1 The turbine and pump works 85
III.4.2.2. Added heat and rejected heat 85
III.4.2.3. Efficiency and quality 86
III.4.3 Heat recovery steam generator 88
III.4.4. Combined-cycle analysis 90
III.4.5 Solar field analysis 92
III.4.6 Integrated solar combined-cycle analysis 95
III.4.7 Economic analysis 96
III.4.7.1 Natural gas consumption and annual savings 96
III.4.7.2 Electricity sales income and profits 97
III.4.8. Closing thoughts and future of the SPP1 98

Conclusion.....100
References.....101
Appendix-A Technical Specifications of SGT-800.....104
Appendix-B Combustion Ratio of Air-Fuel.....105

List of Figures

Figure I.1 CSP applications..... 3

Figure I.2 Solar tower..... 4

Figure I.3 Parabolic dish..... 5

Figure I.4 Fresnel system elements..... 5

Figure I.5 Fresnel collector driving an ammonia-water-chiller in Bergamo, Italy..... 5

Figure I.6 Parabolic trough system..... 6

Figure I.7 Sun tracking control system..... 7

Figure I.8 Aerial View of 5 x 30 MW Solar SEGSs at California, USA..... 7

Figure I.10 Solar thermal power plant with thermal storage system..... 8

Figure I.11 Solar trough system with fossil fuel backup..... 9

Figure I.12 Solar trough plants operation systems a. Solar system using HTF b. Solar system using DSG..... 9

Figure I.13 Direct steam generation in parabolic trough technology..... 10

Figure I.14 Schematic of ISCC..... 11

Figure I.15 Combined cycle power plant scheme..... 12

Figure I.16 Different power plants efficiencies..... 12

Figure I.17 a Solar share in based-load operation, **b** Solar share in mid-load operation..... 14

Figure I.18 a Specific CO_2 emissions in based-load operation, **b** Specific CO_2 emissions in mid-load operation..... 14

Figure I.19 a Increase of electricity cost in based-load operation, **b** Increase of electricity cost in mid-load operation..... 14

Figure II.1 Three main parts of a gas turbine: the compressor, the combustion chamber, and the power turbine..... 19

Figure II.2 a Open cycle; **b** closed air standard Brayton cycle..... 19

Figure II.3 Simple Brayton cycle in **a** temperature-specific entropy diagram; **b** pressure-specific volume diagram..... 21

Figure II.4 a Actual and ideal compression work; **b** actual and ideal expansion work; **c** combination of both processes..... 24

Figure II.5 a Actual and ideal thermal efficiencies; **b** actual and ideal net work. $T_1 = 300\ K$, $T_3 = 1200\ K$, $\eta_T = 0{,}85$ and $\eta_C = 0{,}80$ 25

Figure II.6 a four basic components of a simple Rankine cycle; **b** temperature-specific entropy diagram and Carnot cycle..... 27

Figure II.7 a four basic components of a Rankine cycle with vapor superheating; **b** temperature-specific entropy diagram..... 28
Figure II.8 Configurations of the combined-cycle and cogeneration modes..... 30
Figure II.9 Natural Circulation HRSG..... 31
Figure II.10 Forced Circulation HRSG..... 31
Figure II.11 Once through HRSG..... 31
Figure II.12 Evaporator of single-pressure HRSG..... 32
Figure II.13 Economizer of single-pressure HRSG..... 32
Figure II.14 Superheater of single-pressure HRSG..... 32
Figure II.15 Temperatures profiles in the HRSG..... 33
Figure II.16 Heat transfer diagram of HRSG..... 35
Figure II.17 Evaporator + Superheater heat balance..... 37
Figure II.18 Gas power cycle topping a vapor power cycle..... 38
Figure II.19 Gas turbine cycle, which receives energy at rate $\dot{Q}_h$ from a source at temperature T_h, converts $\dot{W}_{gt} = \eta_{GT}.\dot{Q}_h$ to useful work and sends its "waste" energy at temperature T_{ex}, at rate $\dot{Q}_{ex} = \dot{Q}_h - \dot{W}_{gt}$ to steam turbine cycle..... 39
Figure II.20 a Schematics of a heat engine; **b** T-s diagram for a Carnot cycle..... 43
Figure II.21 Heat exchange between the heat transfer fluid and the steam cycle in solar steam generator..... 44
Figure III.1 The Integrated Solar Combined-Cycle of SPP1..... 46
Figure III.2 Temperature-Entropy diagram of the gas turbine cycle..... 48
Figure III.3 Steam cycle with condensation temperature at $P_1 = 25\text{kPa}$ ($T_{1sat} = 64{,}97°\text{C}$)..... 53
Figure III.4 Steam Carnot cycle condensation temperature $P_1 = 25\text{kPa}$ ($T_{1sat} = 64{,}97°\text{C}$)..... 64
Figure III.5 Steam cycle with condensation temperature $P_1 = 20\text{kPa}$ ($T_{1sat} = 60{,}06°\text{C}$)..... 67
Figure III.6 Steam cycle with condensation temperature at $P_1 = 15\text{kPa}$ ($T_{1sat} = 53{,}97°\text{C}$)..... 73
Figure III.7 Steam cycle with condensation temperature at $P_1 = 10\text{kPa}$ ($T_{1sat} = 45{,}81°\text{C}$)..... 78
Figure III.8 Steam turbine net power and its efficiency versus the condensation temperature..... 84
Figure III.9 Turbine and pump work versus condensation temperature..... 85
Figure III.10 Added heat and rejected heat versus condensation temperature..... 86
Figure III.11 Steam turbine efficiency versus quality versus the condensation temperature..... 86
Figure III.12 Increase and decrease rates versus condensation temperature..... 87

Figure III.13 Economizer heat flux and stack temperature versus condensation temperature……. 88
Figure III.14 Stack temperature and pinch point temperature versus condensation temperature……. 89
Figure III.15 Combined-cycle total net power and efficiency versus condensation temperature……. 90
Figure III.16 Steam turbine efficiency versus combined-cycle efficiency versus condensation temperature……. 91
Figure III.17 Solar net power and efficiency versus condensation temperature……. 93
Figure III.18 Total gas flow rate and savings versus the condensation temperature……. 94
Figure III.19 Savings of daily natural gas consumption……. 95
Figure III.20 Steam turbine and combined-cycle and solar field efficiencies versus condensation temperature…… 96

List of Tables

Table II.1 Important properties of common HTFs..... 42

Table III.1 Entropy and Enthalpy parameters at of $25\ \mathrm{kPa}$ pressure..... 57

Table III.2 States of the vapor cycle 01..... 58

Table III.3 Entropy and Enthalpy parameters at $20\ \mathrm{kPa}$ pressure 68

Table III.4 States of the vapor cycle 02..... 69

Table III.5 Entropy and Enthalpy parameters at t $15\ \mathrm{kPa}$ pressure 74

Table III.6 States of the vapor cycle 03..... 75

Table III.7 Entropy and Enthalpy parameters at $10\ \mathrm{kPa}$ pressure..... 79

Table III.8 States of the vapor cycle 04..... 80

Table III.9 Siemens gas turbine SGT-800 parameters summary..... 82

Table III.10 Steam turbine net power and efficiency versus condensation temperature..... 83

Table III.11 Magnitudes at the four condensation temperatures and gain (or loss) in each parameter..... 84

Table III.12 Stack temperatures and economizer heat fluxes..... 88

Table III.13 Stack temperatures and pinch point temperature differences..... 89

Table III.14 CC Total net power and efficiencies..... 90

Table III.15 Steam turbine and CC efficiencies..... 91

Table III.16 Heat fluxes of the solar field..... 92

Table III.17 Economization of total gas flow rates..... 93

Table III.18 Economization of natural gas consumption..... 94

Table III.19 Economization of natural gas consumption and annual savings..... 96

Table III.20 Electricity sales incomes and annual profits..... 97

Table III.21 Annual electricity sales incomes and percentages of annual profits..... 98

Abbreviations

CSP	Concentrating Solar Power
ISCC	Integrated Solar Combined-Cycle
CC	Combined-Cycle
HRSG	Heat Recovery Steam Generator
SPP1	Solar Power Plant One
TES	Thermal Energy Storage
HTF	Heat Transfer Fluid
SHCC	Solar-Hybrid Combined-Cycle
LEC	Levelized Electricity Cost
DSG	Direct Steam Generating
DLR	German Aerospace Centre
MENA	Mediterranean and North African
CHP	Combined Heat and Power
SEGS	Solar Energy Generating Systems
DNI	Direct Normal Irradiation
HVDC	High-Voltage Direct Current
EU	Europe

Symbols

h $Enthalpy\ (kJ/kg)$

h_s $Enthalpy\ of\ an\ isentropic\ process\ (\Delta s = 0)$

h_f $Enthalpy\ of\ saturated\ liquid\ (kJ/kg.K)$

h_{fg} $Enthalpy\ of\ evaporation\ (kJ/kg.K)$

h_i $Enthalpy\ of\ an\ isentrpic\ expantion\ (kJ/kg.K)$

s $Entorpy\ (kJ/kg.K)$

s_f $Entropy\ of\ saturated\ liquid\ (kJ/kg.K)$

s_{fg} $Entropy\ of\ evaporation\ (kJ/kg.K)$

s_i $Entropy\ of\ an\ isentrpic\ expantion\ (kJ/kg.K)$

P $Pressure\ (kPa, bar, bars)$

T $Temperature\ (°C, K)$

T_c $Temperature\ of\ the\ cold\ source\ (°C, K)$

T_h $Temperature\ of\ the\ hot\ source\ (°C, K)$

T_{s1} $Temperature\ of\ HTF\ entering\ the\ solar\ steam\ generator\ (°C, K)$

T_{s2} $Temperature\ of\ HTF\ leaving\ the\ solar\ steam\ generator\ (°C, K)$

T_{g1} $Temperature\ of\ hot\ gases\ entering\ the\ superheater\ (°C, K)$

T_{g2} $Temperature\ of\ hot\ gases\ entering\ the\ evaporator\ (°C, K)$

T_{g3} $Temperature\ of\ hot\ gases\ entering\ the\ economizer\ (°C, K)$

T_{g4} $Stack\ temperature\ (°C, K)$

T_s $Temperature\ of\ an\ isentropic\ process\ (\Delta s = 0)$

ΔP_{loss} $Pressure\ drop\ in\ the\ combustion\ chamber\ (kPa)$

ΔT $Temperature\ difrence\ (°C, K)$

ΔT_{pp} $Pinch\ point\ temperature\ difrence\ (°C, K)$

ΔT_{eco} $Temperature\ difrence\ between\ the\ hot\ gases\ and\ steam\ at\ the\ economizer\ inlet$

ΔT_{sup} $Temperature\ difrence\ between\ the\ hot\ gases\ and\ steam\ at\ the\ superheater\ inlet$

$\dot{Q}_{eco}$ $Economizer\ heat\ flux\ (kW)$

$\dot{Q}_{eva}$ $Evaporator\ heat\ flux\ (kW)$

$\dot{Q}_{sup}$ $Superheater\ heat\ flux\ (kW)$

$\dot{Q}_{tot}$ $Total\ heat\ flux\ (kW)$

$\dot{Q}_{C}$ $Air-cooled\ condenser\ heat\ flux\ (kW)$

$\dot{Q}_{ex}$ $Exhaust\ gas\ heat\ flux\ (kW)$

$\dot{Q}_{b}$ $Second\ burner\ gases\ heat\ flux\ (kW)$

$\dot{Q}_{h}$ $Hot\ source\ heat\ flux\ (kW)$

$\dot{Q}_{b}$ $Cold\ source\ heat\ flux\ (kW)$

$\dot{Q}_{Srec}$ $Heat\ flux\ recovered\ by\ the\ solar\ field\ (kW)$

$\dot{Q}_{H}$ $Total\ added\ heat\ (kW)$

q_{L} $Rejected\ heat\ (kJ/kg)$

$\dot{Q}_{L}$ $Total\ rdded\ heat\ (kW)$

q_{H} $Added\ heat\ (kJ/kg)$

$\dot{m}$ $Mass\ flow\ rate\ (kg/s)$

$\dot{m}_{h}$ $HTF\ flow\ rate\ \ (kg/s)$

$\dot{m}_{gtd}$ $Total\ hot\ gases\ flow\ rate\ during\ the\ day\ "solar\ field\ working\ hours"\ (kg/s)$

$\dot{m}_{bd}$ $Second\ burner\ gases\ flow\ rate\ during\ the\ day\ "solar\ field\ working\ hours"\ (kg/s)$

$\dot{m}_{g}$ $Exhaust\ gas\ flow\ rate\ (kg/s)$

$\dot{m}_{v}$ $Steam\ flow\ rate\ (kg/s)$

$\dot{m}_{gt}$ $Total\ hot\ gases\ flow\ rate\ (kg/s)$

$\dot{m}_{b}$ $Second\ burner\ gases\ flow\ rate\ (kg/s)$

$\dot{W}_{S}$ $Solar\ field\ total\ net\ work\ (kW)$

$\dot{W}_{ST}$ $Steam\ turbine\ total\ work\ (kW)$

$\dot{W}_{GT}$ $Gas\ turbine\ total\ work\ (kW)$

$\dot{W}_P$ $Total\ pump\ work\ (kW)$

$\dot{W}_T$ $Total\ turbine\ work\ (kW)$

w_T $Turbine\ work\ (kJ/kg)$

w_C $Compressor\ work\ (kJ/kg)$

$\dot{W}_C$ $Total\ compressor\ power\ (kW)$

w $Net\ work\ (kJ/kg)$

$\dot{W}_{net}$ $Total\ net\ power\ (kW)$

w_p $Pump\ work\ (kJ/kg)$

η_{CC} $Combined\ cycle\ efficieny\ (\%)$

η_{ST} $Steam\ turbine\ efficiency\ (\%)$

η_{GT} $Gas\ Turbine\ efficiency\ (\%)$

η_C $Compressor\ efficiency\ (\%)$

η_T $Turbine\ efficiency\ (\%)$

η_{Carnot} $Carnot\ cycle\ efficency\ (\%)$

η_P $Pump\ efficency\ (\%)$

Cp $Specific\ heat\ capacity\ (kJ/kg.K)$

$\overline{Cp}_g$ $Average\ specific\ heat\ capacity\ of\ hot\ gases\ (kJ/kg.K)$

$\overline{Cp}_h$ $Specific\ heat\ capacity\ of\ HTF\ (kJ/kg.K)$

r $Compressor\ pressure\ ratio$

γ $Ratio\ of\ Specif\ Heats$

d $Density\ (kg/m^3)$

Y $Steam\ flow\ rate\ to\ exhaust\ gas\ flow\ rate\ ratio$

v $Specific\ volume\ (m^3/kg)$

General Introduction

Thermo-Solar energy conversion with Rankine cycles offer new technical challenges to achieve acceptable thermal efficiency because of lower temperatures sources than in conventional cycles.

The search for improving the net work of thermal cycles (Rankine cycle, Brayton cycle…etc.), along with their thermal efficiencies has never stopped; and it will continue to grow with the advance in technology and the evolution in metallurgy. In this memoire we will try to lower condensation temperature, of the steam turbine (Rankine cycle) at the solar power plant “One” (Hassi R’mel), and analyze its impact on the power output and thermal efficiency.

In the first chapter, we will discuss the solar thermal power plants in general and compare them. Parabolic trough solar power plants will have the biggest share, since they are the most reliable technology and the most proven in the field. Thermal energy storage is becoming more efficient and less expensive; the advantages of TES with simulations of real solar power plants will be presented in this chapter. The last section is reserved to the presentation of “Solar Power Plant One” of Hassi R’mel.

The second chapter will discuss the thermodynamics of power plants, including the steam turbine, the gas turbine, heat recovery steam generators, the combined cycle and the solar field. In addition, all the applicable equations are presented in this chapter; they are used in calculations presented in the third chapter.

The third chapter has two sections, the first one is the calculation section where we will present all the calculations of solar power plant one (SPP1); the calculations will be done for four different condensation temperatures of the bottom cycle (Rankine cycle) of the combined-cycle.

The second section is the analysis of the results obtained previously, the analysis is divided in two main parts; part one is the impact of the condensation temperature on the steam turbine cycle (Rankine cycle), the combined cycle and the solar field. The second part is a result of the first one; it is about the economy of natural gas consumption. Economic evaluations also are presented.

Chapter I

Introduction to Power Plants

I.1. Introduction

Parabolic trough solar power plants are the most proven system of concentrating solar power (CSP) techniques. The nine parabolic trough solar electricity generating system (SEGS) of California illustrate the capability of this technology to be a reliable, renewable energy resource. This system has been operating commercially in large-scale thermal solar power plants with a total output of $345MW$. CSP plants are promising to be the alternative clean energy resource to meet the increasing energy demand and thus reduce thermal impact on the environment. It is predicted that CSP will play a significant role in providing the energy to meet the world's energy demands which are increasing rapidly in response to the growing economies in both developed and developing countries. Electricity produced by CSP in the Mediterranean and North African (MENA) region can be used to improve the local energy production systems and can be exported to the EU. The TRANS-CSP scheme has been introduced by the Trans-Mediterranean Renewable Energy Cooperation. It aims at interconnecting the electricity grids of Europe and the Mediterranean and North Africa regions, generating power by employing CSP in MENA and exporting it to the EU using a high voltage direct current HVDC network. The goal is to export about $700\ TWh/year$ to the EU by 2050. The anticipated cost is $0.05\ €/kWh$ [17].

Parabolic trough power plants can be operated in different configurations and operating systems. They can be operated in only solar mode where the solar collector's array is the only energy resource for the thermal cycle. Alternatively, they can be operated as a hybrid system, where a backup fossil fuel boiler is used in parallel to the solar collector's array. Most of the existing trough plants use synthetic oils as a heat transfer medium to supply the heat gained by the solar collectors to a Rankine cycle. However, a new concept of direct steam generating (DSG) has been introduced, where the water is evaporated and superheated in the solar collector tubes directly. This operation technique results in a cost reduction of up to 26% and efficiency improvement [17].

One of the most advanced solar operating systems is the integrated solar combined cycle ISCC, where a solar field based on the parabolic trough technology is coupled to a conventional combined cycle power plant. This system's advantages are cost reduction and operating flexibility because there is no need to install a storage system of fossil fuel backup boilers.

I.2. Solar Thermal Power Plants

The sun continuously supplies a massive amount of energy. Because of the nature of this energy, which is spread out at low density, it needs to be collected and concentrated to be useable economically. There are many applications and techniques where solar energy is utilized. In solar thermal power plants, solar energy is absorbed as heat into a heat transfer fluid (HTF) which is then transformed into electricity. Transforming this thermal solar energy into electricity can be achieved by different approaches. The most common techniques are concentrating solar power (CSP) plants. The CSP techniques are: solar tower, parabolic dish, parabolic trough and Fresnel arrays.

I.2.1. Concentrating solar power plants (CSP)

CSP plants provide energy at high temperatures which is used to run conventional power cycles such as the steam turbine, gas turbine and Stirling engine.

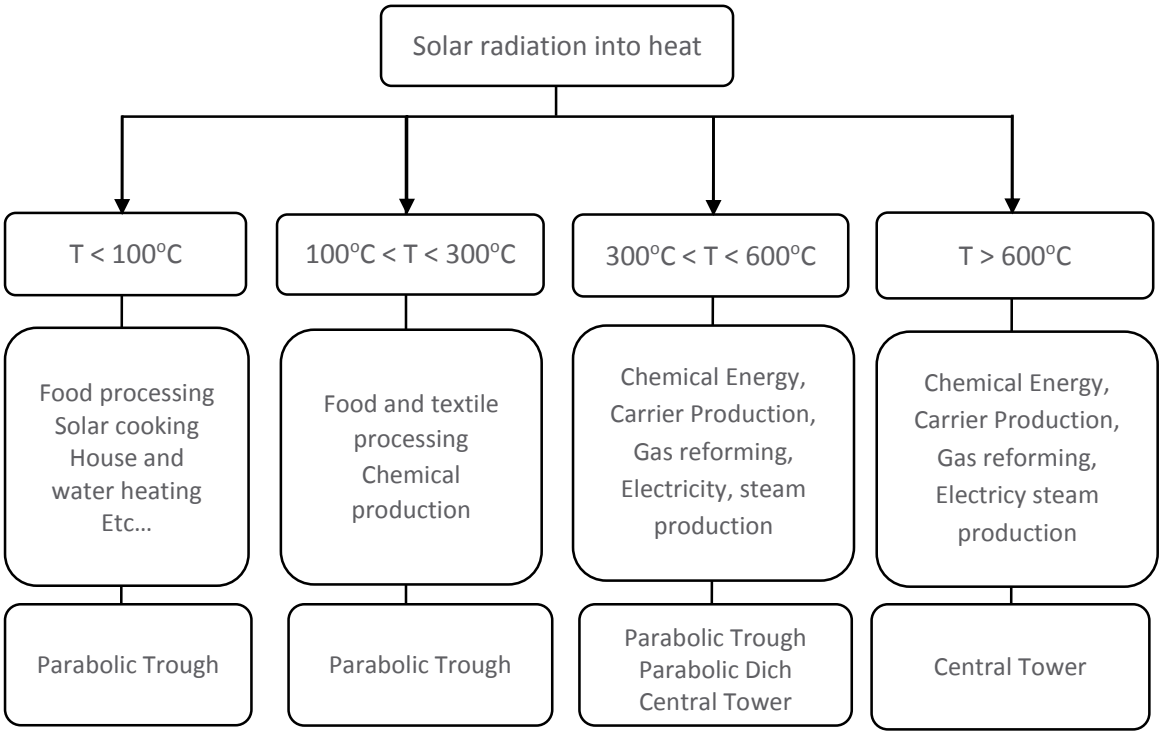

Figure I.1: CSP applications

I.2.1.1. Solar tower system

This technology provides a high ratio of solar radiation concentration of up to 600 which allows solar towers to achieve 1200°C for gas turbines applications. As shown in *Figure I.2*, the solar tower system

consists of heliostat reflectors located in circular array around the solar receiver. The reflectors track continuously the sun's position to ensure directing the sunlight to a receiver. A heat transfer medium is used in the receiver to absorb the concentrated solar energy. The absorbed heat is supplied to run a thermal power plant. The heat transfer fluid in the central receiver can be water, air, molten salt or oils. Research shows that this technique can be used to run a gas turbine where air is pressurized first and then heated up in the receiver to $1000°C$ [18].

Figure I.2: Solar tower [18].

The solar tower is one of the proven CSP technologies in the field. Examples of the operated solar towers are solar one and solar two in the USA. Their capacity is $10\ MW$ each.
Research has shown that the central tower has a potential to be used in a wide range of applications of gas turbines, combined cycles, CHP and some industrial processes [19][20]. In addition projects are being undertaken to investigate the technology potential in metal and hydrogen production.

I.2.1.2. Parabolic dish-engine

The basic concept of this technique is to use a parabolic dish to concentrate the solar radiation on an engine-generator set in the focal point of the reflector. The engine can be Stirling engine or a gas turbine. In terms of efficiency, the parabolic dish is the most efficient technology, its peak efficiency can be as much as 29% [18]. The typical diameter of the parabolic dish varies from 5 to $15\ m$ with an output of 5 to $25\ kW$ [21]. This technology is suitable for decentralized power supply and remote

locations. The barriers facing this technology are its cost and proof of long term reliability. *Figure I.3* shows a parabolic dish solar collector.

Figure I.3: Parabolic dish [27].

I.2.1.3. Linear Fresnel system

This system consists of an array of liner reflectors to concentrate the solar radiation on a central absorber. The absorber tube which is oriented along the focal line of the reflectors receives the concentrated solar radiation and converts the solar energy to heat. *Figure I.4* shows the Fresnel system elements. Heat transfer fluid is used to absorb this energy to be used in the proposed application. This type of collector offers good possibilities for solar energy use and it is suitable for small- and large-scale applications. Linear Fresnel technology was used in the summer of 2006 for the first time in a real industrial application to run an ammonia-water-chiller (see *Figure I.5*). One of the advantages of this collector is that it does not need complex construction materials.

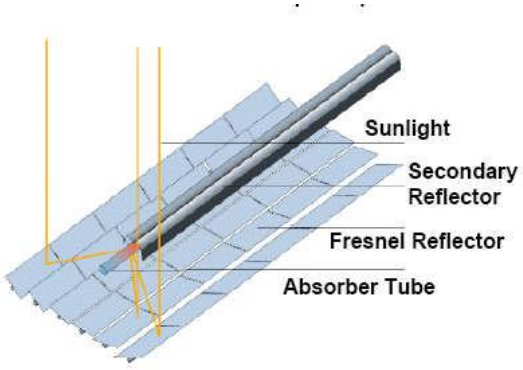

Figure 1.4 Fresnel system elements [18]

Figure 1.5 Fresnel collector driving an Ammonia-water-chiller in Bergamo, Italy

I.2.1.4. Parabolic trough system

The difference between this technology and the Linear Fresnel system is that parabolic trough system uses a parabolic shaped reflector. The concentration ratio can be 80 or more. The collected energy then absorbed by heat transfer fluid runs inside the absorbed tube. Parabolic trough technology supplies energy at a temperature of up to 400°C. This energy is supplied to run either a simple Rankine cycle or hybrid system. The heat transfer fluid which is used to absorb the heat can be either water or synthetic oils. *Figure I.6* shows the parabolic trough system elements [17].

The parabolic trough is the most proven technology so far, in solar thermal power plant applications thanks to the nine SEGS in the California desert, USA. They have been running commercially for more than 20 years in large-scale electric power plants. They are supplying $354\ MW$ to the southern Californian grid and have shown that there is no doubt about the technology's reliability and its potential to be a competitive energy resource. Most of the commercially proposed solar thermal power plants are planned to be operated based on the parabolic trough system.

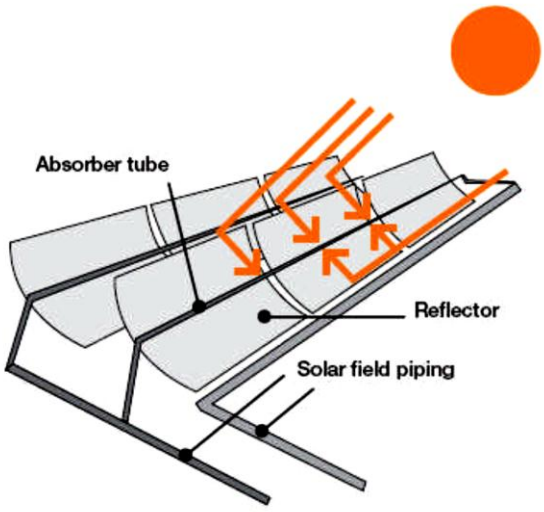

Figure 1.6 Parabolic trough system [22]

I.3. Parabolic Trough Solar Power Plants

I.3.1. The sun tracking control system

Since only direct solar radiation can be concentrated (Jacobson, 2006) parabolic trough systems use a sun tracking control system to ensure maximum efficiency of the concentrating process. For parabolic

trough collectors the most appropriate control system is for a north-south oriented rotation axis, where collectors are aligned on the north-south axis and collectors rotate from east to west tracking the sun's position. The control system continuously drives the collectors from east at sunrise to west at sunset. It is reset to the east position at sundown. Small motors are used to drive this tracking system. *Figure I.7* shows the solar collector control system theory.

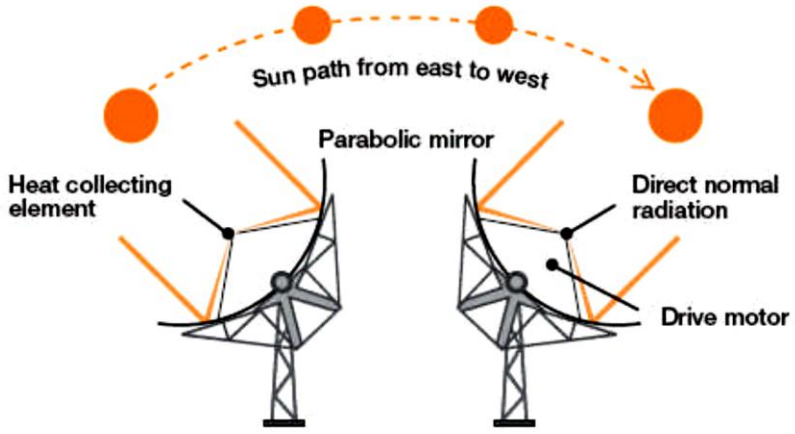

Figure 1.7: Sun tracking control system [22]

I.3.2. Parabolic trough plant configurations

Solar trough systems vary in configurations and operating systems. They can be installed in solar mode only where only heat from the solar field is used to operate the thermal cycle. However, these systems require a thermal storage facility to ensure operation continuously. Hybrid systems use different approaches.

Figure I.8: Aerial View of 5 x 30 MW Solar SEGSs at California, USA

Where the fossil fuel boiler (commonly natural gas fired) is used to supply the required energy for the thermal power plant. Boilers are connected in parallel to the solar field to heat up the feed water or to superheat the generated steam in the thermal cycle. The solar field consists of rows of parabolic trough collectors each row consists of collectors. *Figure I.8* shows an aerial view of a five parabolic trough power plant in the USA.

I.3.2.1. Solar only mode

In this configuration the only energy resource to run the thermal plant is the solar field. There is no backup or assistance from fossil fuels boilers. However, a thermal storage system is needed in this regime for continuous operation. The average solar-operating hours are 10-12 hours during the summer season. For the remaining time the plant is operated by energy from thermal storage. In solar only mode with storage the solar field starts running from sunrise to supply heat to the Rankine cycle. For about 2-3 hours of solar radiation peak, the solar field is operated to supply some energy to storage system in addition to its primary task of running the steam turbine. When solar energy is not sufficient to run the Rankine cycle, the storage system starts to supply energy to the thermal cycle. After sunset the plant runs completely on the storage system (Herrmann, 2004). *Figure I.10* shows a solar thermal power plant with a thermal storage system.

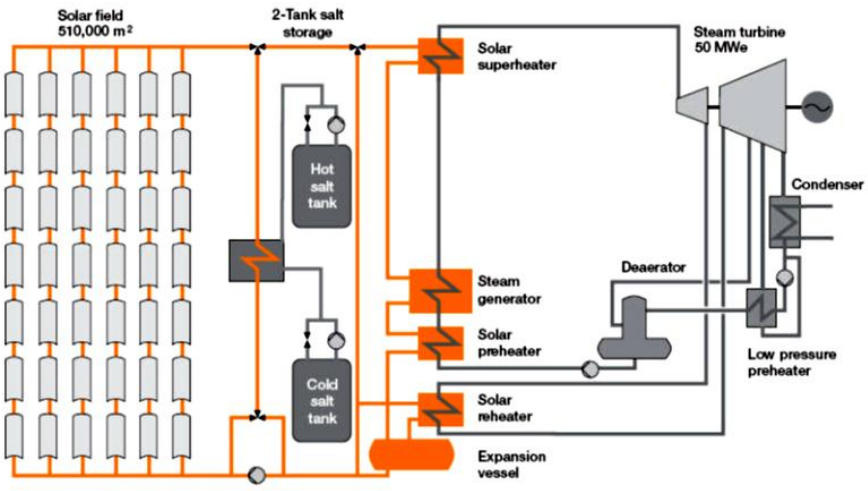

Figure I.10: Solar thermal power plant with thermal storage system [23]

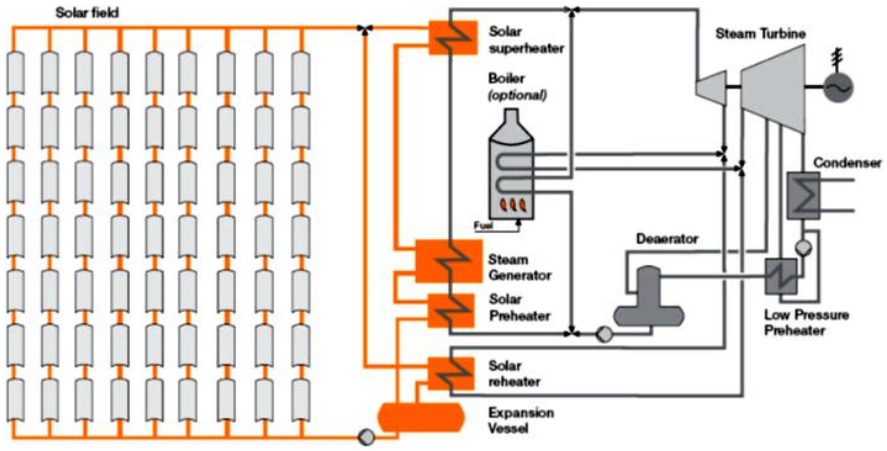

Figure I.11: Solar trough system with fossil fuel backup [22]

I.3.2.2. Hybrid systems

The hybrid system solar power generation concept uses a backup fossil fuel boiler which is used in parallel to the solar field to guarantee reliable operation at night-time or when no solar radiation is available. Many configurations have been introduced as hybrid systems. One fossil fuel boiler or more is used to supply the required energy for the thermal cycle. Boilers can be used to superheat the steam in the thermal cycle. Moreover in the hybrid systems one solar field or more is allocated in different positions either to heat the feed water or superheat the steam [24]. *Figure I.11* shows hybrid trough solar power plant.

I.3.2.3. Direct steam generation

The concept of DSG is to use water as an HTF in the parabolic trough solar field, so that the solar field

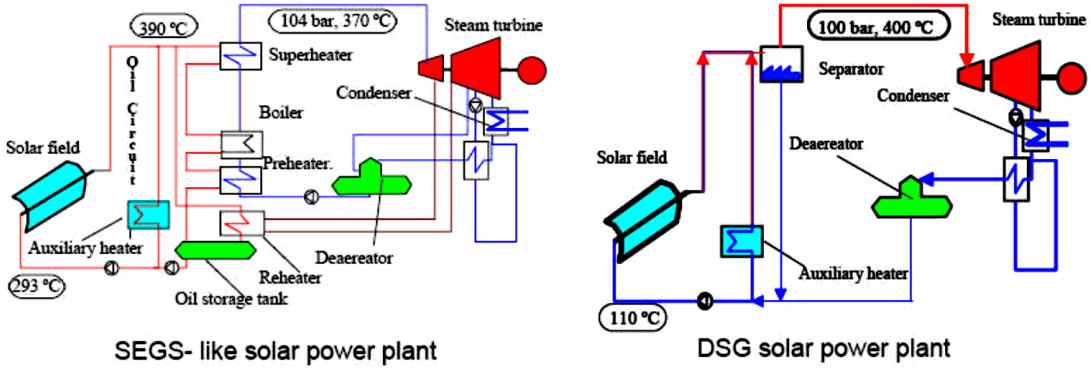

a. Solar system using HTF b. Solar system using DSG

Figure I.12: Solar trough plants operation systems

preheats, evaporates and superheats the water feed. Accordingly, steam can be expanded at a steam turbine directly. The benefits of this operation strategy are to cut capital and operation costs. Using water as an HTF results in eliminating the use of expensive synthetic oils and eliminating the heat exchanger from the power plant. Furthermore, the thermal efficiency of the thermal cycle is increased [17]. Because no temperature limits are imposed by the nature of the fluid. However, collector tubes operate under high steam pressures to be used, which is a less severe operating limit. *Figure I.12* shows a comparison between a DSG operation strategy and operation system with an oil HTF.

Three different operation regimes were tested by the European project DISS. These experimental tests were carried out in southern Spain in real solar radiation conditions and have proven the trough capability to generate steam with good conditions for the Rankine cycle operation. The three operation strategies are once-trough, injection system and recirculation system. These operation systems are shown in *Figure I.13* and described below.

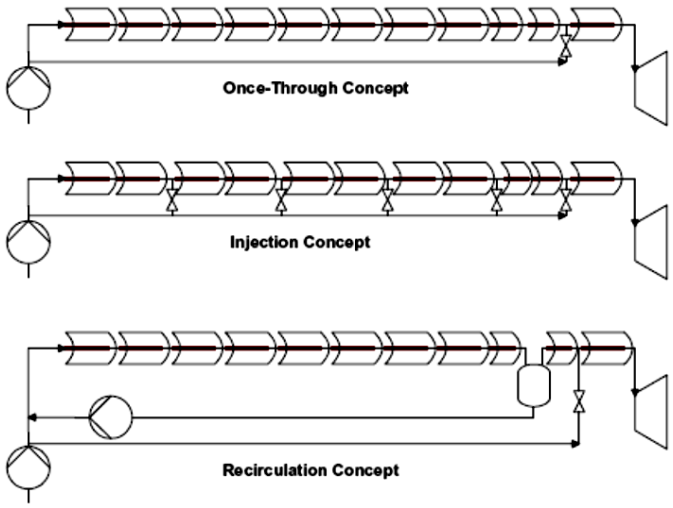

Figure I.13: Direct steam generation in parabolic trough technology

I.3.2.4. Integrated solar combined-cycle (ISCC)

The ISCC system is a combination of a solar field and gas turbine-combined cycle. The waste heat from the gas turbine is used to generate some steam to be expanded in a steam turbine. In addition, the solar field supplies extra heat to the thermal cycle. The additional heat from the solar field results in electricity generation increase during sunlight time. This combination results in improving the overall

thermal efficiency [17]. The benefits of employing this technology are to overcome some problems related to startup and shut down in solar power plants, reduce the capital cost and improve the solar-to-electricity efficiency. *Figure I.14* shows a schematic of ISCC.

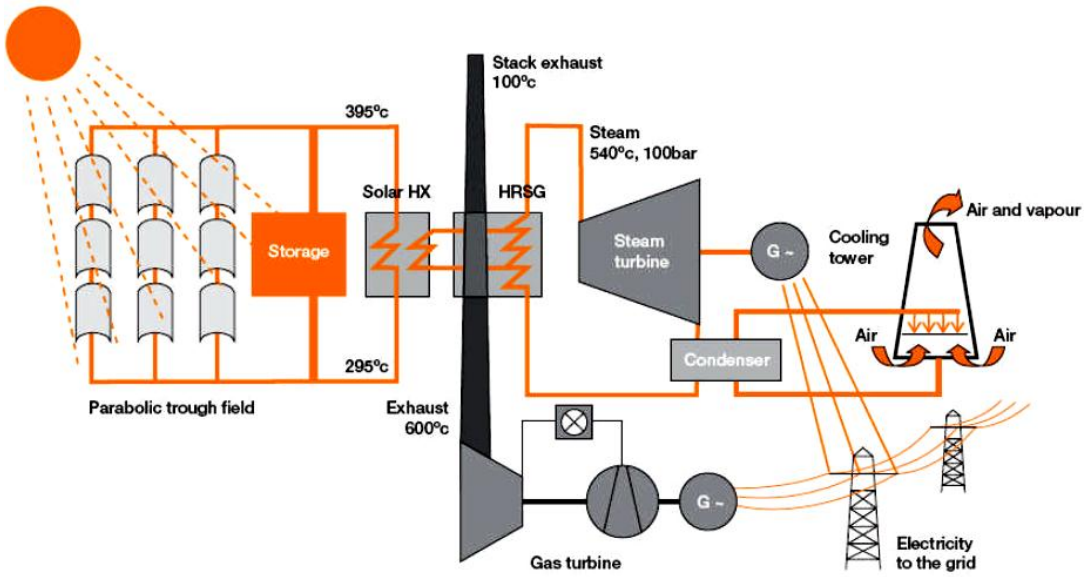

Figure I.14: Schematic of ISCC [22]

I.4. Combined-Cycle Power Plant

Gas turbines reject gases at high temperatures; for a simple gas turbine cycle, the temperature of exhaust gases can be as high as 600°C. Moreover, the simple gas turbine (without heat recovery) has a relatively low thermal efficiency. The design efficiency for commercial advanced turbines can be 36% (ALSTOM, 2007). The average efficiency for the whole operation life cycle is even worse. The exhaust gases from the gas turbine unit can be used as an external boiler for a Rankine cycle, where the heat recovery steam generator (HRSG) is used to generate and superheat some steam which is driven to be expanded in a steam turbine. As a result, more electricity is generated and the overall efficiency of the combined cycle (CC) is increased. *Figure I.15* shows the combined cycle layout. HRSG is a heat exchanger which recovers the energy from the exhaust hot gas and is used commonly in combined cycle power plants. The heat recovery system in the CC is divided to three main sections: heating the feed water to increase the water temperature up to the saturated temperature, the boiling process which converts the water into steam, and the superheating section which increases the steam temperature up to the desired state.

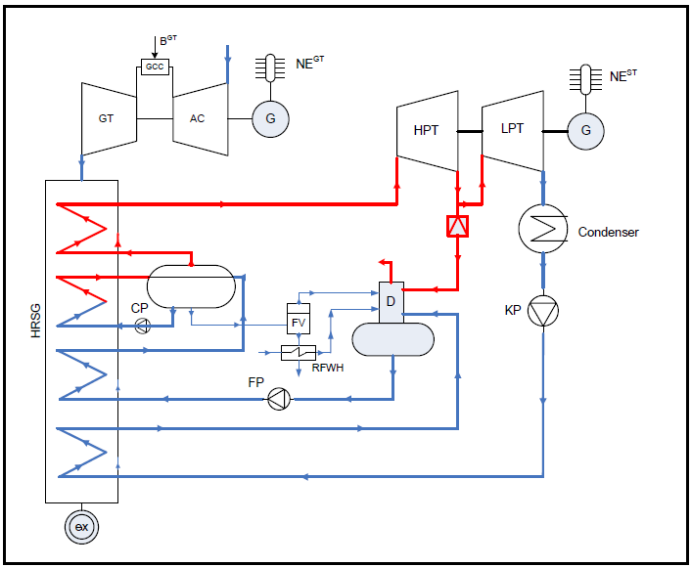

Figure I.15: Combined cycle power plant scheme

Figure I.16 shows a comparison between efficiencies of the common power plant systems. The combination of these two cycle gas turbines and steam turbines drives the total cycle efficiency to up to 60% [33].

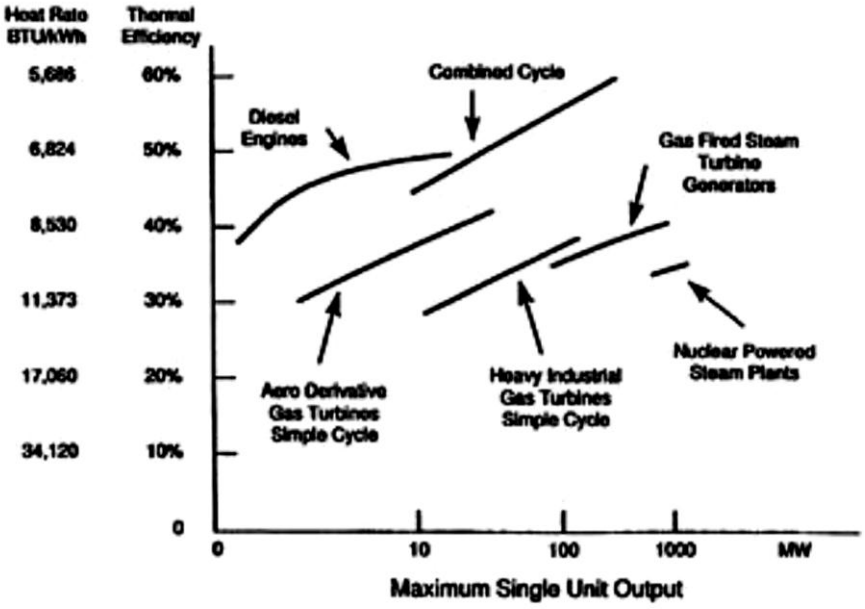

Figure I.16: Different power plants efficiencies [33]

I.5. Thermal Energy Storage (TES)

Adding TES provides several additional sources of value to a CSP plant. First, unlike a plant that must sell electricity when solar energy is available, a CSP plant with TES can shift electricity production to periods of highest prices. Second, TES may provide firm capacity to the power system, replacing conventional power plants as opposed to just supplementing their output. Finally, the dispatch ability of a CSP plant with TES can provide high-value ancillary services such as spinning reserves.
Building a CSP plant with TES introduces several sizing options as the plant essentially consists of three independent but interrelated components that can be sized differently: the power block, the solar field, and the thermal storage tank. The size of the power block is the rated power capacity of the steam turbine.

The size of the solar field, determines the amount of thermal energy that will be available to the power block, this will determine the capacity factor of the CSP plant. Under-sizing the solar field will result in an underused power block and a low capacity factor for the CSP plant, because of the lack of thermal energy. An oversized solar field, on the other hand, will tend to result in thermal energy being wasted because the power block will not have sufficient capacity to use the thermal energy from the solar field in many hours.

The size of storage determines both the thermal power capacity of the heat exchangers between the storage tank and the HTF and the total energy capacity of the storage tank.
For a merchant CSP developer, the decision to build and the choice of the size of a CSP plant will be governed not only by the amount of solar energy available but also by the pattern of solar resource and by electricity prices. Clearly, high electricity prices and an abundance of solar resource are necessary for CSP to be economic, but a lack of correlation between solar availability and electricity prices can make CSP economically unattractive. TES can improve the economics by shifting generation to higher-priced hours, but this adds capital costs and some efficiency losses in the storage cycle [23].

A study done by the German Aerospace Centre (DLR) on solar-hybrid power plants that were designed and modeled for a site in Northern Africa (Hassi R'Mel, Algeria) for a power level of $30\ MW$ with dry cooling towers. Due to the integrated fossil burner each analyzed solar-hybrid p ower plant can be operated in solar-only, fossil-only or solar-hybrid mode. To increase the solar share of the plant a thermal energy storage is used

a) Solar share in base-load operation

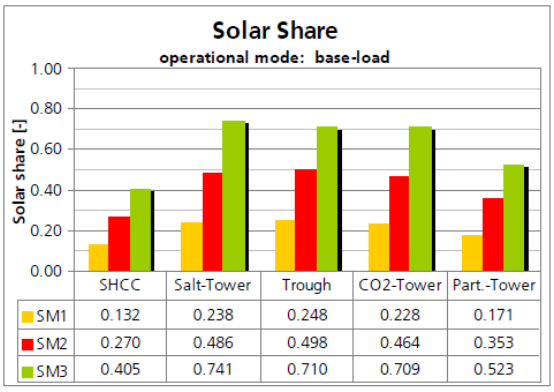

	SHCC	Salt-Tower	Trough	CO2-Tower	Part.-Tower
SM1	0.132	0.238	0.248	0.228	0.171
SM2	0.270	0.486	0.498	0.464	0.353
SM3	0.405	0.741	0.710	0.709	0.523

b) Solar share in mid-load operation

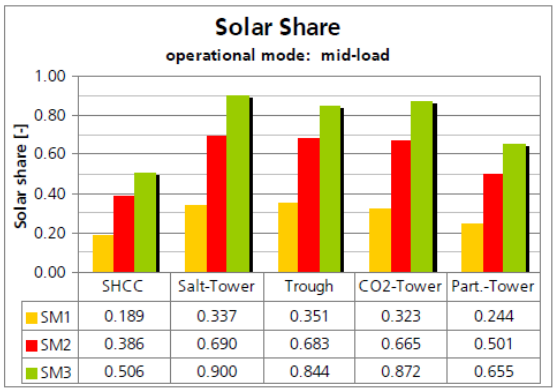

	SHCC	Salt-Tower	Trough	CO2-Tower	Part.-Tower
SM1	0.189	0.337	0.351	0.323	0.244
SM2	0.386	0.690	0.683	0.665	0.501
SM3	0.506	0.900	0.844	0.872	0.655

Figure I.17. a Solar share in based-load operation, b Solar share in mid-load operation [15].

c) Specific CO_2 emissions in base-load operation

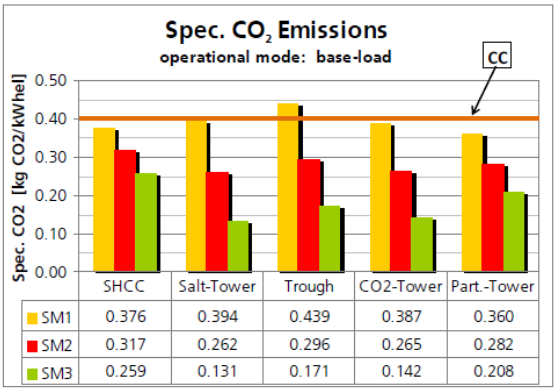

	SHCC	Salt-Tower	Trough	CO2-Tower	Part.-Tower
SM1	0.376	0.394	0.439	0.387	0.360
SM2	0.317	0.262	0.296	0.265	0.282
SM3	0.259	0.131	0.171	0.142	0.208

d) Specific CO_2 emissions in mid-load operation

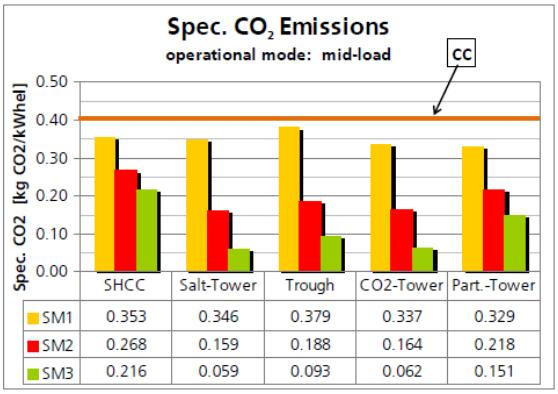

	SHCC	Salt-Tower	Trough	CO2-Tower	Part.-Tower
SM1	0.353	0.346	0.379	0.337	0.329
SM2	0.268	0.159	0.188	0.164	0.218
SM3	0.216	0.059	0.093	0.062	0.151

Figure I.18. a Specific CO_2 emissions in based-load operation, b Specific CO_2 emissions in mid-load operation [15].

e) LEC and solar LEC in base-load operation

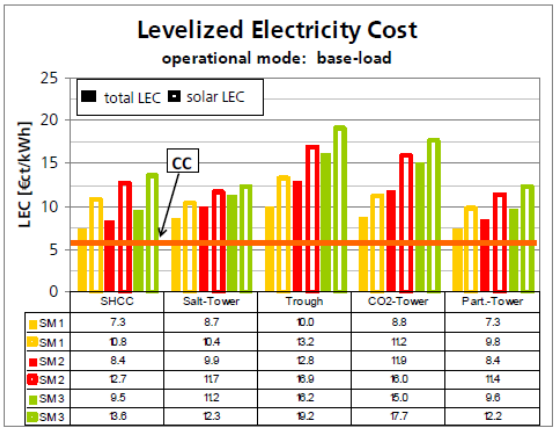

	SHCC	Salt-Tower	Trough	CO2-Tower	Part.-Tower
SM 1	7.3	8.7	10.0	8.8	7.3
SM 1	10.8	10.4	13.2	11.2	9.8
SM 2	8.4	9.9	12.8	11.9	8.4
SM 2	12.7	11.7	16.9	16.0	11.4
SM 3	9.5	11.2	16.2	15.0	9.6
SM 3	13.6	12.3	19.2	17.7	12.2

f) LEC and solar LEC in mid-load operation

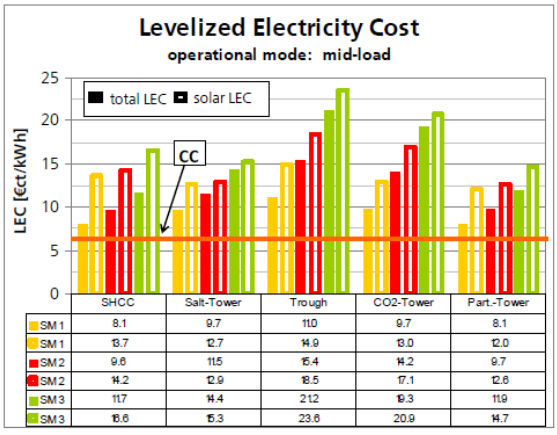

	SHCC	Salt-Tower	Trough	CO2-Tower	Part.-Tower
SM 1	8.1	9.7	11.0	9.7	8.1
SM 1	13.7	12.7	14.9	13.0	12.0
SM 2	9.6	11.5	15.4	14.2	9.7
SM 2	14.2	12.9	18.5	17.1	12.6
SM 3	11.7	14.4	21.2	19.3	11.9
SM 3	18.6	15.3	23.6	20.9	14.7

Figure I.19. a Increase of electricity cost in based-load operation, b Increase of electricity cost in mid-load operation [15].

The results of this study showed that in comparison to a conventional fossil fired combined cycle the potential to reduce the CO_2 emissions is high, especially with large solar fields and high storage

capacities. However, for dispatchable power generation and supply security it is obvious that in any case a certain amount of additional fossil fuel is required. No analyzed solar-hybrid power plant shows at the same time advantages in terms of low CO_2 emissions and low LEC. While power plants with solar-hybrid combined cycle (SHCC, Particle-Tower) show interesting LEC, the power plants with steam turbine (Salt-Tower, Parabolic Trough, CO2-Tower) have low CO_2 emissions (especially those with large solar fields and high storage capacities). All solar-hybrid power plants show increasing LEC with increasing solar field sizes and storage capacities. This is mainly caused by the high investment cost of the TES. However, those are a fundamental requirement for low CO_2 emissions for base-load operation of solar thermal power plants. The LEC could generally be reduced by choosing a site with better solar resources. However, to be competitive to conventional fired combined cycles in *base-load operation*, it is necessary in future to further reduce the investment cost of the solar-hybrid power plants and/ or to increase the efficiency and/ or the increase the solar share. Higher cost of fossil fuels and higher cost for carbon trading can generally reduce the advantage in LEC for the fossil fired combined cycles. However, this will also dramatically increase the cost of common electricity supply [15].

So despite these benefits, TES cannot be economically justified on energy value alone, because TES cannot be installed anywhere in the world, first because of the large area needed that some regions cannot afford; secondly due to the high cost investment. The results can be uneconomic.

I.6. Solar Power Plant One (SPP1)

I.6.1. Presentation of SPP1

The first Gas-Solar hybrid power plant in Algeria was first inaugurated July the 14th 2011, located in Hassi R'mel. This power plant was named "Solar Power Plant One" (SPP1). The major shareholders of SPP1 are ABENER with 51%, NEAL (New Energy Algeria) with 20%, COFIDES (Spanish company of projects finance in developing countries) with 15% and SONATRACH with a share of 14%.
The Power Plant SPP1 is located $494.5\ km$ south of the capital Algiers, at the south frontiers of city of Laghouat. It is installed on land that extends over a surface of $150\ hectares$. It is reached by the national highway $N1$, the existence of electrical grid alongside of the national highway $N1$ and Hassi R'mel gas field were factors this site was chosen.

The region of Hassi R'mel is characterized by the average meteorological conditions:

- Relative humidity 24%.
- Atmospheric pressure: $0.928\ bar$.
- Wind velocity: $2.14 - 4.15\ m/s$.
- Extreme temperatures: -10°C (winter) $+50$ °C (summer)
- Direct normal irradiation (DNI): $950\ W/m^2$ in the summer time.

The SPP1 is hybrid. By this we mean that it operates on natural gas and solar energy. It produces $150\ MW$ (net power ISO) with a solar contribution of 17% of the rated power which is $25\ MW$. This unit is composed of two parts, the solar field and the combined cycle.
The Combined cycle consists of two gas turbines (with natural gas) with a rated power of $47\ MW$ each. The combustion heat of these turbines is recovered in two horizontal natural circulation HRSGs (Heat Recovery Steam Generator). These supply the steam turbine with a rated power of $80\ MW$.

It is noted that the strength of the SPP1 is the addition of the steam produced by the solar field to the steam recovered from the burned gases of the gas-turbine to run the steam-turbine, the electrical power produced by the plant increases accordingly.
The construction of this central SPPI lasted 3 years. In perspective, it is planned to build three new hybrid plants in the coming years (SPP II Meghaïer in 2014, SPP III Naâma in 2016 and SPP IV Hassi R'Mel 2018) [35].

I.6.2. Components

I.6.2.1. Gas turbine

The gas-turbines are of the SIEMENS type (SGT800). Each turbine is coupled with an alternator of rated power of $40\ MW$,$11\ KV$, cooled with air. The air intake of the compressor, goes through a chiller (Chilled water-Heat exchanger) to approach the ISO conditions at the compressor inlet (15°C, $1.0131\ bar$, and relative humidity 60%) to maintain the turbine efficiency in the extreme conditions. Speed $6600\ rpm$, overspeed 110%, the net power per gas turbine at 100% load is $47\ MW$ in ISO conditions, ISO efficiency 37.5%.

I.6.2.2. Heat recovery steam generator

The heat recovery steam generator (HRSG) allows to recover the burnt gases from the gas turbine exhaust to produce the necessary steam for the operating of the steam turbine. The HRSG is horizontal and natural circulation flow and one level of HP pressure. The heat exchange is done in cross flow configuration through several levels of exchangers, some of which are equipped with burners (post combustion).

I.6.2.3. Steam turbine

The steam turbine is of SIEMENS "SST-900 C" type, one HP body. The condensation of the steam occurs in air cooled condensers. The turbine rotates with $3000\ rpm$ an alternator of rated power of $80\ MW$; at a corresponding efficiency of 33.25%.

I.6.2.4. Air-cooled condenser

The air cooled condenser is composed of six air heat exchangers disposed in inverted V-shaped, through which ambient air is blown by 15 fans. The condensed water is recovered in a condensate tank. These condensates are re-injected into the heat recovery steam generator at the required pressure.

I.6.2.5. Solar field

The park of collectors of the plant consists of two solar fields; one in the north of the site and the other to the south with a total area of opening mirrors $183{,}120\ m^2$ and a ground engaging over $600{,}000\ m^2$, the total surface area of land on which the plant occupies is $150\ hectares$. The two solar fields (north-south) include:

- 56 Loops in a centralized provision;
- A loop comprises four collectors connected in series;
- A collector consists of 12 modules arranged in series;
- 2688 Modules which each have 28 curved mirrors to get a parabolic profile.

The orientation of the field (north-south), and tracking the sun is done on (east - west) trajectories. Collectors are equipped with tracking systems (tracking) on one axis and controlled from the control room. In case of maintenance or breakdown, it is possible to isolate a loop without affecting the operation of the rest of the field. Also in the case of a minor operation or washing of a collector, it can be put out of operation (de-focused position) without affecting the operation of the rest of the loop.

Washing mirrors is a systematic operation (15 to 20 days to wash all the mirrors); it is done using a truck equipped with a system of jet water treated by reverse osmosis. The two fields are joined together by carbon steel pipes carrying oil (HTF: heat transfer fluid) to the solar steam generator.

I.7 Aim of This Study

The objective of this study is to analyze the physical and performance characteristics of the power plant SPP1 (recently obtained by M.TRAD), we are aiming particularly at the operation of the air-cooled condensers on the steam cycle efficiency. We are looking to quantify the gains of power and thermal efficiency by lowering the temperature of condensation of the steam turbine, either by increasing the blowing velocity of air-cooled condensers, or by humidifying the air blown. Precise energy evaluations will be conducted.

Chapter II

Thermodynamics of Power Plants

II.1. Gas Turbine

Gas turbines are complex turbo machines. Nevertheless, gas turbines have three main parts that perform the fundamental thermodynamic processes involved in the mechanical shaft power production from the fuel chemical energy as illustrated in *Figure II.1*. First, the income atmospheric air must undergo a compression process in the compressor section where both pressure and temperature are increased. Next, the compressed air is driven to a combustion chamber where fuel is injected into the compressed air stream and burnt increasing the temperature at a constant pressure process. Finally, the combustion products at a high temperature and pressure are expanded in the power turbine section generating shaft power to drive the compressor as well as an electrical generator or any other rotary device attached to the rotary shaft. The combustion products are exhausted through a nozzle into the atmosphere [6].

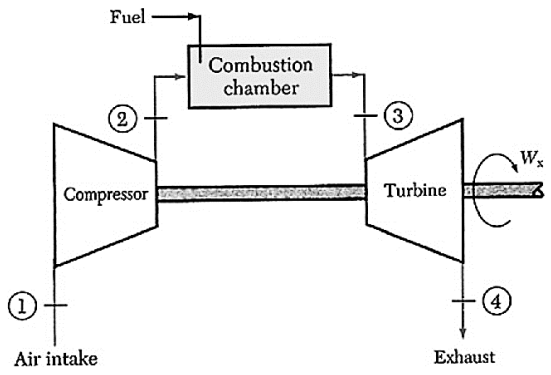

Figure II.1. Three main parts of a gas turbine: the compressor, the combustion chamber, and the power turbine

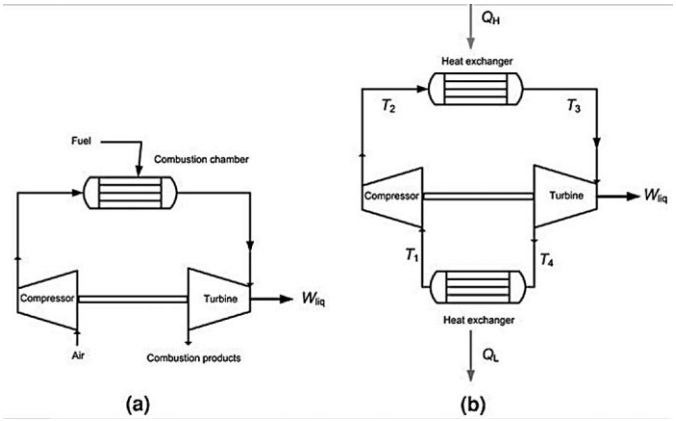

Figure II.2. a Open cycle; b closed air standard Brayton cycle

II.1.1. Simple Brayton cycle

In an actual gas turbine, the working fluid changes from atmospheric air to combustion products that exhaust back to the atmosphere, as illustrated in *Figure II.2*a. However, in order to evaluate the machine from the thermodynamic point-of-view, some assumptions are needed. Firstly, the working fluid is assumed to be plain air, without any chemical transformation due to the combustion. In doing so, the air-fuel combustion process is replaced by a heat addition process at a constant pressure [1]. Secondly, the exhaust and admission processes are replaced by a heat transfer process to the environment, which makes the air to flow continuously in a closed loop as indicated in *Figure II.2*b. In the closed cycle, air at environment pressure and temperature is first compressed, next it receives heat Q_H and it is followed by an expansion process in the turbine section to, finally, reject heat Q_L at constant pressure. This is the Air-Standard Brayton Cycle [1][6].

Having the cycle of *Figure II.2*b. in mind along with the ideal gas behavior and constant thermodynamic properties, one may obtain the working equations for each cycle component:

Heat addition

$$q_H = h_3 - h_2 = Cp.(T_3 - T_2) \tag{1}$$

Heat rejection

$$q_L = h_4 - h_1 = Cp.(T_4 - T_1) \tag{2}$$

Compression work

$$w_C = h_2 - h_1 = Cp.(T_2 - T_1) \tag{3}$$

Turbine work

$$w_T = h_3 - h_4 = Cp.(T_3 - T_4) \tag{4}$$

Cycle net work

$$w = q_H - q_L = w_T - w_C \tag{5}$$

Equations (1) through (5) are on mass basis whose unit is kJ/kg in the international system of units, SI. We assume that both kinetic and potential forms of energy are here [1].

So for instance, if one needs the total compressor power $\dot{W}_C$, it may be obtained by multiplying the equations (1) to (5) by the mass flow rate $\dot{m}$.

$$\dot{W} = \dot{m}.w \quad and \quad \dot{Q} = \dot{m}.q \tag{6}$$

Figure II.3 gives two important thermodynamic diagrams for cycle analysis. The first one is the temperature-entropy diagram and the second one is the pressure-specific volume diagram. The simple Brayton cycle formed by its four basic ideal gas processes is indicated in both diagrams. The cycle net work is given by the enclosed area shown in figures. First, air is compressed ideally (isentropic) in the compressor (1–2) increasing both pressure and temperature at expenses of using compression work w_C which is supplied by the turbine itself. Second, heat q_H is added at constant pressure making up the process 2–3, which heats up the air to the highest cycle temperature T_3. Next, the high pressure and temperature air undergoes an expansion process (3–4) that generates work w_T enough to drive the compressor and produce net shaft work w. Finally, heat q_L is rejected to the environment (4–1) at constant low pressure closing the cycle [1] [6]. Thermal efficiency η_{GT} of a cycle is defined as the ratio between the cycle net work and heat added. By applying the First Law for the whole cycle, one easy can show that:

$w = q_H - q_L$. Therefore, one obtains [1]:

$$\eta_{GT} = 1 - \frac{q_L}{q_H} \tag{7}$$

Finally, using Eqs. (1) and (2), it yields [1]:

$$\eta_{GT} = 1 - \frac{Cp.(T_4 - T_1)}{Cp.(T_3 - T_2)} = \frac{T_1.(T_4/T_1 - 1)}{T_2.(T_3/T_1 - 1)} \tag{8}$$

By examining the temperature-entropy diagram in *Figure II.3*a, one can easily notice that T_3 is the

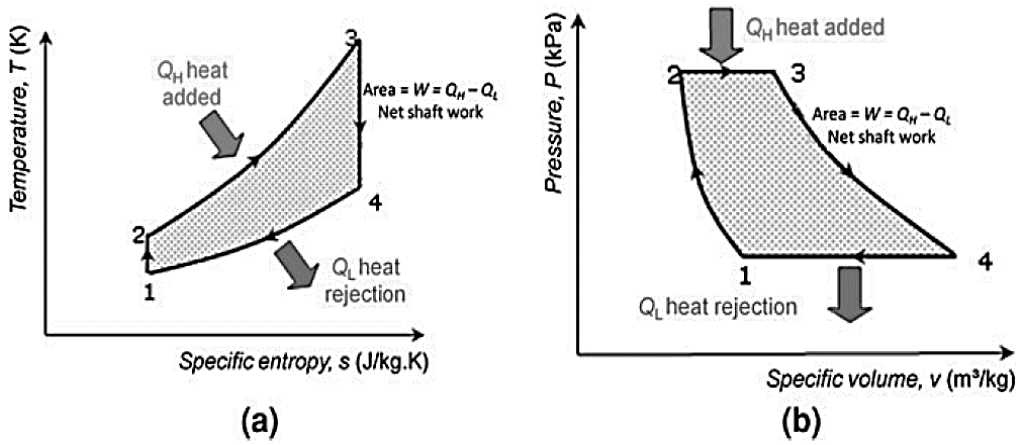

Figure II.3. Simple Brayton cycle in a temperature-specific entropy diagram; b pressure-specific volume diagram

maximum cycle temperature, also known as the firing temperature, while T_1 is the minimum one (usually the environment temperature).

By using isentropic ideal gas relationships between pressure and temperature, it is straightforward to show that [1].

$$\frac{T_2}{T_1} = \left(\frac{P_2}{P_1}\right)^{\frac{\gamma-1}{\gamma}} \; and \;\; \frac{T_3}{T_4} = \left(\frac{P_3}{P_4}\right)^{\frac{\gamma-1}{\gamma}} \tag{9}$$

Also, from the diagram of *Figure II.3*b, one may notice that [6].

$$r = \frac{P_2}{P_1} = \frac{P_3}{P_4} \tag{10}$$

Where, r is the ratio of maximum and minimum cycle pressures. Using the isentropic compression and expansion processes and constant pressure heat transfer, one may show that $T_3/T_2 = T_4/T_1$. Finally, substituting that in Eq. (8), one obtains [1] [6].

$$\eta_{GT} = \frac{\dot{W}_{net}}{\dot{Q}_H} = 1 - \frac{T_1}{T_2} = 1 - \frac{1}{\left(\frac{P_2}{P_1}\right)^{\frac{\gamma-1}{\gamma}}} = 1 - \frac{1}{(r)^{\frac{\gamma-1}{\gamma}}} \tag{11}$$

Figure II.4 shows a graphics of the thermal efficiency as a function of the pressure ratio for air as given by Eq. (11), for air (value of $\gamma = 1{,}4$). Generally, it is not enough to carry out a simple thermal efficiency analysis to find the best operational condition of a Brayton cycle. A non-negligible amount of work is required to compress the air from the inlet to the maximum cycle pressure and this work must be supplied by the turbine itself. Therefore, one should examine the net work produced by the system compressor-turbine as a whole. In order to achieve that, first subtract Eq. (3) from Eq. (4), to obtain the net work [1][7]:

$$w = w_T - w_C = Cp.(T_3 - T_4) - Cp.(T_2 - T_1) \tag{12}$$

II.1.2. Inefficiencies and actual Brayton cycle

The actual Brayton cycle is based on real turbo machines that deviate from ideal ones (isentropic). Substantial part of the work produced in the turbine section is drawn by the compressor, which can reach figures as high as 80% of turbine shaft work. If compressor and turbine efficiencies are not high enough, no net shaft work will be generated. Therefore, it is quite important to analyze how much

process losses are introduced on the overall performance of the turbine due to machine inefficiency. First, two isentropic definitions must be introduced:

Compressor isentropic efficiency, η_C, is defined as the ratio of ideal or isentropic compression work, w_{C-s}, to the actual compression work, w_C. *Figure II.6*a indicates the ideal and the actual compression processes in the T-s diagram [1][6][8].

$$\eta_C = \frac{w_{C-s}}{w_C} = \frac{h_{2s} - h_1}{h_2 - h_1} \tag{13}$$

Turbine isentropic efficiency, η_T, is defined as the ratio of the turbine actual work, w_T, to the ideal or isentropic turbine work, w_{T-s}. *Figure II.6*b indicates the ideal and the actual expansion process in the T-s diagram [1][6][8].

$$\eta_T = \frac{w_T}{w_{T-s}} = \frac{h_3 - h_4}{h_3 - h_{4s}} \tag{14}$$

In *Figure II.4*, one can see both processes of compression (a); both processes of expansion in the turbine section (b); and, finally, on can see the overall combination (c) of those processes.

Using the definition of isentropic compression work Eq.(13), one can obtain the following equation for the actual compression work and ideal gas assumption with constant specific heat [8]:

$$w_C = \frac{Cp.T_1}{\eta_C}\left((r)^{\frac{\gamma-1}{\gamma}} - 1\right) \tag{15}$$

And similarly for the actual turbine work Eq.(14) [8]:

$$w_T = \eta_T.(1+f).Cp.T_3\left(1 - \frac{1}{(r)^{\frac{\gamma-1}{\gamma}}}\right) \tag{16}$$

By subtracting previous equations, one obtains the actual net shaft work produced by the gas turbine cycle. To take into account polytropic efficiencies of compressor and turbine with n replacing γ , we write:

$(r)^{\frac{\gamma-1}{\gamma}} = (r)^{\frac{n-1}{n}} = r^{\alpha}$, and obtain the net power as [8]:

$$w = w_T - w_C = Cp.T_1.\left[(1+f).\frac{T_3}{T_1}.\eta_T.\left(1 - \frac{1}{(r)^{\alpha}}\right) - \frac{1}{\eta_C}.((r)^{\alpha} - 1)\right] \tag{17}$$

In a similar fashion, it is possible to show that the actual pressure ratio where the maximum actual net work takes place for a given temperature ratio, T_3/T_1, considering the isentropic machine efficiencies:

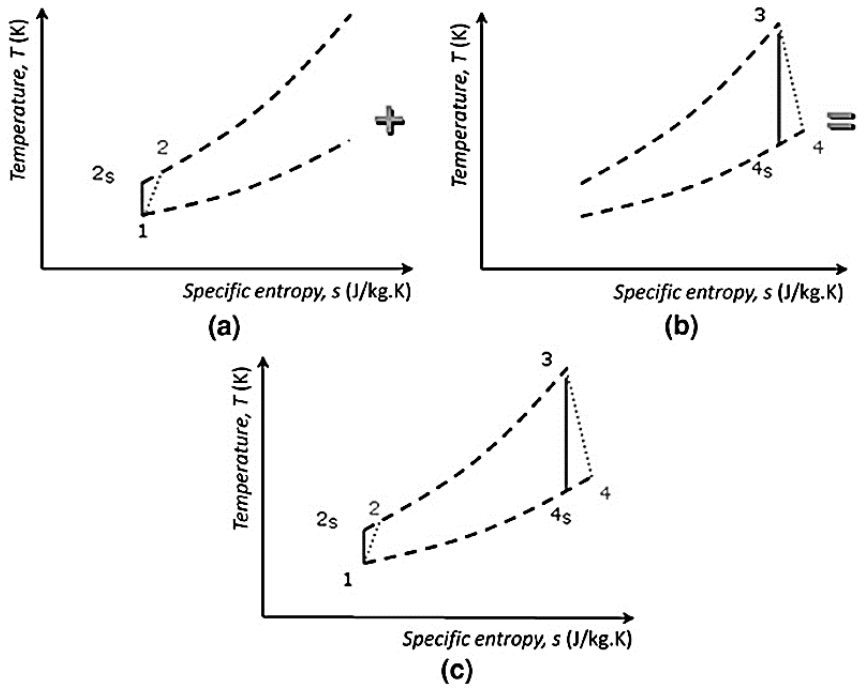

Figure II.4 a Actual and ideal compression work; b actual and ideal expansion work; c combination of both processes

Taking the first derivative of net power with respect to pressure ratio i.e., $\partial w/\partial r)_{T_3/T_1} = 0$, one obtains the necessary but also sufficient condition for the optimum compression ratio at maximum power [8]:

$$r_{max} = \left(\frac{P_2}{P_1}\right) = \left((1+f).\eta_C \eta_T \frac{T_3}{T_1}\right)^{\frac{1}{2\alpha}} \tag{18}$$

One may also obtain the actual thermal efficiency, η_{GT}, as the ratio of the actual net power and the added flux heat [8]:

$$\eta_{GT} = \frac{\dot{w}_{net}}{\dot{q}_H} = \frac{\left[(1+f).\frac{T_3}{T_1}.\eta_T.\left(1-\frac{1}{(r)^{\alpha}}\right)-\frac{1}{\eta_C}.((r)^{\alpha}-1)\right]}{(1+f).\left(\frac{T_3}{T_1}-\frac{1}{\eta_C}.((r)^{\alpha}-1)-1\right)} \tag{19}$$

*Figure II.5*a displays the ideal and actual thermal efficiencies and *Figure II.7*b shows the net work. As seen in those graphics, machines efficiencies are quite relevant.

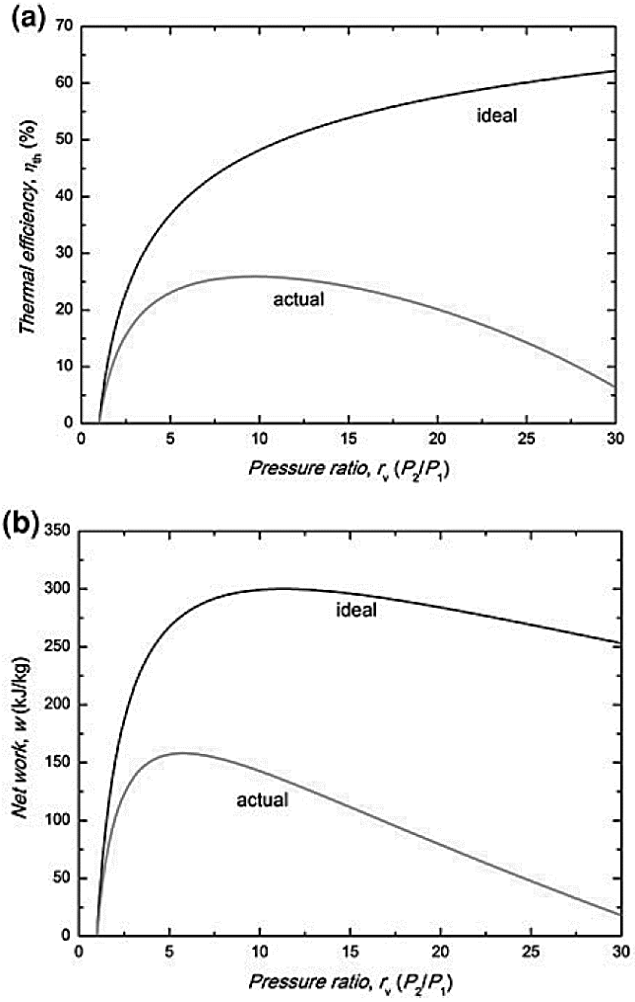

Figure II.5. a Actual and ideal thermal efficiencies; b actual and ideal net work. $T_1 = 300\ K$, $T_3 = 1200\ K$, $\eta_T = 0{,}85$ *and* $\eta_C = 0{,}80$

II.2. Steam Turbine

II.2.1. Rankine cycle

Rankine cycle is the one used in steam power plants. The most common fluid used in this cycle is water, but other fluids can also be used. Lately, ROC, Rankine Organic Cycles have been devised using organic fluids, rather than water. ROC is mostly used in small to medium installations and they are usually powered by solar energy or recovered waste heat. Industrial and large thermal power plants use conventional Rankine Cycles, which are revised in this section. First, the simplest Rankine cycle is presented and the necessary variations are discussed.

II.2.1.1 The simple Rankine cycle

The ideal Rankine cycle is the one based on four reversible processes as shown in *Figure II.6*a. Saturated liquid 1 undergoes an isentropic compression process to reach compressed liquid at state 2. Next, the compressed liquid is driven to the steam generator, where heat Q_h is added to obtain saturated vapor at state 4. Useful work is produced in an expansion machine, such as a steam turbine, in an isentropic process yielding fluid at state 5. Finally, there occurs condensation by removing heat Q_l in the condenser to close the cycle and the fluid returns to the initial state 1. All processes are ideal. The diagram T-s in *Figure II.6*b shows the corresponding Carnot Cycle 1'-3-4-5-1'. Clearly, one can see that the Carnot cycle has a higher thermal efficiency than the simple Rankine cycle by simply reasoning that heat is delivered to the Rankine cycle at an average temperature (between T_2 and T_H) lower than the one for the Carnot cycle T_H.

Thermal balances around the components of the Rankine cycle are:

Heat addition (steam generator)

$$q_h = h_4 - h_2 \tag{20}$$

Heat rejection (condenser)

$$q_l = h_5 - h_1 \tag{21}$$

Compression work (pump)

$$w_P = h_2 - h_1 \tag{22}$$

Expansion work (turbine)

$$w_T = h_4 - h_5 \tag{23}$$

Cycle net work

$$w = w_T - w_P = q_h - q_l \tag{24}$$

Magnitudes in Eqs.(20) to (24) are on mass basis. For instance, if one needs the cycle total net power $\dot{W}_{net}$, it may be obtained according to Eq.(25).

$$\dot{W}_{net} = \dot{m}.w = \dot{m}.(w_T - w_P) = \dot{m}.[(h_4 - h_5) - (h_2 - h_1)] \tag{25}$$

Where, $\dot{m}$ is the mass flow rate.

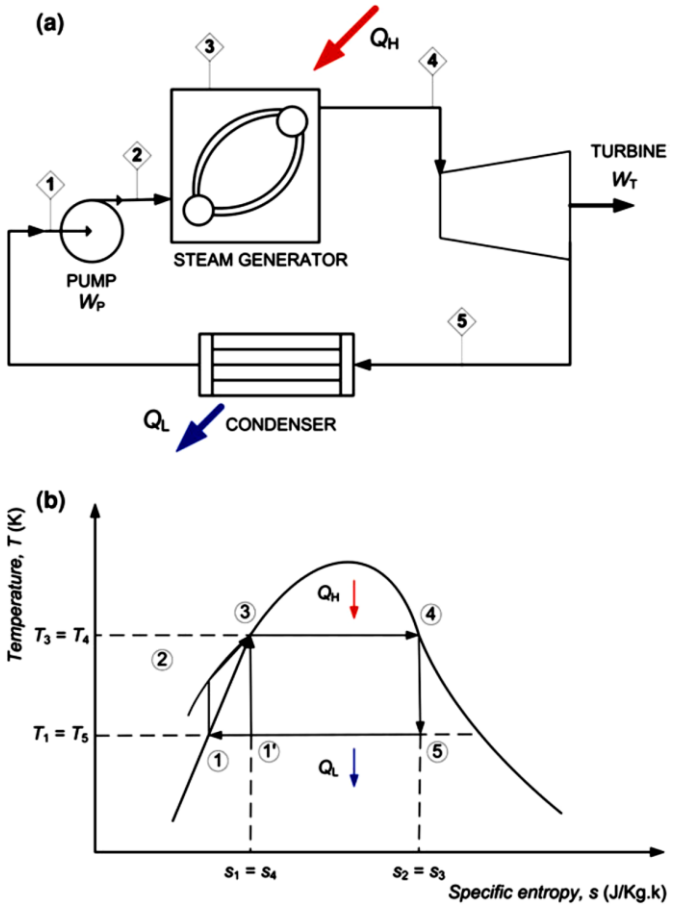

Figure II.6: a- four basic components of a simple Rankine cycle; b- temperature-specific entropy diagram and Carnot cycle

By assuming incompressible liquid, it is also a common practice to obtain the ideal pumping work by the following expression [8]:

$$w_p = v.(P_2 - P_1) \tag{26}$$

Where v is the liquid specific volume.

II.2.1.2 Rankine cycle with vapor superheating

By closely examining the T-s diagram of the simple Rankine cycle (*Figure II.7*b), it is possible to notice that at the exit of the expansion machine (turbine) a mixture of liquid and vapor is present (state 5). Usually, a vapor quality at and below around 90% can cause damage to the turbine blades by erosion due to the impact of droplets at high velocity. The way to get around the blade impact problem is done by introducing a first modification on the simple Rankine Cycle. A super-heater is installed at the exit of the steam generator in order to superheat the saturated vapor to higher temperatures T_5 as

seen in *Figure II.7*a. The super-heater is an additional heat exchanger integrated to the steam generator.

The T-s diagram is shown in *Figure II.7*b. Clearly, by heating up the working fluid to higher temperatures, a higher thermal efficiency and specific power will also be obtained without any additional increase in the working pressure. However, there is an additional cost of the steam superheating installation.

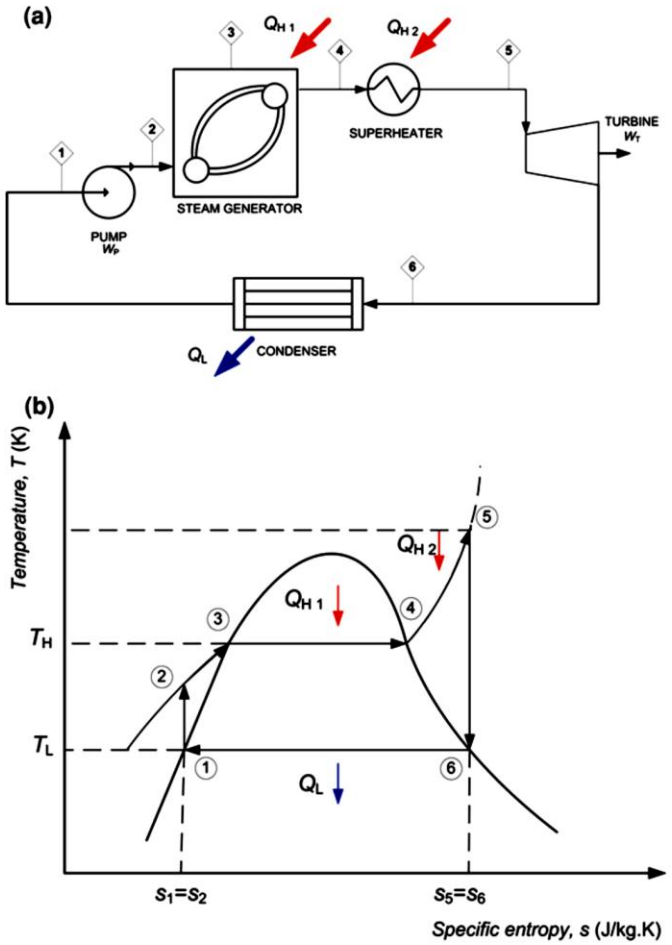

Figure II.7. a- four basic components of a ideal Rankine cycle with vapor superheating;

b- temperature-specific entropy diagram

During the vaporization process of water, the substance is a mixture of saturated liquid and saturated vapor. Quality x is defined to describe the fraction of saturated vapor in the mixture.

$$x = \frac{m_{vapor}}{m_{total}} \tag{27}$$

Quality has a value between 0 and 1. x equals 1 for saturated vapor and x equals 0 for saturated liquid according to its definition.

A saturated mixture is a two-phase system. For convenience, it can be treated as a homogenous mixture and the properties of this mixture are simply the average properties of the saturated liquid and saturated vapor. At truly constant temperature [8]:.

$$x = \frac{s - s_f}{s_{fg}} = \frac{h - h_f}{h_{fg}} \tag{28}$$

II.2.2 Working fluid

With the exception of a few specialized applications, the working fluid predominantly used in vapor power cycles is water. Water is the best working fluid presently available, but it is far from being the ideal one. The binary cycle is an attempt to overcome some of the shortcomings of water and to approach the ideal working fluid by using two fluids. Let us list the characteristics of a working fluid most suitable for vapor power cycles:

1. A high critical temperature and a safe maximum pressure. A critical temperature above the metallurgically allowed maximum temperature (about 620°C) makes it possible to transfer a considerable portion of the heat isothermally at the maximum temperature as the fluid changes phase. This makes the cycle approach the Carnot cycle. Very high pressures at the maximum temperature are undesirable because they create material-strength problems.
2. Low triple-point temperature. A triple-point temperature below the temperature of the cooling medium prevents any solidification problems.
3. A condenser pressure that is not too low. Condensers usually operate below atmospheric pressure. Pressures well below the atmospheric pressure create air-leakage problems. Therefore, a substance whose saturation pressure at the ambient temperature is too low is not a good candidate.
4. A high enthalpy of vaporization h_{fg} so that heat transfer to the working fluid is nearly isothermal (is needed to reduce mass flow rate and equipment size).
5. A saturation dome that resembles an inverted U. This eliminates the formation of excessive moisture in the turbine and the need for reheating.
6. Good heat transfer characteristics (high thermal conductivity).
7. Low viscosity to reduce pressure drop.

8. Other properties such as being inert, inexpensive, readily available, and nontoxic.

No fluid possesses all these characteristics. Water comes the closest, although it does not fare well with respect to characteristics 1, 3, and 5. We can cope with its sub-atmospheric condenser pressure by careful sealing, and with the inverted V-shaped saturation dome by reheating, but there is not much we can do about item 1. Water has a low critical temperature (374°C, well below the metallurgical limit) and very high saturation pressures at high temperatures ($16.5\ MPa$ at 350°C).

II.3. Heat Recovery Steam Generator (HRSG)

The HRSG forms a major part of the steam system. In the combined-cycle mode, the efficiency of the combined gas-turbine + HRSG system can reach $55 - \ 60\%$ (LHV basis) with the current advanced machines, while in the cogeneration mode, system efficiency can be as high as $75 - 85\%$.

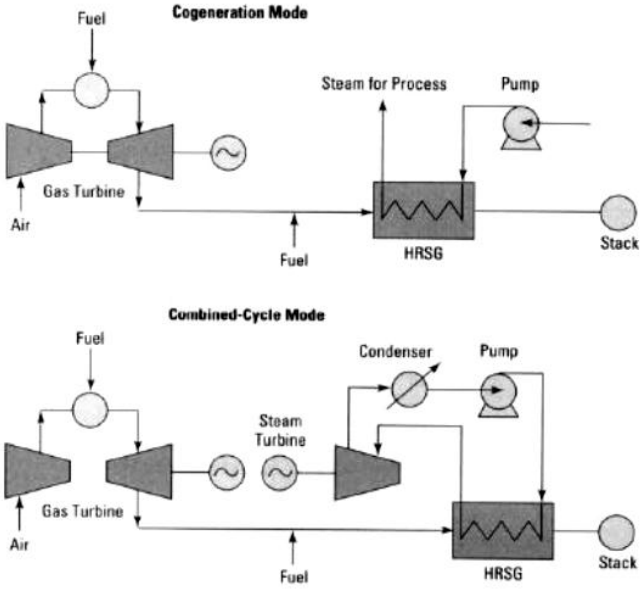

Figure II.8. Configurations of the combined-cycle and cogeneration modes

Recent trends in HRSG design include multiple-pressure units for maximum energy recovery, the use of high temperature superheaters or reheaters in combined cycle plants, and auxiliary firing for efficient steam generation. In addition, furnace firing is often employed in small capacity units when the exhaust gas is raised to temperatures of $2{,}400 - \ 3{,}000°F$ to maximize steam generation and thus improve fuel utilization [3].

II.3.1. Types of heat recovery steam generators

There are basically three types of heat recovery steam generators [3][11]:

II.3.1.1. Natural circulation HRSG

- Typically horizontal gas flow and vertical tubes
- Tube bundles typically grow thermally down
- For gas turbines less than $50\ MW$, evaporator is shipped to site in single unit
- For larger gas turbines the evaporator is shipped in multiple sections

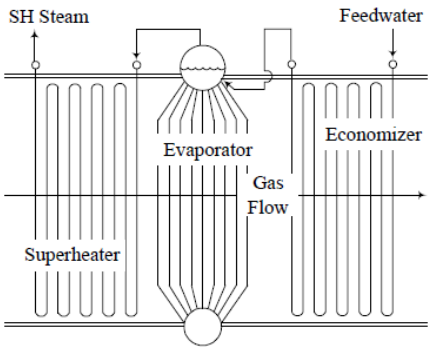

Figure II.9. Natural Circulation HRSG

II.3.1.2. Forced circulation HRSG

- Typically vertical gas flow and horizontal tubes.
- Steam/water mixture circulation through evaporator tubes and to/from drum with a pump.

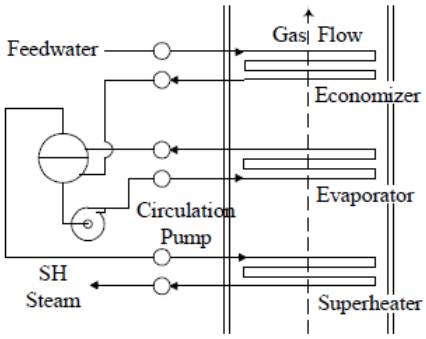

Figure II.10. Forced Circulation HRSG

II.3.1.2. Once through HRSG

- Typically vertical gas flow and horizontal tubes
- OTSGs eliminate the need for steam drums
- Phase change from water to steam is free to move throughout the bundle

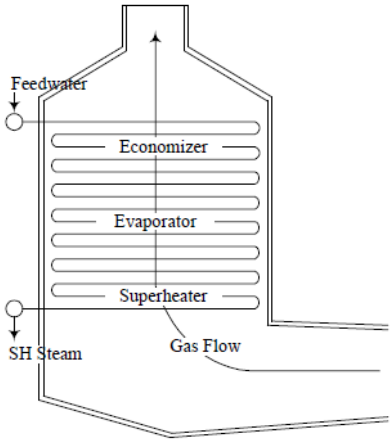

Figure II.11.: Once through HRSG

II.3.2. Heat recovery steam generator components

In a single-pressure HRSG, the heat recovery from gas turbine exhaust is normally done in 3 steps [5].

II.3.2.1. The evaporator

- Vaporize water and produce steam
- Water/steam circulates from lower drum to steam drum
- Steam exits from the steam drum after passing through steam separating equipment
- Water level must be carefully maintained

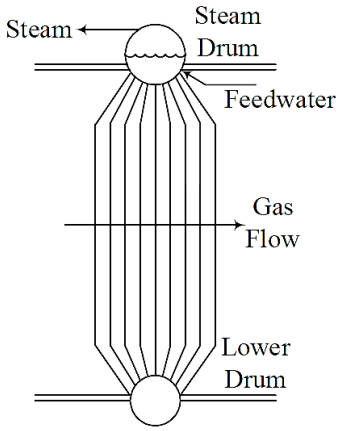

Figure II.12. Evaporator of single-pressure HRSG

II.3.2.2. The economizer

- Preheats water prior to entry into the steam drum
- Desirable to prevent steam from forming in the economizer

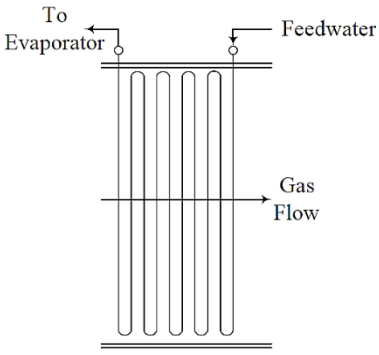

Figure II.13. Economizer of single-pressure HRSG

II.3.2.3. The superheater

- Saturated steam from evaporator is sent to superheater to produce dry steam
- Dry steam is required for steam turbines

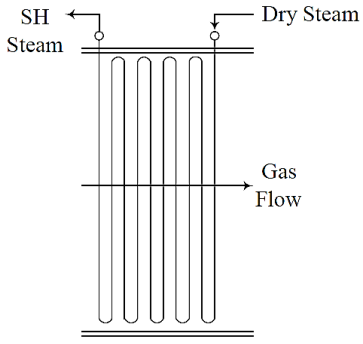

Figure II.14. Superheater of single-pressure HRSG

II.3.3. HRSG temperature profiles and steam generation

The starting point in the engineering of a HRSG is the evaluation of its steam generation capability and gas and steam temperature profiles. For a conventional fired steam generator, one can assume a desired steam flow rate and exit gas temperature and then fire the necessary amount of fuel to meet the steam demand. A HRSG behaves differently due to the low inlet gas temperature ($482 - 565°F$ in the unfired mode) and the large gas/steam ratio. Arbitrarily assuming an exit gas temperature or steam generation rate can lead to "temperature cross situations" or pinching.

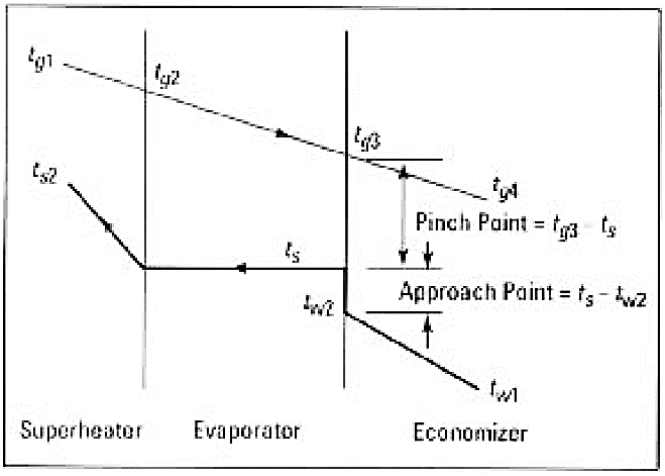

Figure II.15. Temperatures profiles in the HRSG.

Figure II.17 shows the typical gas and steam temperature profiles in a HRSG consisting of a superheater, evaporator, and economizer operating at a single pressure. Because of the low gas temperature entering the HRSG, the steam generation will also be lower than in conventional steam generators for the same gas flow [3][4].

In conventional steam generators the adiabatic combustion temperature of the fuels used start out at $1760°C$ or so. Hence, the economizer duty in the HRSG will also be low, leading to a high exit gas temperature. Also (again unlike in a conventional steam generator), the effect of steam pressure is significant, the higher the steam pressure, the higher the exit gas temperature from the evaporator and the lower the steam generation rate, leading to a smaller duty in the economizer and a higher exit gas temperature. This is the reason for considering multiple pressure units, as well as deaeration steam coils and condensate heaters in HRSGs operating at high pressures [3].

Two variables that directly affect steam production and the gas and steam temperature profiles are the pinch point and the approach point *Figure II.15*. The pinch point is the difference between the gas

temperature leaving the evaporator and the temperature of saturated steam. The approach point is the difference between the temperature of saturated steam and the temperature of the water entering the evaporator. The pinch and approach points for unfired HRSGs are usually in the range of $5°C$ to $15°C$. (If one specifically wants to generate less steam, such as in a multiple-pressure HRSG generating more low-pressure steam than high-pressure steam, then a larger pinch and approach may be used).

Pinch and approach points are selected for a particular case or exhaust gas condition called the "design case." Unlike in a conventional steam generator, where the steam demand drives the design case, in a HRSG steam production is affected by the conditions of the exhaust gas leaving the gas turbine [3][9]. Once selected, the pinch and approach points will vary if gas flow and exhaust gas temperature vary. These cases are called "off-design" cases. For example, at different ambient conditions and gas turbine loads, one can have different exhaust gas parameters, or one may have to burn auxiliary fuel to generate a desired quantity of steam. There is only one design case, but several off-design cases.

Prudent engineering calls for the pinch and approach points to be established in the unfired mode rather than in the fired mode, for several reasons [3]:

1. Designs that can be physically and economically shipped can be established if pinch and approach points are chosen in the range suggested in the unfired mode at the design ambient conditions.
2. A HRSG simulation approach is required to evaluate the pinch and approach points at fired conditions or at different ambient conditions. If the pinch and approach were selected in the fired mode (which is not recommended), it is likely that the pinch point in the unfired mode could be too low, resulting in a huge, unwieldy, and uneconomical HRSG. Also, a low approach point in the fired mode could result in steaming in the economizer under unfired conditions.
3. If a superheater is used, it is not possible to estimate the degree of oversizing if the pinch and approach are selected in the fired mode. If the steam temperature is to be maintained over a wide load range, it is likely that the steam temperature will be lower than desired under unfired conditions. If pinch and approach points along with the desired steam temperature are selected in the unfired mode, then the steam temperature can certainly be maintained under fired conditions and can be controlled using steam attemperation or other means.

II.3.4. Heat transfer diagram and heat balances

The three steps of heat recovery in the HRSG can be illustrated in a temperature-heat transfer diagram Figure II.16. The aim of such a diagram is to facilitate analysis of different parameters in the HRSG. The upper line illustrates the cooling of exhaust gas from inlet to outlet in the HRSG. The lower line illustrates the water to steam process, where evaporation takes place at constant temperature. The area between the exhaust profile and the water profile is a measure of the heat loss in the HRSG, and consequently in the power produced.

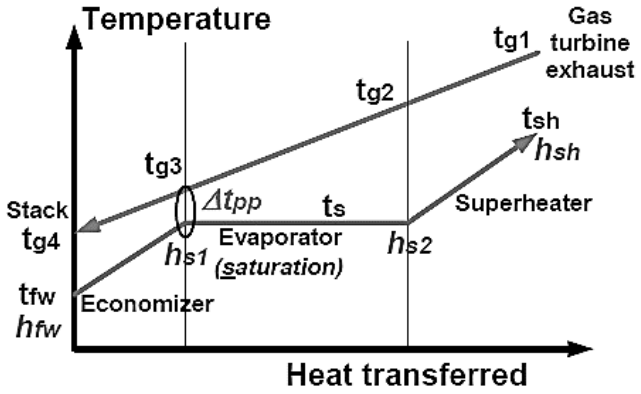

Figure II.16. Heat transfer diagram of HRSG.

Different parameters of importance for analyzing the combined cycle are found through heat balances in the HRSG. The larger the temperature difference between the two media, the lower the effectiveness of the heat exchange, and thus less heat is recovered. The lower the heat recovery (and thus effectiveness), the higher the exit temperature of the cooled medium.

II.3.4.1. Pinch point temperature difference

The pinch point temperature difference ΔT_{pp} is the difference between the temperature of exhaust exiting the evaporator T_{g3} and the temperature of water evaporation T_s

$$\Delta T_{pp} = T_{g3} - T_s \tag{29}$$

The water evaporation takes place at constant temperature (isothermal process) at the saturation pressure prevailing in the drum. Without considering pressure losses in the water-steam tubes, the pressure in the boiler drum equals the pressure after the feed-water pump.

II.3.4.2. Heat balances in the HRSG

From this section and on the approach point is not considered. The heat recovered from the flue gas can be balanced both from the exhaust side viewpoint and from the water profile viewpoint according to [4][9][10]:

Gas side

$$\dot{Q}_{recovered} = \dot{m}_g . \overline{Cp}_g . \left(T_{g1} - T_{g4}\right) \quad (30)$$

Steam side

$$\dot{Q}_{recovered} = \dot{m}_v . \left(h_{sh} - h_{fw}\right) \quad (31)$$

Heat balances for each component in the HRSG are as follows (without the economizer approach temperature):

Economizer:

$$\dot{m}_g . \overline{Cp}_g . \left(T_{g3} - T_{g4}\right) = \dot{m}_v . \left(h_{s1} - h_{fw}\right) \quad (32)$$

Evaporator:

$$\dot{m}_g . \overline{Cp}_g . \left(T_{g2} - T_{g3}\right) = \dot{m}_v . \left(h_{s2} - h_{s1}\right) \quad (33)$$

Superheater:

$$\dot{m}_g . \overline{Cp}_g . \left(T_{g1} - T_{g2}\right) = \dot{m}_v . \left(h_{sh} - h_{s2}\right) \quad (34)$$

The specific heat $\overline{Cp}_g$, is temperature dependent and thus taken as an integrated average value between the two gas temperatures.

The enthalpies h_{s1} and h_{s2} are found in water-steam saturation tables for the pressure prevailing in the boiler drum. Without consideration of pressure losses, the drum pressure equals the steam turbine inlet pressure.

.

Thus, by combining Eqs.(33) and (34), a very convenient heat balance is obtained (as shown in *Figure II.17*):

$$\dot{m}_g . \overline{Cp}_g . \left(T_{g1} - T_{g3}\right) = \dot{m}_v . \left(h_{sh} - h_{s1}\right) \quad (35)$$

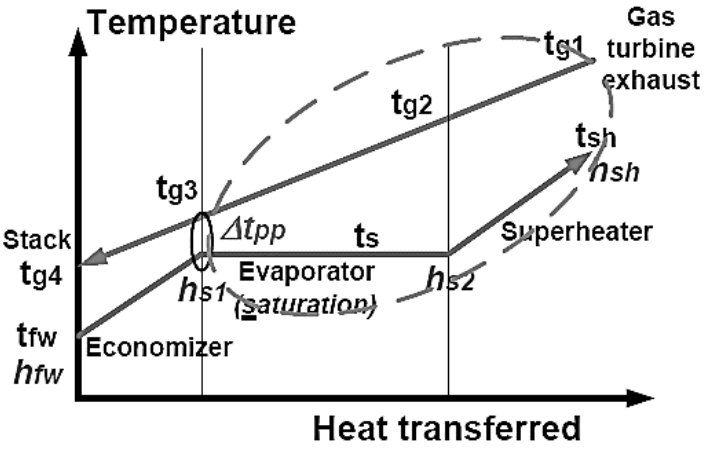

Figure II.17 Evaporator + Superheater system heat balance

Also, another parameter that should be introduced, is the ratio of the steam flow rate to the hot gases flow rate. Such parameter shows the capability of hot gases to produce steam, this ratio is usually referred as Y, and it is defined as [7][8]:

$$Y = \frac{\dot{m}_v}{\dot{m}_g} \tag{36}$$

It is also important to note that the lower pressure should be low, say, $25\ to\ 100\ kPa$, so that water vaporization can take place with low value exhaust heat. Water at $100\ kPa$ boils at $99.63°C$. The higher pressure should be relatively high, say, $80\ bars$, this will create high pressure difference that will drives steam through the turbine with high velocity, so he steam turbine power is maximized.

II.4. The Combined-Cycle

The continued quest for higher thermal efficiencies has resulted in rather innovative modifications to conventional power plants. The binary vapor cycle. A more popular modification involves a gas power cycle topping a vapor power cycle, which is called the combined gas–vapor cycle, or just the combined cycle. The combined cycle of greatest interest is the gas-turbine (Brayton) cycle topping a steam-turbine (Rankine) cycle, which has a higher thermal efficiency than either of the cycles executed individually.

Gas-turbine cycles typically operate at considerably higher temperatures than steam cycles. The maximum fluid temperature at the turbine inlet is about $620°\text{C}$ for modern steam power plants, but over $1425°\text{C}$ for gas-turbine power plants. It is over $1500°\text{C}$ at the burner exit of turbojet engines. The use of higher temperatures in gas turbines is made possible by recent developments in cooling

the turbine blades and coating the blades with high-temperature-resistant materials such as ceramics. Because of the higher average temperature at which heat is supplied, gas-turbine cycles have a greater potential for higher thermal efficiencies. However, the gas-turbine cycles have one inherent disadvantage, the gas leaves the gas turbine at very high temperatures (usually above $500°C$) depending on the pressure ratio, which limits any potential gains in thermal efficiency. The efficiency can be improved somewhat by using regeneration for low pressure ratios, but the improvement is limited. It makes engineering sense to take advantage of the very desirable characteristics of the gas-turbine cycle at high temperatures and to use the high temperature exhaust gases as the energy source for the bottoming cycle such as a steam power cycle. The result is a combined gas–steam cycle, as shown in *Figure II.18.* In this cycle, energy is recovered from the exhaust gases by transferring it to the steam in a heat exchanger that serves as the boiler. In general, more than one gas turbine is needed to supply sufficient heat to the steam turbine without additional firing. Also, the steam cycle may involve regeneration as well as reheating, but usually does not.

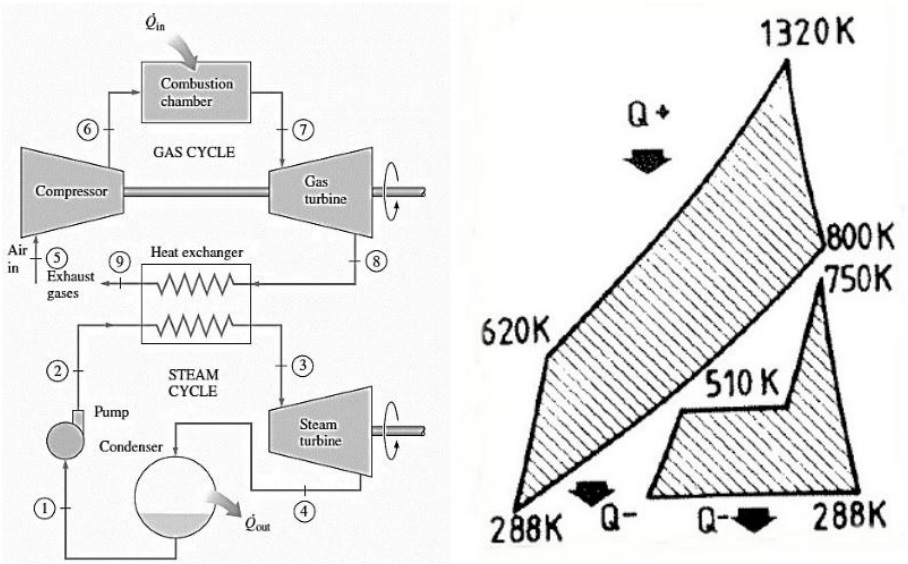

Figure II.18 Gas power cycle topping a vapor power cycle [2].

A gas turbine cycle is depicted symbolically in *Figure II.24*. As demonstrate earlier, the efficiency of the gas turbine is given by:

$$\eta_{GT} = \frac{\dot{W}_{net}}{\dot{Q}_H} = \frac{\dot{W}_{gt}}{\dot{Q}_h} \tag{37}$$

Where $\dot{Q}_h$ is the energy input from the high-temperature source at temperature T_h, and $\dot{W}_{gt}$ is the power output delivered to an electric generator. By energy conservation, the rate of energy transfer to the lower-temperature reservoir at the exhaust temperature T_{ex} is [2].

$$\dot{Q}_{ex} = \dot{Q}_h - \dot{W}_{gt} \tag{38}$$

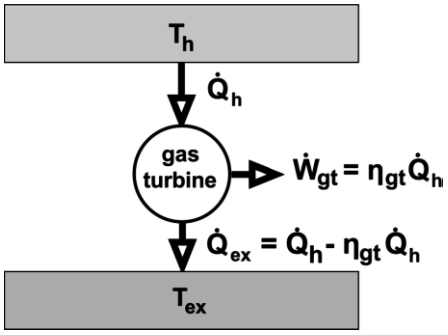

Figure II.19 Gas turbine cycle, which receives energy at rate $\dot{Q}_h$ from a source at temperature T_h, converts $\dot{W}_{gt} = \eta_{GT}.\dot{Q}_h$ to useful work and sends its "waste" energy at temperature T_{ex}, at rate $\dot{Q}_{ex} = \dot{Q}_h - \dot{W}_{gt}$ to steam turbine cycle.

Adrian Bejan [12] cites various sources of irreversibility that plague gas turbines and explains how clever engineering designs, entailing regenerative heat exchangers, reheaters, and intercoolers, can bring higher efficiencies. However, even greater efficiency gains are possible for electricity generation by using the high-temperature exhaust of the gas turbine to power a steam cycle. For example, a gas turbine with inlet and exhaust temperatures $1673\ K$ and $873K$, respectively, might use the exhaust gases to heat a steam turbine that has exit temperature $350K$, achieving the overall temperature range, $1673\ K -> \ 350\ K$.A single gas turbine cycle cannot match this.

In this regard, Bejan writes "…gas-turbine cycles are better suited for efficient operation at high temperatures than steam-turbine cycles. On the other hand, the steam-turbine cycle is more attractive from the point of view of minimizing the temperature gap between the cold end of the cycle and the low-temperature reservoir… The engineering challenge that remains is to mesh optimally the two cycles along that range of intermediate temperatures where the upper cycle must act as a heat source for the lower one." [12] The bottom line is that existing combined cycles are more efficient than any currently achievable single cycle.

In the simplest combined-cycle design, the gas turbine drives one electric generator and the steam turbine runs another. Ignoring losses in the heat exchanger, the inlet temperature to the steam turbine is T_{ex}. Combining Eq.(37) and Eq.(38), the "waste" energy rate [2].

$$\dot{Q}_{ex} = \dot{Q}_h - \eta_{GT}.\dot{Q}_h \tag{39}$$

In the exhaust gases becomes the input power for the steam turbine cycle, whose efficiency we call η_{ST} [1][8]:

$$\eta_{ST} = \frac{\dot{W}_{net}}{\dot{Q}_H} = \frac{\dot{W}_{st}}{\dot{Q}_{ex}} \tag{40}$$

Thus, the power output delivered by the steam turbine

$$\dot{W}_{st} = \eta_{ST}.\dot{Q}_{ex} = \eta_{ST}.\left(\dot{Q}_h - \eta_{GT}.\dot{Q}_h\right) \tag{41}$$

Combining Eqs.(37),(41), the total power delivered by the gas and steam turbine combination (combined-cycle) is [8]

$$\dot{W}_{tot} = \dot{W}_{gt} + \dot{W}_{st} = [\eta_{GT} + \eta_{ST}.(1 - \eta_{GT})].\dot{Q}_h \tag{42}$$

and the combined-cycle efficiency is

$$\eta_{CC} = \frac{\dot{W}_{tot}}{\dot{Q}_h} \tag{43}$$

So that and with consideration of the HRSG effectiveness ε, [8]:

$$\eta_{CC} = \eta_{GT} + \varepsilon.(1 - \eta_{GT}).\eta_{ST} \tag{44}$$

Typically, with a steam turbine efficiency of 0.40, a gas turbine efficiency of 0.37 and an 85% HRSG effectiveness, the combined-cycle efficiency is $\eta_{CC} = 0{,}584$.

II.5. The Solar Field

II.5.1. Heat transfer fluid

Common operating fluids may be either synthetic oil, molten salt, pressurized steam or air. Operating temperatures of the technologies using synthetic oil as heat transfer fluid (HTF) are limited to 400°C. Molten salt, usually a mixture of nitrate salts, is used in concentrated solar thermal systems because it is a liquid at atmospheric pressure and temperature higher than $800\ K$.

The operating temperatures are similar with usual steam turbines and it is non-flammable and non-toxic. The typical composition of the molten salts is 60% by weight of Sodium Nitrate ($NaNO_3$) and 40% by weight of Potassium Nitrate (KNO_3). The melting point is of the nitrate salts of 221°C.Currently the operating temperatures are up to 600°C. Operating temperatures of 700°C to 800°C can be reached with liquid fluoride salts.

Further research on materials and techniques has to be done for commercial use. Pressurized steam or air as working medium at very high temperatures allows gas or steam turbines to be powered directly without a heat exchanger which improves its efficiency. Also with these fluids further development and improvement are required.
A HTF has to fulfil certain requirements:

- High evaporation temperature
- Low freezing temperature
- Thermal stability
- High heat capacity
- High heat conductivity
- Low viscosity
- Low Investment cost
- Availability
- Environmental compatibility
- Low inflammability
- Low explosivity

Some criteria are more important than others. Evaporation temperature and thermal stability, for instance, are very important criteria because they determine the maximum steam cycle temperature, which on its part determines the power block efficiency. Low inflammability, on the contrary, is not always considered a decisive selection criterion (Table II.1 shows most common HTFs criteria).

Table II.1 Important properties of common HTFs

Medium	Max Temperature (°C)	Heat Capacity $(J/kg.K)$	Heat Conductivity $(W/m.K)$	Vol. Spez. Heat Capacity $(kWh/m^3.K)$	Cost
Mineral Oil	300	2600	0.12	0.55	+
Synthetic Oil	400	2300	0.11	0.57	-
Silicon Oil	400	2100	0.1	0.525	-
Nitride Salt	450	1500	0.5	0.75	o
Nitrate Salt	565	1600	0.5	0.8	+
Carbonate Salt	850	1800	2.0	1.05	-
Sodium (Liquid)	850	1300	71.0	0.3	o
+ Low		- High		o Moderate	

The importance of the different criteria also depends on the system configuration. For instance, if the power plant contains a thermal storage, then it could be an advantage to use the HTF also as storage medium because this means that no additional heat transfer step between HTF and storage medium is required. In this case, when very large quantities of the HTF are needed, economic criteria may be more important than in other cases [17].

II.5.2. Solar energy conversion

II.5.2.1. The Carnot cycle

On studying heat engines and thermal machines, one is faced with a question very relevant: Given two sources of thermal energy at two different temperatures, one at a high temperature T_h and the other at a low temperature T_l, what is the maximum conversion of heat drawn from the source at high temperature that can be converted into useful work in an ideal heat engine (reversible one) that operates continuously in a closed thermodynamic cycle? First, the Kelvin-Planck statement of the Second Law of Thermodynamics tells us that it is impossible to have a heat engine that will convert all the heat received from the high temperature source, Q_H, into useful work in a thermodynamic cycle. It is necessary to reject part of the received heat to the low temperature source Q_L. In other words, it is impossible to have a 100% efficiency heat engine [1][12][25]. A schematic of an operating heat engine according to Kelvin-Planck is shown in *Figure II.20*a.

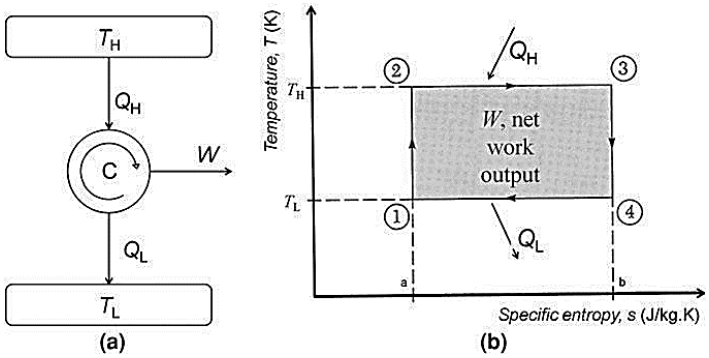

Figure II.20 a Schematics of a heat engine; b T-s diagram for a Carnot cycle

Second, Carnot devised that the heat engine that can achieve the maximum efficiency in continuously converting heat into work operating between the two heat sources is the one made up of four reversible processes as illustrated in the temperature-entropy diagram in *Figure II.20*b, which are [1]:

1. Process 1–2: temperature raise from T_l to T_h in an adiabatic reversible process (isentropic).
2. Process 2–3: heat addition, Q_H, in an isothermal reversible process at T_h.
3. Process 3–4: temperature decrease from T_h to T_l in an adiabatic reversible process (isentropic).
4. Process 4–1: heat rejection, Q_L, in an isothermal reversible process at T_l. The thermal efficiency of any power cycle η_{th}; is the ratio of the network W, and the heat received Q_H.

$$\eta_{th} = \frac{W}{Q_H} = \frac{Q_H - Q_L}{Q_H} = 1 - \frac{Q_L}{Q_H} \tag{45}$$

With $Q_H = T_h.\Delta s$ and $Q_L = T_l.\Delta s$, one obtains the final form of the Carnot efficiency η_{Carnot} which is:

$$\eta_{Carnot} = 1 - \frac{T_l}{T_h} \tag{46}$$

This remarkable result shows that the maximum conversion of heat into work in heat engine operating continuously between two heat sources is limited by the ratio between the two heat sources temperatures. The lower the temperature ratio, the higher the Carnot efficiency. As a final remark, no 100% conversion can take place because it would require either a $0\ K$ low temperature source, or an extremely high temperature source (mathematically, an infinite one), or both. However, it must be understood that T_l and $T_h$are the fluid, not the source, temperatures, for otherwise the Carnot cycle will convert zero power [8].

II.5.2.2. The solar heat flux and balance in the HRSG

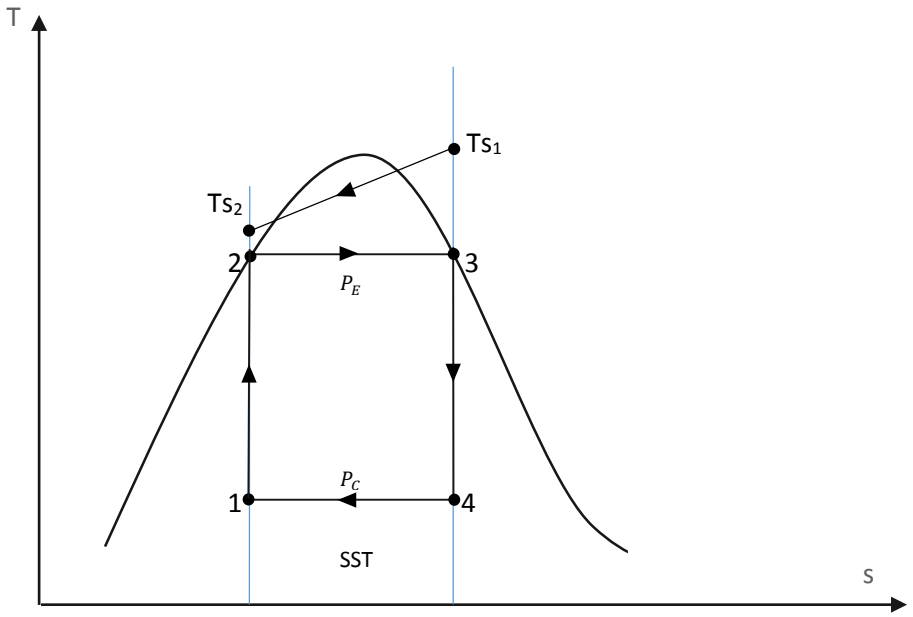

FigureII.21 Heat exchange between the heat transfer fluid and the steam cycle in solar steam generator

The heat recovered from the hot oil, trough the evaporator can be defined by the following equation

$$\dot{Q}_{Srec} = \dot{m}_h . \overline{Cp}_h . (T_{s1} - T_{s2}) \quad (47)$$

Where $\dot{m}_h$is the hot oil flow rate, and $\overline{Cp}_h$ is the specific heat capacity of oil.

The net work of the solar field $\dot{W}_S$ is obtained by the following equation

$$\dot{W}_S = \eta_{Carnot} . \eta_T . \dot{Q}_{Srec} \quad (48)$$

Where, η_T is the turbine efficiency and η_{Carnot} is the Carnot cycle efficiency.

Combining the two Eqs.(47) and (48) we obtain:

$$\dot{W}_S = \eta_{Carnot} . \eta_T . \left(\dot{m}_h . \overline{Cp}_h . (T_{s1} - T_{s2})\right) \quad (49)$$

II.6. Conclusion

All the thermodynamic concepts and equations presented in this chapter, are important to carry out with the next chapter; In order to analyze and evaluate the performance of the SPP1 power plant (Hassi R'mel).

Chapter III

Performance Analysis of SSP1

III.1. Operating of SPP1 Solar Hybrid Power Plant

This power plant is located near the Hassi R'Mel natural gas field and its production center. It is connected to national electrical grid. The following information is obtained courtesy of M. TRAD.

Two gas-turbines each coupled to a generator, produce electricity from the combustion of natural gas, the energy contained in the exhaust gas of the gas-turbine is recovered at temperature of 544°C and pressure of $0.95\ bar$ through the HRSG which generate the cycle's steam. The steam produced at pressure of $83\ bars$, runs the steam-turbine that rotate a third generator. In the output of the steam-turbine, the steam is condensed in an air-cooled condenser to be re-injected in the water-steam circuit at the pressure of $83\ bars$.

During sunny periods (operating parameters meet: direct normal irradiation and eligible wind velocity), the solar field contribute to the functioning of the power plant by participating in the steam production.

A heat transfer fluid is heated through tubular receptors by concentrating solar radiation to reach a temperature of 393°C at a pressure of $14\ bars$. The gained heat is used to participate in the production of steam at a temperature of 372°C and a pressure of $87.2\ bars$ by a heat exchange oil-water in a steam generator. This steam is injected into the HRSG.

During sunny periods, the power plant operates in the hybrid cycle (ST-GT-Solar field). Therefore the solar field helps reduce the gas consumption.

During non-sunny periods, the solar field does not intervene in the functioning of the power plant thus the solar field contribution is replaced by an addition in the gas consumption in the burners of the HRSG

The power unit has two identical gas-turbines $47MW$ and one steam-turbine $80MW$ that operates in conventional combined-cycle, which is hybridized with a solar-field that contribute with $25MW$ injected at a suitable temperature level.

Figure III.1 shows an approximate schematic scheme of the SPP1 based on these information.

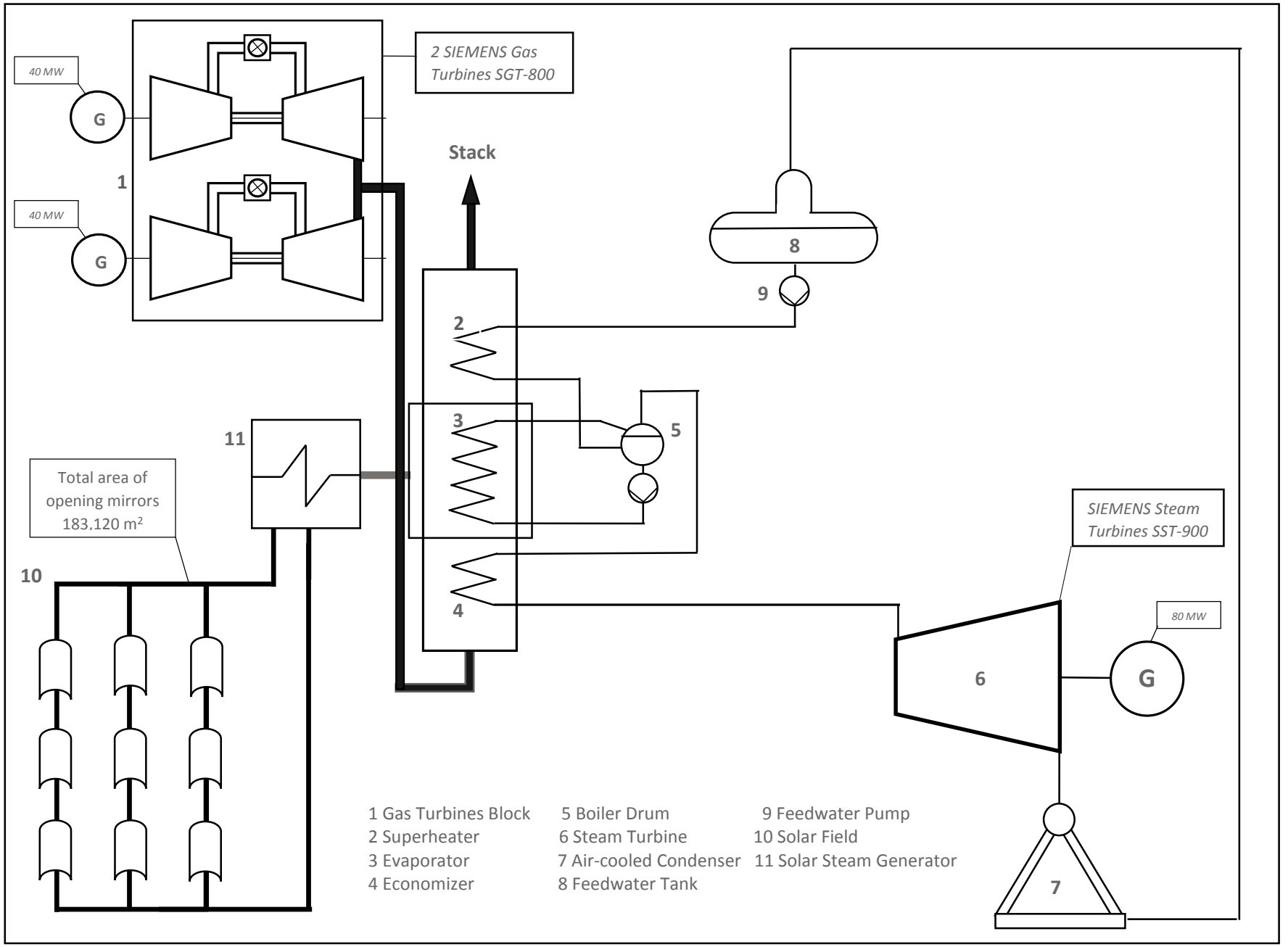

Figure III.1 The Intergrated Solar Combined-Cycle of SPP1

III.2. Objectives

The objectives of this chapter are as follow:

1- Calculations of the gas turbine power cycle.
2- Calculations of the steam turbine power cycle with four different condensation temperatures.
3- Calculations of the combined-cycle with the results of the previous four steam turbine power cycles.
4- Calculations of the solar field.
5- Calculation of the economization of natural gas consumption.
6- Analysis of the gas turbine performance.
7- Analysis and discussion of the impact of the condensation temperature on the steam turbine, combined-cycle and the solar field.

III.3. Calculations

III.3.1. Gas turbine calculations

The air at ambient temperature enters the chiller for the cooling process (1'-1), then enters the compressor at 15^{o}C. The burnt gases leave the turbine at temperature of 544^{o}C (as illustrated in *Figure III.2*). We assume a perfect gas behavior.

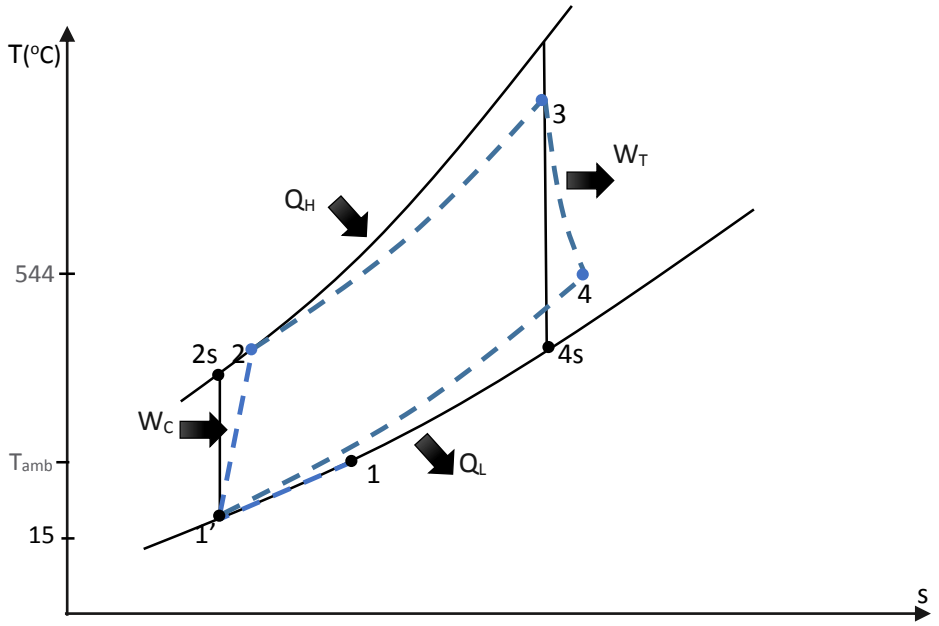

Figure III.2: Temperature-Entropy diagram of the gas turbine cycle

The compressor inlet state (state1) is fixed,

$P_1 = 1{,}0131\ bar$

$T_1 = 15^{o}\text{C} = 288\ K$

The turbine outlet state (state4) is fixed,

$P_4 = 0{,}95\ bar$

$T_4 = 544^{o}\text{C} = 817\ K$

Since the compressor and the turbine efficiencies are not known, it's up to us to assume them.

$\eta_C = 0{,}95,\ \eta_T = 0{,}85$

Compressor compression ration $r = 19$ (Appendix-A).

We consider the compressor first

Control volume: Compressor

Inlet state: P_1, T_1 known, fixed state.

Exit state: P_2 known.

The first law gives Eq.(3)

$$w_C = h_2 - h_1 = Cp.(T_2 - T_1)$$

Using Eq.(10) we get:

$$P_2 = r.P_1 = 19.(1{,}0131) = 19{,}25\ bar$$

For air $\gamma = 1{,}4$ so:

$$\frac{\gamma - 1}{\gamma} = 0{,}286$$

And the second law gives (isentropic process)

$$s_2 = s_1$$

By Eq.(9) and solving for T_{2s} we get

$$T_{2s} = T_{1.}\left(\frac{P_2}{P_1}\right)^{\frac{\gamma-1}{\gamma}}$$

$T_{2s} = 668{,}5\ K$

Using Eq.(15) we get

$$\eta_C = \frac{h_{2s} - h_1}{h_2 - h_1} = \frac{T_{2s} - T_1}{T_2 - T_1} = 0{,}95$$

Solving for T_2

$$T_2 = \frac{T_{2s} - T_1}{\eta_C} + T_1$$

$$T_2 = \frac{668{,}5 - 288}{0{,}95} + 288 = 688{,}52\ K$$

Therefore,

$$w_C = 1{,}004.(688{,}52 - 288) = 402{,}12\ kJ/kg$$

Then the total compressor work is obtained by the Eq.(6)

$$\dot{W}_C = \dot{m}.w_C = 131{,}5.(424{,}46\ ) = 52878{,}78\ kW$$

Considering the turbine next,

Control volume: Turbine

Inlet state: P_3 known.

Exit state: $P_4,\ T_4$ known, fixed state.

The first law gives Eq.(4)

$$w_T = h_3 - h_4$$

Using Eq.(10) we get:

$$P_3 = r.P_4 = 19.(0{,}95) = 18{,}05\ bar$$

Comparing the pressure at the combustion chamber inlet P_2 and at the exit P_3 we see some pressure loss ΔP_{loss}

$$\Delta P_{loss} = P_3 - P_2 = -18{,}05 - 19{,}25 = -1{,}2\ bar$$

The second law gives (isentropic process)

$$s_2 = s_1$$

From Eq.(9) we solve for T_3

$$T_3 = T_{4s}.\left(\frac{P_3}{P_4}\right)^{\frac{\gamma-1}{\gamma}}$$

Using Eq.(14) we have

$$\eta_T = \frac{h_3 - h_4}{h_3 - h_{4s}} = \frac{T_3 - T_4}{T_3 - T_{4s}} = 0{,}85$$

We solve for T_{4s} we get

$$T_{4s} = T_3 - \frac{T_3 - T_4}{\eta_T}$$

We replace $T_{4s}$by its expression we get:

$$T_3 = \left(T_3 - \frac{T_3 - T_4}{\eta_T}\right).\left(\frac{P_3}{P_4}\right)^{\frac{\gamma-1}{\gamma}}$$

$$T_3 = \left(T_3.\left(1 - \frac{1}{\eta_T}\right) + \frac{T_4}{\eta_T}\right).\left(\frac{P_3}{P_4}\right)^{\frac{\gamma-1}{\gamma}}$$

$$T_3 = T_3.\left(1 - \frac{1}{\eta_T}\right).\left(\frac{P_3}{P_4}\right)^{\frac{\gamma-1}{\gamma}} + \frac{T_4}{\eta_T}.\left(\frac{P_3}{P_4}\right)^{\frac{\gamma-1}{\gamma}}$$

$$T_3.\left(1 - \left(1 - \frac{1}{\eta_T}\right).\left(\frac{P_3}{P_4}\right)^{\frac{\gamma-1}{\gamma}}\right) = \frac{T_4}{\eta_T}.\left(\frac{P_3}{P_4}\right)^{\frac{\gamma-1}{\gamma}}$$

$$T_3 = \frac{\frac{T_4}{\eta_T}.\left(\frac{P_3}{P_4}\right)^{\frac{\gamma-1}{\gamma}}}{\left(1 - \left(1 - \frac{1}{\eta_T}\right).\left(\frac{P_3}{P_4}\right)^{\frac{\gamma-1}{\gamma}}\right)}$$

Finally,

$$T_3 = \frac{\frac{817}{0{,}85}.(19)^{0{,}286}}{\left(1 - \left(1 - \frac{1}{0{,}85}\right).(19)^{0{,}286}\right)} = 1582{,}7\ K$$

From Eq.(4)

$$w_T = h_3 - h_4 = Cp.(T_3 - T_4) = 1{,}004.(1582{,}77 - 817) = 768{,}84\ kJ/kg$$

Then the total turbine work by Eq.(6)

$$\dot{W}_T = \dot{m}_g.w_T = 131{,}5.(768{,}84) = 101102{,}46\ kW$$

The Cycle net work is obtained by Eq.(5)

$$w = w_T - w_C = 768{,}84 - 402{,}12 = 366{,}72\ kJ/kg$$

$52878{,}78\ kW$ of the turbine work is given to the compressor (the turbine rotates the compressor), what remains is the net power of the gas turbine

$$\dot{W}_{net} = \dot{m}_g.w = \dot{W}_T - \dot{W}_C = 101102{,}46 - 52878{,}78\ = 48223{,}68\ kW \approx 48{,}2\ MW$$

Control volume: High-temperature heat exchanger

Inlet state: State 2 fixed.

Exit state: State 3 fixed.

The first law is Eq.(1)

$$q_H = h_3 - h_2 = Cp.(T_3 - T_2)$$

$$q_H = 1.004.(\ 1582{,}7 - 688{,}52\ ) = 897{,}75\ kJ/kg$$

As for the total heat flux $\dot{Q}_H$ is given by Eq.(6)

$$\dot{Q}_H = \dot{m}_g.q_H = 131{,}5.(897{,}75\ ) = 118054{,}12\ kW$$

Control volume: Low-temperature heat exchanger

Inlet state: State 4 fixed.

Exit state: State 1 fixed.

The first law is Eq.(2)

$$q_L = h_4 - h_1 = Cp.(T_4 - T_1)$$

$$q_L = 1{,}004.(\ 817 - 288\ ) = 531{,}12\ kJ/kg$$

As for the total heat flux $\dot{Q}_L$ is given by Eq.(6)

$$\dot{Q}_L = \dot{m}_g.q_L = 131{,}5.(531{,}12\ ) = 69841{,}75\ kW$$

That leaves us with only the thermal efficiency to determine which is defined in Eq.(11)

$$\eta_{GT} = \frac{\dot{W}_{net}}{\dot{Q}_H} = \frac{48223{,}68}{118054{,}12} = 0{,}408 \approx 40{,}8\%$$

Which is also verified by the Equation

$$\eta_{GT} = \frac{\eta_T \cdot \frac{T_3}{T_1} \cdot \left(1 - \frac{1}{(r)^{\frac{\gamma-1}{\gamma}}}\right) - \frac{1}{\eta_C} \cdot \left((r)^{\frac{\gamma-1}{\gamma}} - 1\right)}{\frac{T_3}{T_1} - \frac{1}{\eta_C} \cdot \left((r)^{\frac{\gamma-1}{\gamma}} - 1\right) - 1}$$

$$\eta_{GT} = \frac{0{,}85 \cdot \frac{1582{,}7}{288} \cdot \left(1 - \frac{1}{(19)^{0{,}286}}\right) - \frac{1}{0{,}95} \cdot ((19)^{0{,}286} - 1)}{\frac{1582{,}7}{288} - \frac{1}{0{,}95} \cdot ((19)^{0{,}286} - 1) - 1} = 0{,}408 = 40{,}8\%$$

III.3.2. Cycle 01: Condensation at $25\ kPa$ (saturation temperature $64,97°C$).

III.3.2.1 The steam turbine calculations

The feed water enters the pump with pressure of $25\ kPa$ (state 1), the pump raises its pressure to $83\ bars$ (state 2') to start the evaporation (process 2'-3), until it becomes saturated steam (state 3), then the steam enters the superheater to raise its temperature (process 3-4). The hot steam drives the turbine and loses its energy (Pressure and temperature), finally the steam leaves the turbine and enters the air-cooled condenser (state 5) to start the condensation (process 5-1).

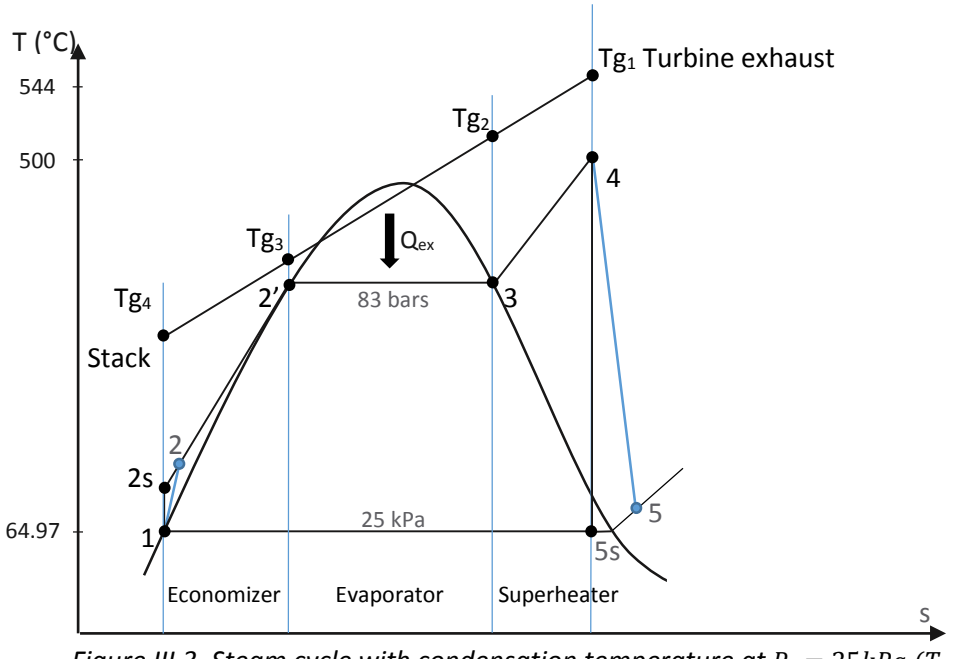

Figure III.3. Steam cycle with condensation temperature at $P_1 = 25kPa$ ($T_{1sat} = 64{,}97°C$)

We have to fully identify all the states of the steam cycle 1-2-2'-3-4-5-1.

State 1:

As we can see in the *Figure III.3*, state 1 represent saturated liquid water at the pressure of $25\ kPa$.

Using the tables of thermodynamic properties *(table A4*), we read the saturation temperature, enthalpy, entropy…etc.

$P_1 = 25kPa.$

$T_1 = 64{,}97\ ^{o}C.$

$h_1 = 271{,}93\ kJ/kg.$

$s_1 = 0{,}8931\ kJ/kg.K.$

State 2:

In order to identify state 2, first we need to calculate the pump work, that raise the water pressure from $25\ kPa$ to $83\ bars$ $(8{,}3\ MPa)$.

Using Eq.(26) and introducing the pump efficiency $\eta_P = 0{,}8$

$$w_p = \frac{1}{\eta_P}.v.(P_2 - P_1) = \frac{1}{0{,}8}.0{,}001020.(8300 - 25)$$

$$w_p = 10{,}55\ kJ/kg$$

Knowing the pump work w_p and h_1 we can determine h_2 trough Eq.(22).

$$h_2 = h_1 + w_p = 282{,}48\ kJ/kg$$

Using the tables of thermodynamic properties for compressed liquid water, we read the temperature T_2 and the entropy s_2.

$P_2 = 8300\ kPa.$

$T_2 = 65{,}84°C$ *(Interpolated value)*

$h_2 = 282{,}48\ kJ/kg.$

$s_2 = 0{,}8979\ kJ/kg.K$ *(Interpolated value)*

State 2':

State 2' is saturated liquid water at the pressure of $83\ bars$.

Using the tables of thermodynamic properties for compressed liquid water, we read the temperature T_2, the enthalpy h_2, and the entropy $s_{2'}$.

The temperature T_2, is not directly readable from the tables, it is necessary to interpolate to determine the correct temperature.

$P_{2'} = 8300\ kPa$ (Saturated liquid water)

$P_{2'_-} = 8000\ kPa \longrightarrow T_{2'_-} = 295{,}01\ ^oC.$

$P_{2'_+} = 9000\ kPa \longrightarrow T_{2'_+} = 303{,}35\ ^oC.$

$$\frac{T_{2'}-T_{2'_-}}{P_{2'}-P_{2'_-}} = \frac{T_{2'_+}-P_{2'_-}}{P_{2'_+}-P_{2'_-}} \longrightarrow T_{2'} = 295{,}01 + (8300 - 8000)\frac{303{,}35-295{,}01}{9000-8000} = 297{,}51\ ^oC.$$

$P_{2'} = 8300\ kPa$

$T_{2'} = 297{,}51\ ^oC$ *(Interpolated value)*

$h_{2'} = 1331{,}005\ kJ/kg$ *(Interpolated value)*

$s_{2'} = 3{,}2313\ kJ/kg.K$ *(Interpolated value)*

State 3:

State 3 is saturated water steam at the pressure of $83\ bars$.

Using the tables of thermodynamic properties for compressed liquid water, we read the temperature T_3 the enthalpy h_3, and the entropy s_3.

$P_3 = P_2 = 8300\ kPa$

$T_3 = T_2 = 297{,}51\ ^oC$

$h_3 = 2753{,}23\ kJ/kg$ *(Interpolated value)*

$s_3 = 5{,}7252\ kJ/kg.K$ *(Interpolated value)*

State 4:

In a real situation, temperature at state 4 is a variable determined by heat transfer calculations on the superheater. These calculations are made concomitantly for the steam generator and the economizer.

Each piece of heat exchanger is governed by three equations and three unknowns. In the situation at hand, we have to guess the value used at the Hassi R'Mel power plant.

Compared to other steam cycles working on combined cycles, the temperature can easily reach 500°C, giving the fact that the difference between the exhaust gases T_{g1} and the temperature of the superheated steam T_4 should be considered. Because if the difference between the two temperatures ΔT is too low, that can lead to a very expensive super-heater.

We suppose $T_4 = 500$°C.

Now that we have two know properties; we can read from the tables of superheated steam the enthalpy h_4, and the entropy s_4.

$P_4 = P_3 = 8300\ kPa$

$T_4 = 500$°C

$h_4 = 3395{,}87\ kJ/kg$ *(Interpolated value)*

$s_4 = 6{,}7075\ kJ/kg.K$ *(Interpolated value)*

State 5:

State 5 is mix of both steam and liquid water, the percentage of steam in the mix determine the quality of the steam that is x_5.

Considering the process from 4 to 5 is an isentropic expansion in the turbine.

The second law of thermodynamic gives:

$$s_4 = s_{5i} = 6{,}7075\ kJ/kg.K$$

By the definition of quality in Eq.(28) we get:

$$x_{5i} = \frac{s_{5i} - s_f}{s_{fg}}$$

Table III.1 Entropy and Enthalpy parameters at the pressure of 25 kPa

Pressure (kPa)	Entropy $(kJ/kg.K)$		Enthalpy (kJ/kg)	
25	s_f	s_{fg}	h_f	h_{fg}
	0,8931	6,9383	271,93	2346,3

$$x_{5i} = \frac{6{,}7075 - 0{,}8931}{6{,}9383} = 0{,}84$$

Now that we have the steam quality x_{5i} it should be easy to determine the enthalpy h_{5i} trough Eq.(28).

$$h_{5i} = h_f + x_5 . h_{fg}$$

$$h_{5i} = 271{,}93 + (0{,}84).2346{,}3 = 2242{,}82\ kJ/kg$$

These properties (entropy, enthalpy and vapor quality) are for an isentropic expansion in the turbine, assuming a turbine isentropic efficiency $\eta_T = 0{,}85$. We get the actual ones:

$$h_5 = h_4 - \eta_T . (h_4 - h_{5i})$$

$$h_5 = 3395{,}87 - 0{,}85.(3395{,}87 - 2242{,}82) = 2415{,}8\ kJ/kg$$

$$x_5 = \frac{2415{,}8 - 271{,}93}{2346{,}3} = 0{,}914$$

$$s_5 = 0{,}8931 + 0{,}914.(6{,}9383) = 7{,}2347\ kJ/kg.K$$

This means $91{,}4\%$ of the mix is steam, the rest is water bulbs. The quality of steam is above $0{,}90$; usually a one lower can cause the turbine performance to drop.

State 5 is fixed,

$P_5 = P_1 = 25\ kPa$

$T_5 = T_1 = 64{,}97\ ^oC$

$h_5 = 2415{,}8\ \ kJ/kg$

$s_5 = 7{,}2347\ kJ/kg.K$

Now that all states are fixed, the following table summarize them.

Table III.2 States of the vapor cycle 01

State	Temperature (^oC)	Pressure (kPa)	Enthalpy (kJ/kg)	Entropy $(kJ/kg.K)$
1	64,97	25	271,93	0,8931
2	65,84	8300	282,48	0,8979
2’	297,51	8300	1331,005	3,2313
3	297,51	8300	2753,23	5,7252
4	500	8300	3395,87	6,7075
5	64,97	25	2415,8	7,2347

III.3.2.2 The heat recovery steam generator calculations

Using the heat balances of evaporator and superheater Eq.(33) and (34) we obtain the following equation as in Eq.(35):

$$\dot{m}_g.\overline{Cp}_g.\left(T_{g1}-T_{g3}\right)=\dot{m}_v.(h_4-h_{2'})$$

$\dot{m}_g$: $Exhaust\ gas\ flow\ rate.$

$\dot{m}_v$: $Steam\ flow\ rate.$

This equation represent the heat balance of the system (evaporator + super-heater).

We solve for $\dot{m}_v$:

$$\dot{m}_v=\frac{\dot{m}_g.\overline{Cp}_g.\left(T_{g1}-T_{g3}\right)}{(h_4-h_{2'})}$$

Now using Eq.(32) to write the energy balance in the economizer.

$$\dot{m}_g.\overline{Cp}_g.\left(T_{g3}-T_{g4}\right)=\dot{m}_v.(h_{2'}-h_2)$$

To obtain the steam flow rate, we need to determine the specific heat capacity of the exhaust gas $\overline{Cp}_g$, and the temperature of the exhaust gas leaving the evaporator and entering the economizer T_{g3}.

From thermodynamics class notes, the specific heat of the exhaust gas is correlated between the temperature of the exhaust gas leaving the HRSG (stack) and the temperature of the exhaust gas entering the HRSG with the linear regression $C_p = 0{,}7903 + 0{,}0005107T$. These figures have been obtained from the Sonelgaz-Hamma gas turbine power plant.

$$\overline{Cp}_g = \frac{\int_{T_{g4}}^{T_{g1}} C_p dT}{\Delta T} \qquad with \qquad \Delta T = T_{g1} - T_{g4}$$

Knowing that the temperature of the exhaust gas leaving the HRSG will be between 100 and 200^oC, we correlate the specific heat capacity between 144^oC $(417\ K)$ and 544^oC $(817\ K)$.

$$\overline{Cp}_g = \frac{\left[0{,}7903T + \frac{0{,}0005107T^2}{2}\right]_{417}^{817}}{817 - 417} = 1.105\ kJ/kg.K$$

The temperature T_{g3}, is a very important parameter that cannot be assumed randomly, because doing so can lead to impossible situation "A temperature cross situation" as already discussed.

The pinch point temperature difference ΔT_{pp} is the difference between the temperature of exhaust gas leaving the evaporator T_{g3}, and the temperature of water leaving the economizer $T_{2'}$.

Using Eq.(29) we obtain:

$$T_{g3} = T_{2'} + \Delta T_{pp}$$

Assuming $\Delta T_{pp} = 10$°C gives:

$$T_{g3} = 297{,}51 + 10 = 307{,}51°C$$

Now that we have all parameters to determine the steam flow rate $\dot{m}_v$.

The exhaust gas flow $\dot{m}_g$ of gas turbine SGT-800 rate is giving in (Appendix-A)

$\dot{m}_g = 131{,}5\ kg/s$; We have two gas turbines so the new exhaust gas flow rate will be $2.(131{,}5) = 263\ kg/s$ (the two turbines can be considered as one machine).

$$\dot{m}_v = \frac{263.1{,}105.(544 - 307{,}51)}{(3395{,}87 - 1331{,}005)} = 33{,}28\ kg/s$$

We check if this steam flow rate capable of producing the $67{,}9MW$ net power of the steam turbine SST-900 giving by M.TRAD Ameur.

The net power of the steam turbine is calculated by the Eq.(25)

$$\dot{W}_{net} = \dot{W}_T - \dot{W}_P = \dot{m}_v.[(h_4 - h_5) - (h_2 - h_1)]$$

$$= 33{,}28.[(3395{,}87 - 2415{,}8) - (282{,}48 - 271{,}93)]$$

$$\dot{W}_{net} = 32265{,}63\ kW$$

The net power produced by the steam turbine is approximately $32{,}2\ MW$, that is too low compared to the actual net power that is $67{,}9MW$.

This comes to realize that there is a second burner that contribute in the production of the steam necessary, to deliver the energy to produce the $67{,}9MW$ net power.

To obtain the additional gas flow rate coming from the second burner, we need first to calculate the necessary steam flow rate that produce the actual net power.

The reverse process, assuming that the net power of the steam turbine is $67{,}9MW$ will give us the steam flow rate $\dot{m}_v$ that deliver it.

Using Eq.(25) we get:

$$\dot{m}_v = \frac{\dot{W}_{net}}{[(h_4 - h_5) - (h_2 - h_1)]}$$

Then,

$$\dot{m}_v = \frac{67900}{[(3395{,}87 - 2415{,}8\ ) - (282{,}48 - 271{,}93)]} = 70{,}03\ kg/s$$

The new total gas flow rate is calculated by using the Eq.(35)

$$\dot{m}_{gt}.\overline{Cp}_g.\left(T_{g1} - T_{g3}\right) = \dot{m}_v.(h_4 - h_{2'})$$

$$\dot{m}_{gt} = \frac{\dot{m}_v.(h_4 - h_{2'})}{\overline{Cp}_g.\left(T_{g1} - T_{g3}\right)}$$

$$\dot{m}_{gt} = \frac{70{,}03.(3395{,}87 - 1331{,}005)}{1{,}105.(544 - 307{,}51)} = 553{,}35\ kg/s$$

Now that we have the total gas flow rate, we can determine the gas flow rate of the second burner $\dot{m}_b$.

$$\dot{m}_{gt} = \dot{m}_g + \dot{m}_b$$

Then,

$$\dot{m}_b = \dot{m}_{gt} - \dot{m}_g = 553{,}35 - 263 = 290{,}35\ kg/s.$$

This is the flow rate of the hot gases coming from the second burner.

The stack temperature is determined from an energy balance on the economizer Eq.(32)

$$\dot{m}_{gt}.\overline{Cp}_g.\left(T_{g3} - T_{g4}\right) = \dot{m}_v.(h_{2'} - h_2)$$

This gives:

$$T_{g4} = T_{g3} - \frac{\dot{m}_v.(h_{2'} - h_2)}{\dot{m}_{gt}.\overline{Cp}_g}$$

$$T_{g4} = 307{,}51 - \frac{70{,}03.(1331{,}005 - 282{,}48)}{553{,}35.1{,}105} = 187{,}42^{o}\text{C}.$$

The temperature difference in the economizer between the stack temperature T_{g4} and the temperature of water entering the economizer T_2

$$\Delta T_{eco} = T_{g4} - T_2$$

$$\Delta T_{eco} = 187{,}42 - 65{,}84 = 121{,}58°\text{C}$$

The temperature of exhaust gases when leaving the super-heater and entering the evaporator is determined from an energy balance on the super-heater Eq.(34)

$$\dot{m}_{gt}.\overline{Cp}_g.\left(T_{g1} - T_{g2}\right) = \dot{m}_v.(h_4 - h_3)$$

This gives:

$$T_{g2} = T_{g1} - \frac{\dot{m}_v.(h_4 - h_3)}{\dot{m}_{gt}.\overline{Cp}_g}$$

$$T_{g2} = 544 - \frac{70{,}03.(3395{,}87 - 2753{,}23)}{553{,}35.1{,}105} = 470{,}39^{o}\text{C}.$$

The temperature difference in the super-heater between the temperature of exhaust gases entering evaporator T_{g2} and the temperature of vapor entering the super-heater T_3 is:

$$\Delta T_{sup} = T_{g2} - T_3$$

$$\Delta T_{sup} = 470{,}39 - 297{,}51 = 172{,}88^{o}\text{C}.$$

The ratio of mass flows rates is determined from the Eq.(36)

$$Y = \frac{\dot{m}_v}{\dot{m}_{gt}} = \frac{70{,}03}{553{,}35} = 0{,}127$$

That is, $1\ kg$ of hot gases can heat only $0{,}127\ kg$ of steam from $65{,}84$ to 500°C as they are cooled from 544 to $187{,}42$°C.

The heat extracted from the hot gases in the three heat exchangers (*Economizer, Evaporator, Superheater*), is determined by Eqs.(32) (33) (34).

$$\dot{Q}_{eco} = \dot{m}_v.(h_{2'} - h_2) = \dot{m}_{gt}.\overline{Cp}_g.\left(T_{g3} - T_{g4}\right) = 553{,}35.1.105.(307{,}51 - 187{,}42)$$

$$\dot{Q}_{eco} = 73429{,}24\ kW \approx 73{,}4\ MW.$$

$$\dot{Q}_{eva} = \dot{m}_v.(h_3 - h_{2'}) = \dot{m}_{gt}.\overline{Cp}_g.\left(T_{g2} - T_{g3}\right) = 553{,}35.1.105.(470{,}39 - 307{,}51)$$

$$\dot{Q}_{eva} = 99593{,}26\ kW \approx 99{,}6\ MW.$$

$$\dot{Q}_{sup} = \dot{m}_v.(h_4 - h_3) = \dot{m}_{gt}.\overline{Cp}_g.\left(T_{g1} - T_{g2}\right) = 553{,}35.1.105.(544 - 470{,}39)$$

$$\dot{Q}_{sup} = 45008{,}96\ kW \approx 45\ MW.$$

The total heat extracted from the hot gases is giving by the Eqs.(30) (31).

$$\dot{Q}_{tot} = \dot{m}_v.(h_4 - h_2) = \dot{m}_{gt}.\overline{Cp}_g.\left(T_{g1} - T_{g4}\right) = 553{,}35.1.105.(544 - 187{,}42)$$

$$\dot{Q}_{tot} = 218031{,}47\ kW \approx 218\ MW.$$

Or simply calculated by adding the heat fluxes of each heat exchanger.

$$\dot{Q}_{tot} = \dot{Q}_{eco} + \dot{Q}_{eva} + \dot{Q}_{sup}$$

$$\dot{Q}_{tot} = 73429{,}24 + 99593{,}26 + 45008{,}96 = 218031{,}46\ kW \approx 218\ MW.$$

The turbine work is defined by the Eq.(23)

$$w_T = h_4 - h_5$$

$$w_T = 3395{,}87 - 2415{,}8 = 980{,}07\ kJ/kg.$$

$$\dot{W}_T = \dot{m}_v . w_T = 70{,}03.(980{,}07\ ) = 68634{,}3\ kW \approx 68{,}6\ MW$$

The heat flux rejected to the air-cooled condenser is

$$\dot{Q}_C = \dot{Q}_{tot} - \dot{W}_T = 218031{,}46 - 68634{,}3 = 149397{,}16\ kW \approx 149{,}4\ MW$$

Then the thermal efficiency of the steam turbine is calculated using Eq.(40)

$$\eta_{ST} = \frac{\dot{W}_{net}}{\dot{Q}_{tot}}$$

$$\eta_{ST} = \frac{67900}{218031{,}46} = 0{,}311 \approx 31{,}1\%$$

III.3.2.3 The Combined-cycle calculations

Since there is another burner that contributes to the production of steam, we note that the combined-cycle efficiency defined in Eq.(44), is no longer applicable.

To determine the combined-cycle efficiency, we must first determine the additional heat coming from the second burner, noted $\dot{Q}_b$

We know that the total heat flux given to the steam turbine $\dot{Q}_{tot}$ is in fact the sum of heat flux of the exhaust gas $\dot{Q}_{ex}$ and the heat flux of the second burner $\dot{Q}_b$

$$\dot{Q}_{tot} = \dot{Q}_{ex} + \dot{Q}_b$$

This gives,

$$\dot{Q}_b = \dot{Q}_{tot} - \dot{Q}_{ex}$$

The heat flux of the exhaust gas $\dot{Q}_{ex}$ is defined in the Eq.(38)

$$\dot{Q}_{ex} = \dot{Q}_h - \dot{W}_{gt}$$

Replacing $\dot{Q}_{ex}$ by its expression and since there are two gas turbines, we obtain:

$$\dot{Q}_b = \dot{Q}_{tot} - 2.(\dot{Q}_h - \dot{W}_{gt})$$

So we get:

$$\dot{Q}_b = 218031{,}46 - 2.(118054{,}12 - 48223{,}68) = 78370{,}58\ kW$$

Now the combined-cycle efficiency η_{CC} is determined as follows

$$\eta_{CC} = \frac{\dot{W}_{tot}}{\dot{Q}_h + \dot{Q}_b} = \frac{\dot{W}_{ST} + \dot{W}_{GT}}{\dot{Q}_h + \dot{Q}_b}$$

Also, since there are two gas turbines we get

$$\eta_{CC} = \frac{\dot{W}_{ST} + 2\dot{W}_{GT}}{2\dot{Q}_h + \dot{Q}_b} = \frac{67900 + 2.(48223{,}68)}{2.(118054{,}12) + 78370{,}58} = 0{,}523 \approx 52{,}3\%$$

It is clearly that the second burner lowers the efficiency of the combined-cycle, however it compensates in increasing the net power. On the other hand, the combined-cycle efficiency is higher than both, gas turbine and steam turbine efficiencies individually.

III.3.2.4 The Solar field calculations

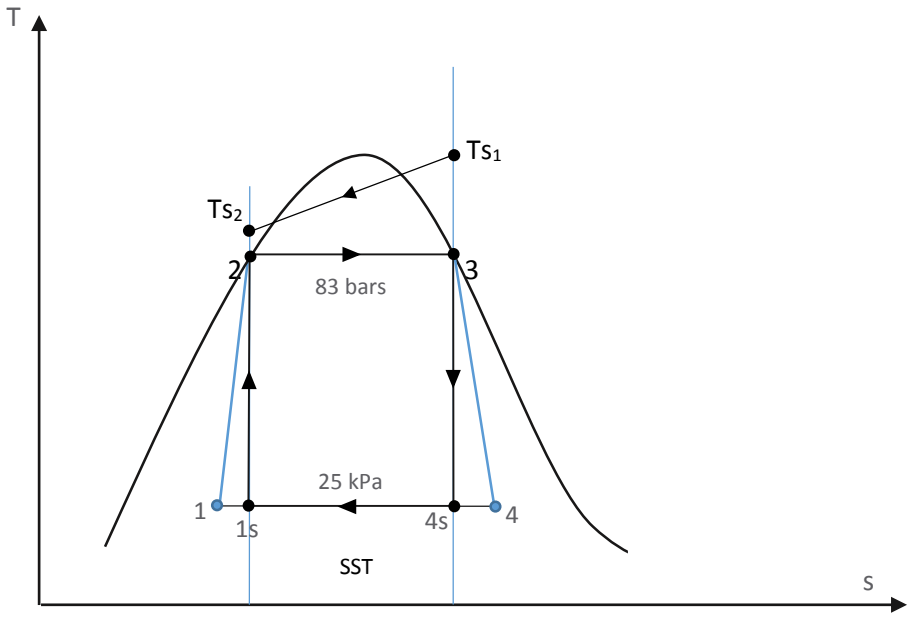

Figure III.4. Steam Carnot cycle condensation temperature $P_1 = 25kPa$ ($T_{1sat} = 64{,}97$°C)

The quantity of heat extracted from the sunlight during the day is calculated by the Eq.(48)

$$\dot{Q}_{Srec} = \frac{\dot{W}_S}{\eta_{Carnot} \cdot \eta_T}$$

Knowing the net power produced by the solar field that is $25MW$, and the turbine efficiency which is assumed to be equal to $0{,}85$, we still have only the Carnot cycle efficiency to be determined.

The Carnot cycle efficiency is calculated by the Eq.(46)

$$\eta_{Carnot} = 1 - \frac{T_c}{T_h}$$

Known: $T_c = 337.97\ K$ and $T_h = 570.51\ K$

$$\eta_{Carnot} = 1 - \frac{337.97}{570.51} = 0.407$$

The quantity of heat extracted from the sunlight is then

$$\dot{Q}_{Srec} = \frac{25000}{0{,}407.0.85} = 73529{,}41\ kW \approx 73.5\ MW$$

Using the heat balance Eq.(47), we'll be able to determine the hot oil flow rate $\dot{m}_h$.

$$\dot{Q}_{Srec} = \dot{m}_h . \overline{Cp}_h . (T_{s1} - T_{s2})$$

Solving for $\dot{m}_h$ we get:

$$\dot{m}_h = \frac{\dot{Q}_{Srec}}{\overline{Cp}_h . (T_{s1} - T_{s2})}$$

$\overline{Cp}_h$ is chosen from Table II.1 (Synthetic oil is chosen, because it has better heat capacity and conductivity)

$$\dot{m}_h = \frac{73529{,}41}{2{,}3. (372 - 307{,}51)} = 495{,}73\ kg/s$$

The solar field contribution during sunshine hours will economize the consumption of natural gas.

Because of the difference between the Rankine cycle and solar field cycle efficiencies, the new gas flow rate $\dot{m}_{gtd}$cannot be obtained through the following equation, the result will be false.

$$\dot{m}_{gtd} = \frac{\dot{Q}_{tot} - \dot{Q}_{Srec}}{\overline{Cp}_g . (T_{g1} - T_{g4})}$$

So we base our calculation on the difference between the net powers of both cycles $\dot{W}_{net} - \dot{W}_S$ rather than the difference between the heat fluxes given to each cycle $\dot{Q}_{tot} - \dot{Q}_{Srec}$ the new gas flow rate $\dot{m}_{gtd}$ is:

$$\dot{m}_{gtd} = \frac{\frac{\dot{W}_{net} - \dot{W}_S}{\eta_{ST}}}{\overline{Cp}_g . (T_{g1} - T_{g4})}$$

$\dot{W}_{net} = 67900\ kW$, $\dot{W}_S = 25000\ kW$, $\eta_{ST} = 0{,}367$, $T_{g4} = 187{,}18$°C

So that will give:

$$\dot{m}_{gtd} = \frac{\frac{67900 - 25000}{0{,}311}}{1{,}105.(544 - 187{,}42)} = 350{,}1\ kg/s$$

It is important to note, that the consumption of natural gas, is at the level of the second burner, because reducing the gas flow rate to the gas turbine, will decreases its performance and ultimately the plant overall net power. The new gas flow rate of the second burner $\dot{m}_{bd}$ is:

$$\dot{m}_{bd} = \dot{m}_{gtd} - \dot{m}_g$$

$$\dot{m}_{bd} = 350{,}1 - 263 = 87{,}1\ kg/s$$

$$\frac{553{,}35 - 350{,}1}{553{,}35} = 0{,}367 \approx 36{,}7\%$$

The mass ratio of Air-Methane for stoichiometric combustion is $r = 17{,}2$ (see Appendix-B), then we need $17{,}2\ kg$ of air for every $1\ kg$ of Methane.

The total gas flow rate is $553{,}35\ kg/s$ $(1992060\ kg/h)$, so the total natural gas flow rate is $115817{,}44\ kg/h$. And with a density of Methane is $d_{CH4} = 0{,}717\ kg/m^3$. This gives a total natural gas flow rate of $161530{,}6\ m^3/h$.

So during sunny non-windy periods the average of natural gas economy is:

$$(0{,}367).(161530{,}6) = 59281{,}73\ m^3/h$$

During the time the solar field is operating which is approximately six hours per day in winter, we save $36{,}7\%$ of the total gas flow rate and as a result $36{,}7\%$ of natural gas. But as we said this goes only for six hours per day, so:

$$\frac{0{,}367.(161530{,}6).6}{(161530{,}6).24} = 0.092 \approx 9.2\%$$

This means the average natural gas economization is 9.2% per day. In comparison to the solar field share percentage per day which is $4{,}2\%$, I believe the contrast between the two is due to the fact that the solar field is more efficient than the steam turbine.

III.3.3. Cycle 02: Condensation at $20\ kPa$ (saturation temperature $60,06$°C)

III.3.3.1. The steam cycle calculations

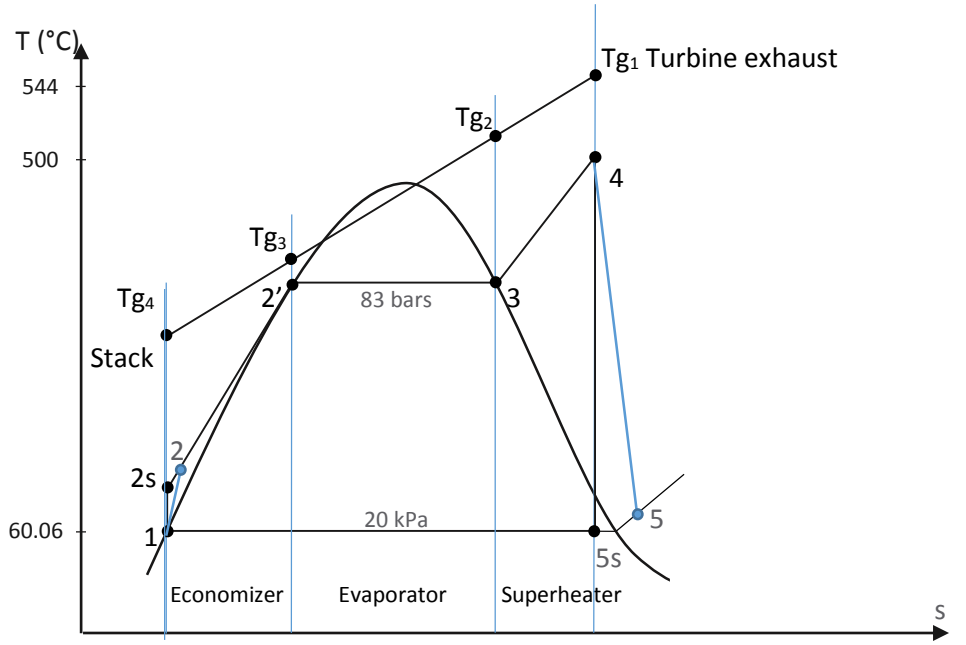

Figure III.5. Steam cycle with condensation temperature $P_1 = 20kPa$ ($T_{1sat} = 60{,}06$°C)

State 1:

State 1 represent saturated liquid water at the pressure of $20kPa$. using the tables of thermodynamic properties, we read:

$P_1 = 20kPa.$

$T_1 = 60{,}06$ °C.

$h_1 = 251{,}42\ kJ/kg.$

$s_1 = 0.8320\ kJ/kg.K.$

State 2:

In order to identify state 2, first we need to calculate the pump work, that raise the water pressure from $20\ kPa$ to $8{,}3\ MPa$ $(83\ bars)$.

Using Eq.(26)

$$w_p = \frac{1}{\eta_P}.v.(P_2 - P_1) = \frac{1}{0{,}8}.0.001017.(8300 - 20)$$

$$w_p = 10{,}52\ kJ/kg$$

Knowing the ideal pump work w_p and h_1 we can determine h_2.

$$h_2 = h_1 + w_p = 261{,}94\ kJ/kg.$$

Using the tables of thermodynamic properties for compressed liquid water, we read the temperature T_2 and the entropy s_2.

$P_2 = 8300\ kPa.$

$T_2 = 60{,}91°C$

$h_2 = 261{,}94\ kJ/kg.$

$s_2 = 0.8381\ kJ/kg.K$

The states 2', 3, 4 remains the same as in cycle 01 simply because the higher pressure $83\ bars$ in the Rankin-Cycle did not change.

State 5:

State 5 is mix of both steam and liquid water. Considering the process from 4 to 5 is an isentropic expansion in the turbine. The second law of thermodynamic gives:

$$s_4 = s_{5i} = 6{,}7075\ kJ/kg.K$$

And,

Table III.3 Entropy and Enthalpy parameters at the pressure of 20 kPa

Pressure (kPa)	Entropy $(kJ/kg.K)$		Enthalpy (kJ/kg)	
20	s_f	s_{fg}	h_f	h_{fg}
	0,8320	7,0752	251,42	2357,5

$$x_{5i} = \frac{6{,}7075 - 0{,}8320}{7{,}0752} = 0.83$$

$$h_{5i} = 251{,}42 + (0{,}83).2357{,}5 = 2208{,}14\ kJ/kg.$$

These properties (entropy, enthalpy and vapor quality) are for an isentropic expansion in the turbine, assuming a turbine isentropic efficiency $\eta_T = 0{,}85$. We get the actual ones:

$$h_5 = h_4 - \eta_T.(h_4 - h_{5i})$$

$$h_5 = 3395{,}87 - 0{,}85.(3395{,}87 - 2208{,}14) = 2386{,}3\ kJ/kg$$

$$x_5 = \frac{2386{,}3 - 251{,}42}{2357{,}5} = 0{,}906$$

$$s_5 = 0{,}8320 + 0{,}906.(7{,}0752) = 7{,}2347\ kJ/kg.K$$

So,

$P_5 = P_1 = 20kPa.$

$T_5 = T_1 = 60{,}06$ °C.

$h_5 = 2386{,}3\ kJ/kg.$

$s_5 = 7{,}2421\ kJ/kg.K$

The following table summarize the states that have changed.

Table III.4 States of the vapor cycle 02

State	Temperature (^oC)	Pressure (kPa)	Enthalpy (kJ/kg)	Entropy $(kJ/kg.K)$
1	60,06	20	251,42	0.8320
2	60,91	8300	261,94	0,8381
5	60,06	20	2386,3	7,2421

III.3.3.2 The heat recovery steam generator calculations

The stack temperature is determined from an energy balance on the economizer Eq.(32). This gives:

$$T_{g4} = T_{g3} - \frac{\dot{m}_v.(h_{2'} - h_2)}{\dot{m}_{gt}.\overline{Cp}_g}$$

$$T_{g4} = 307{,}51 - \frac{70{,}03\ .(1331{,}005 - 261{,}94)}{553{,}35\ .1{,}105} = 185.07°C.$$

The temperature difference in the economizer between the stack temperature T_{g4} and the temperature of water entering the economizer T_2

$$\Delta T_{eco} = 185{,}07 - 60{,}91 = 124{,}2°C$$

The heat extracted from the hot gases in the three heat exchangers (*Economizer, Evaporator, Super-heater*), are determined by Eqs.(32) (33) (34).

$$\dot{Q}_{eco} = \dot{m}_v.(h_{2'} - h_2) = \dot{m}_g.\overline{Cp}_g.\left(T_{g3} - T_{g4}\right) = 553{,}35\ .1.105.(307{,}51 - 185{,}07)$$

$$\dot{Q}_{eco} = 74866{,}15\ kW \approx 74{,}15\ MW.$$

The heat flux of the evaporator and the superheater are as in cycle 01.

$\dot{Q}_{eva} = 99593{,}26\ kW \approx 99{,}6\ MW.$

$\dot{Q}_{sup} = 45008{,}96\ kW \approx 45\ MW.$

The total heat extracted from the hot gases is giving by Eqs.(30) (31).

$$\dot{Q}_{tot} = \dot{m}_v.(h_4 - h_2) = \dot{m}_g.\overline{Cp}_g.\left(T_{g1} - T_{g4}\right) = 553{,}35.1.105.(544 - 185{,}07\ )$$

$$\dot{Q}_{tot} = 219468{,}38\ kW \approx 219{,}5\ MW.$$

The turbine work is defined by the Eq.(23)

$$w_T = h_4 - h_5$$

$$w_T = 3395{,}87 - 2386{,}3 = 1009{,}57\ kJ/kg.$$

$$\dot{W}_T = \dot{m}_v.w_T = 70{,}03.(1009{,}57) = 70700{,}19\ kW \approx 70{,}7\ MW$$

Then the heat flux rejected to the air-cooled condensers is:

$$\dot{Q}_C = \dot{Q}_{tot} - \dot{W}_T = 219468{,}38\ - 70700{,}19\ = 148768{,}2\ kW \approx 148{,}8\ MW$$

The net power $\dot{W}_{net}$ is calculated by the Eq.(25)

$$\dot{W}_{net} = \dot{m}_v.[(h_4 - h_5) - (h_2 - h_1)]$$

$$\dot{W}_{net} = 70{,}03.[(3395{,}87 - 2386{,}3) - (261{,}94 - 251{,}42)] = 69963{,}47\ kW$$

$$\dot{W}_{net} \approx 70\ MW$$

Then the thermal efficiency of the steam turbine is calculated using Eq.(40)

$$\eta_{ST} = \frac{\dot{W}_{net}}{\dot{Q}_{tot}}$$

$$\eta_{ST} = \frac{69963,47}{219468,38} = 0,319 \approx 31,9\%$$

III.3.3.3 The Combined-cycle calculations

The total heat flux given to the steam turbine $\dot{Q}_{tot}$ is in fact the sum of heat flux of the exhaust gas $\dot{Q}_{ex}$ and the heat flux of the second burner $\dot{Q}_b$ so:

$$\dot{Q}_b = \dot{Q}_{tot} - \dot{Q}_{ex}$$

The heat flux of the exhaust gas $\dot{Q}_{ex}$ is defined in the Eq.(40)

$$\dot{Q}_{ex} = \dot{Q}_h - \dot{W}_{gt}$$

So we get:

$$\dot{Q}_b = 219468,38 - 2.(118054,12 - 48223,68) = 79807,5\ kW$$

Now the combined-cycle efficiency η_{CC} is determined as follows

$$\eta_{CC} = \frac{\dot{W}_{tot}}{\dot{Q}_h + \dot{Q}_b} = \frac{\dot{W}_{ST} + \dot{W}_{GT}}{\dot{Q}_h + \dot{Q}_b}$$

Also, since there are two gas turbines we get

$$\eta_{CC} = \frac{\dot{W}_{ST} + 2\dot{W}_{GT}}{2\dot{Q}_h + \dot{Q}_b} = \frac{69963,47 + 2.(48223,68)}{2.(118054,12\ ) + 79807,5} = 0,527 \approx 52,7\%$$

III.3.3.4. The Solar field calculations

The quantity of heat extracted from the sunlight during the day is calculated by the Eq.(48)

$$\dot{Q}_{Srec} = \frac{\dot{W}_S}{\eta_{Carnot}.\eta_T}$$

Knowing the net power produced by the solar field that is $25\ MW$, and the turbine efficiency which is assumed to be equal to $0,85$, we still have only the Carnot cycle efficiency to be determined.

The Carnot cycle efficiency is calculated by the Eq.(46)

$$\eta_{Carnot} = 1 - \frac{T_c}{T_h}$$

Known: $T_c = 333,06\ K$ and $T_h = 570,51\ K$

$$\eta_{Carnot} = 1 - \frac{333{,}06}{570{,}51} = 0{,}416$$

The heat extracted from the sunlight is calculable

$$\dot{Q}_{Srec} = \frac{25000}{0{,}416.0{,}85} = 70701{,}35\ kW \approx 70{,}7\ MW$$

We notice that the solar field needs now only $70{,}7\ MW$ instead of $73.5\ MW$ to produce the $25\ MW$

Another approach is that we know the heat flux $\dot{Q}_s$the solar field is capable of extracting from sunlight during the day, it was calculated in the first cycle which is equal to $73529{,}41\ kW$

So the new net power retrieved is then:

$$\dot{W}_S = \dot{Q}_s . \eta_{Carnot} . \eta_T$$

$$\dot{W}_S = 73529{,}41.(0{,}85).(0{,}416) = 25999{,}99 \approx 26\ MW$$

The solar field contribution during sunshine hours will economize the consumption of natural gas.

The new gas flow rate $\dot{m}_{gtd}$is:

$$\dot{m}_{gtd} = \frac{\frac{\dot{W}_{net} - \dot{W}_S}{\eta_T}}{\overline{Cp}_g . (T_{g1} - T_{g4})}$$

$\dot{W}_{net} = 69963{,}47\ kW$, $\dot{W}_S = 25999{,}99\ kW$, $\eta_{ST} = 0{,}319$, $T_{g4} = 185{,}07$°C

$$\dot{m}_{gtd} = \frac{\frac{69963{,}47 - 25999{,}99}{0{,}319}}{1{,}105.(544 - 185{,}07)} = 347{,}48\ kg/s$$

The new gas flow rate of the second burner $\dot{m}_{bd}$

$$\dot{m}_{bd} = \dot{m}_{gtd} - \dot{m}_g$$

$$\dot{m}_{bd} = 347{,}48 - 263 = 84{,}48\ kg/s$$

$$\frac{553{,}35 - 347{,}48}{553{,}35} = 0{,}372 \approx 37{,}2\%$$

So during sunny non-windy periods the average of natural gas economy is:

$$(0{,}372).(161530{,}6) = 60089{,}38\ m^3/h$$

$$\frac{(0{,}372).6}{24} = 0.093 \approx 9.3\%$$

III.3.4. Cycle 03: Condensation at $15\ kPa$ (saturation temperature $53,97$°C)

III.3.4.1. The steam cycle calculations

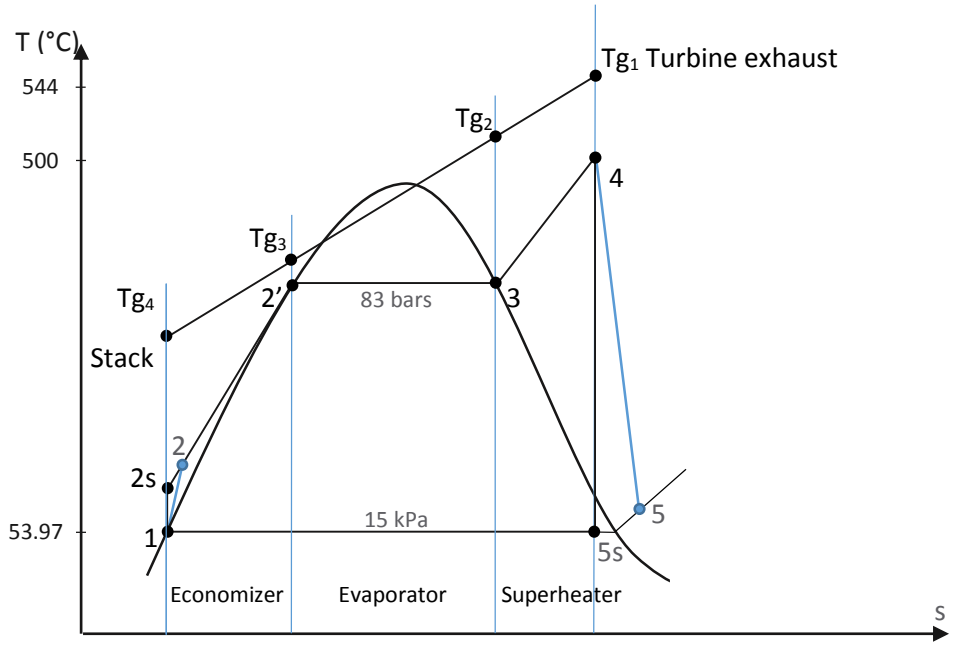

Figure III.6. Steam cycle with condensation temperature at $P_1 = 15kPa$ ($T_{1sat} = 53{,}97$°C)

State 1:

$P_1 = 15kPa.$

$T_1 = 53{,}97$°C.

$h_1 = 225{,}94\ kJ/kg.$

$s_1 = 0.7549\ kJ/kg.K.$

State 2:

Using Eq.(26)

$$w_p = \frac{1}{\eta_P}.v.(P_2 - P_1) = \frac{1}{0{,}8}.0.001014.(8300 - 15)$$

$$w_p = 10{,}50\ kJ/kg$$

Knowing the pump work w_p and h_1 we can determine h_2.

$$h_2 = h_1 + w_p = 236{,}44\ kJ/kg.$$

State2 is fixed,

$P_2 = 8300\ kPa$

$T_2 = 54.79°\text{C}$

$h_2 = 236{,}44\ kJ/kg$

$s_2 = 0.7598\ kJ/kg.K$

State 5:

Table III.5 Entropy and Enthalpy parameters at the pressure of 15 kPa

Pressure (kPa)	Entropy $(kJ/kg.K)$		Enthalpy (kJ/kg)	
15	s_f	s_{fg}	h_f	h_{fg}
	0,7549	7,2536	225,94	2373,1

$$x_{5i} = \frac{6{,}7075 - 0{,}7549}{7{,}2536} = 0{,}82$$

$$h_{5i} = 225{,}94 + (0{,}82).2373{,}1 = 2171{,}88\ kJ/kg$$

These properties (entropy, enthalpy and vapor quality) are for an isentropic expansion in the turbine, assuming a turbine isentropic efficiency $\eta_T = 0{,}85$. We get the actual ones:

$$h_5 = h_4 - \eta_T.(h_4 - h_{5i})$$

$$h_5 = 3395{,}87 - 0{,}85.(3395{,}87 - 2171{,}88) = 2355{,}48\ kJ/kg$$

$$x_5 = \frac{2355{,}48 - 225{,}94}{2373{,}1} = 0{,}897$$

The quality of steam is below $0{,}90$. This will cause the turbine performance to drop and eventually the net power produced by the turbine.

$$s_5 = 0{,}7549 + 0{,}897.(7{,}2536) = 7{,}2614\ kJ/kg.K$$

State 5 is fixed,

$P_5 = P_1 = 15kPa.$

$T_5 = T_1 = 53{,}97$°C.

$h_5 = 2355{,}48\ kJ/kg.$

$s_5 = 7{,}2614\ kJ/kg.K$

The following table summarize the states that have changed.

Table III.6 States of the vapor cycle 03

State	Temperature $(°C)$	Pressure (kPa)	Enthalpy (kJ/kg)	Entropy $(kJ/kg.K)$
1	53,97	15	225,94	0,7549
2	54.79	8300	236,44	0.7598
5	53,97	15	2355,48	7,2614

III.3.4.2 The heat recovery steam generator calculations

The stack temperature is determined from an energy balance on the economizer Eq.(34)

This gives:

$$T_{g4} = T_{g3} - \frac{\dot{m}_v.(h_{2'} - h_2)}{\dot{m}_{gt}.\overline{Cp}_g}$$

$$T_{g4} = 307{,}51 - \frac{70{,}03.(1331{,}005 - 236{,}44\ )}{553{,}35.1{,}105} = 182{,}15°\text{C}.$$

The temperature difference in the economizer between the stack temperature T_{g4} and the temperature of water entering the economizer T_2

$$\Delta T_{eco} = 182{,}15 - 54{,}79 = 127{,}36°\text{C}$$

The heat extracted from the hot gases in the three heat exchangers (*Economizer, Evaporator, Super-heater*), are determined by Eqs.(32) (33) (34).

$$\dot{Q}_{eco} = \dot{m}_v.(h_{2'} - h_2) = \dot{m}_g.\overline{Cp}_g.\left(T_{g3} - T_{g4}\right) = 553{,}35.1{,}105.(307{,}51 - 182{,}15)$$

$$\dot{Q}_{eco} = 76651{,}59\ kW \approx 76{,}7\ MW.$$

The total heat extracted from the hot gases is giving by Eqs.(30) (31).

$$\dot{Q}_{tot} = \dot{m}_v.(h_4 - h_2) = \dot{m}_g.\overline{Cp}_g.(T_{g1} - T_{g4}) = 553{,}35.1.105.(544 - 182.15)$$

$$\dot{Q}_{tot} = 221253{,}82\ kW \approx 221{,}3\ MW.$$

The turbine work is defined by the Eq.(23)

$$w_T = h_4 - h_5$$

$$w_T = 3395{,}87 - 2355{,}48 = 1040{,}39\ kJ/kg.$$

$$\dot{W}_T = \dot{m}_v.w_T = 70{,}03.(1040{,}39) = 72858{,}51\ kW \approx 72{,}9\ MW$$

Then the heat flux rejected to the air-cooled condensers is:

$$\dot{Q}_C = \dot{Q}_{tot} - \dot{W}_T = 221253{,}82 - 72858{,}51 = 148395{,}31\ kW \approx 148{,}4\ MW$$

The net power $\dot{W}_{net}$ is calculated by the Eq.(25)

$$\dot{W}_{net} = \dot{m}_v.[(h_4 - h_5) - (h_2 - h_1)]$$

$$\dot{W}_{net} = 70{,}03.[(3395{,}87 - 2355{,}48) - (236{,}44 - 225{,}94)] = 72123{,}2\ kW \approx 72{,}1\ MW$$

Then the thermal efficiency of the steam turbine is calculated using Eq.(40)

$$\eta_{ST} = \frac{\dot{W}_{net}}{\dot{Q}_{tot}}$$

$$\eta_{ST} = \frac{72123{,}2}{221253{,}82} = 0{,}326 \approx 32{,}6\%$$

III.3.4.3 The Combined-Cycle calculations

The total heat flux given to the steam turbine $\dot{Q}_{tot}$ is in fact the sum of heat flux of the exhaust gas $\dot{Q}_{ex}$ and the heat flux of the second burner $\dot{Q}_b$

$$\dot{Q}_b = \dot{Q}_{tot} - \dot{Q}_{ex}$$

So we get:

$$\dot{Q}_b = 221253{,}82 - 2.(118054{,}12 - 48223{,}68) = 81592{,}94\ kW$$

Now the combined-cycle efficiency η_{CC} is determined as follows:

$$\eta_{CC} = \frac{\dot{W}_{tot}}{\dot{Q}_h + \dot{Q}_b} = \frac{\dot{W}_{ST} + \dot{W}_{GT}}{\dot{Q}_h + \dot{Q}_b}$$

Also, since there are two gas turbines we get

$$\eta_{CC} = \frac{\dot{W}_{ST} + 2\dot{W}_{GT}}{2\dot{Q}_h + \dot{Q}_b} = \frac{72123{,}2 + 2.(48223{,}68)}{2.(118054{,}12) + 81592{,}94} = 0{,}531 \approx 53{,}1\%$$

III.3.4.4 The Solar field calculations

The heat extracted from the sunlight during the day is calculated by the Eq.(49)

$$\dot{Q}_{Srec} = \frac{\dot{W}_S}{\eta_{Carnot} \cdot \eta_T}$$

$$\eta_{Carnot} = 1 - \frac{T_c}{T_h}$$

Known: $T_c = 326{,}97\ K$ and $T_h = 570{,}51\ K$

$$\eta_{Carnot} = 1 - \frac{326{,}97}{570{,}51} = 0{,}43$$

So,

$$\dot{Q}_{Srec} = \frac{25000}{0{,}43.0{,}85} = 68399{,}45\ kW \approx 68{,}4\ MW$$

Or the new net power retrieved is then:

$$\dot{W}_S = 73529{,}41.(0{,}85).(0{,}43) = 26874{,}99 \approx 26{,}8\ MW$$

The solar field contribution during sunshine hours will economize the consumption of natural gas.

The new gas flow rate $\dot{m}_{gtd}$is:

$\dot{W}_{net} = 72123{,}2\ kW$, $\dot{W}_S = 26874{,}99\ kW$, $\eta_T = 0{,}326$, $T_{g4} = 182{,}15$°C

$$\dot{m}_{gtd} = \frac{\frac{72123{,}2 - 26874{,}99}{0{,}326}}{1{,}105.(544 - 182{,}15)} = 347{,}13\ kg/s$$

The new gas flow rate of the second burner $\dot{m}_{bd}$is:

$$\dot{m}_{bd} = 347{,}13 - 263 = 84{,}13\ kg/s$$

$$\frac{553{,}35 - 347{,}13}{553{,}35} = 0{,}373 \approx 37{,}3\%$$

So during sunny non-windy periods the average of natural gas economy is:

$$(0{,}373).(161530{,}6) = 60250{,}91\ m^3/h$$

$$\frac{(0{,}373).6}{24} = 0.0933 \approx 9.33\%$$

III.3.5. Cycle 04: Condensation at $10\ kPa$ (saturation temperature $45,81$°C)

III.3.5.1. The steam cycle calculations

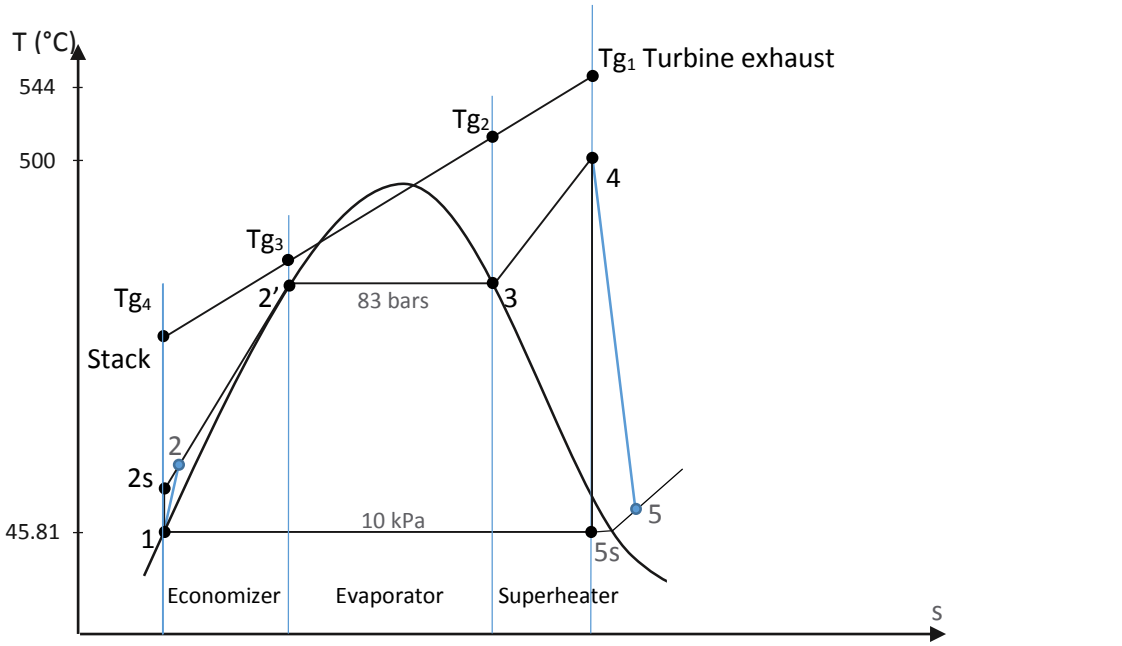

Figure III.7. Steam cycle with condensation temperature at $P_1 = 10kPa$ ($T_{1sat} = 45{,}81$°C)

State 1:

$P_1 = 10\ kPa.$

$T_1 = 45{,}81$°C.

$h_1 = 191{,}81\ kJ/kg.$

$s_1 = 0.6492\ kJ/kg.K.$

State 2:

Using Eq.(26),

$$w_p = \frac{1}{\eta_P}.v.(P_2 - P_1) = \frac{1}{0{,}8}.0.001010.(8300 - 10) = 10{,}47\ kJ/kg$$

$$h_2 = h_1 + w_p = 200{,}18\ kJ/kg.$$

State 2 is fixed,

$P_2 = 8300\ kPa.$

$T_2 = 46{,}71$°C

$h_2 = 202{,}28\ kJ/kg.$

$s_2 = 0{,}6557\ kJ/kg.K$

State 5:

Table III.7 Entropy and Enthalpy parameters at the pressure of 10 kPa

Pressure (kPa)	Entropy $(kJ/kg.K)$		Enthalpy (kJ/kg)	
10	s_f	s_{fg}	h_f	h_{fg}
	0,6492	7,4996	191,81	2392,1

$$x_{5i} = \frac{6{,}7075 - 0{,}6492}{7{,}4996} = 0{,}80$$

$$h_{5i} = 191{,}81 + (0{,}80).2392{,}1 = 2105{,}49\ kJ/kg$$

The actual properties are:

$$h_5 = 3395{,}87 - 0{,}85.(3395{,}87 - 2105{,}49) = 2299{,}04\ kJ/kg$$

$$x_5 = \frac{2299{,}04 - 191{,}81}{2392{,}1} = 0{,}88$$

The quality of steam is below $0{,}90$. This will cause the turbine performance to drop and even damages the turbine blades.

$$s_5 = 0{,}6492 + 0{,}88.(7{,}4996) = 7{,}2488\ kJ/kg.K$$

State 5 is fixed,

$P_5 = P_1 = 10kPa.$

$T_5 = T_1 = 45{,}81$°C.

$h_5 = 2299{,}04\ kJ/kg.$

$s_5 = 7{,}2488\ /kg.K$

The following table summarize the states that have changed.

Table III.8 States of the vapor cycle 04

State	Temperature (^oC)	Pressure (kPa)	Enthalpy (kJ/kg)	Entropy $(kJ/kg.K)$
1	45,81	10	191,81	0.6492
2	46,71	8300	202,28	0,6557
5	45,81	10	2299,04	7,2488

III.3.5.2 The heat recovery steam generator calculations

The stack temperature is determined from an energy balance on the economizer Eq.(32)

This gives:

$$T_{g4} = T_{g3} - \frac{\dot{m}_v.(h_{2'} - h_2)}{\dot{m}_{gt}.\overline{Cp}_g}$$

$$T_{g4} = 307{,}51 - \frac{70{,}03.(1331{,}005-202{,}28)}{553{,}35.1{,}105} = 178.24^oC.$$

$$\Delta T_{eco} = 178{,}24 - 46{,}71 = 131{,}53°C$$

$$\dot{Q}_{eco} = \dot{m}_v.(h_{2'} - h_2) = \dot{m}_g.\overline{Cp}_g.\left(T_{g3} - T_{g4}\right) = 553{,}35.1{,}105.(307{,}51 - 178{,}24)$$

$$\dot{Q}_{eco} = 79042{,}37\ kW \approx 79\ MW.$$

The total heat extracted from the hot gases is giving by the Eqs.(30) (31).

$$\dot{Q}_{tot} = \dot{m}_v.(h_4 - h_2) = \dot{m}_g.\overline{Cp}_g.\left(T_{g1} - T_{g4}\right) = 553{,}35.1.105.(544 - 178{,}24\ )$$

$$\dot{Q}_{tot} = 223644{,}6\ kW \approx 223{,}6\ MW.$$

The turbine work is defined by the Eq.(23)

$$w_T = h_4 - h_5$$

$$w_T = 3395{,}87 - 2299{,}04 = 1096{,}83\ kJ/kg.$$

$$\dot{W}_T = \dot{m}_v.w_T = 70{,}03.(1096{,}83) = 76811\ kW \approx 76{,}8\ MW$$

Then the heat flux rejected to the air-cooled condenser is

$$\dot{Q}_C = \dot{Q}_{tot} - \dot{W}_T = 223644{,}6 - 76811 = 146833{,}6\ kW \approx 146{,}8\ MW$$

The net power $\dot{W}_{net}$ is calculated by the Eq.(25)

$$\dot{W}_{net} = \dot{m}_v.[(h_4 - h_5) - (h_2 - h_1)]$$

$$\dot{W}_{net} = 70{,}03.[(3395{,}87 - 2299{,}04) - (202{,}28 - 191{,}81)] = 76077{,}8\ kW \approx 76{,}1\ MW$$

Then the thermal efficiency of the steam turbine is calculated using Eq.(40)

$$\eta_{ST} = \frac{\dot{W}_{net}}{\dot{Q}_{tot}}$$

$$\eta_{ST} = \frac{76077{,}8}{223644{,}6} = 0{,}34 \approx 34\%$$

III.3.5.3 The Combined-Cycle calculations

The total heat flux given to the steam turbine $\dot{Q}_{tot}$ is the sum of heat flux of the exhaust gas $\dot{Q}_{ex}$ and the heat flux of the second burner $\dot{Q}_b$

$$\dot{Q}_{tot} = \dot{Q}_{ex} + \dot{Q}_b$$

Replacing $\dot{Q}_{ex}$ by its expression and since there are two gas turbines, we obtain:

$$\dot{Q}_b = 223644{,}6 - 2.(118054{,}12 - 48223{,}68) = 83983{,}72\ kW$$

Now the combined-cycle efficiency η_{CC} is determined as follows

$$\eta_{CC} = \frac{\dot{W}_{tot}}{\dot{Q}_h + \dot{Q}_b} = \frac{\dot{W}_{ST} + \dot{W}_{GT}}{\dot{Q}_h + \dot{Q}_b}$$

Also, since there are two gas turbines we get

$$\eta_{CC} = \frac{\dot{W}_{ST} + 2\dot{W}_{GT}}{2\dot{Q}_h + \dot{Q}_b} = \frac{76077{,}8 + 2.(48223{,}68)}{2.(118054{,}12\ ) + 83983{,}72} = 0{,}539 \approx 53{,}9\%$$

III.3.5.4 The Solar field calculations

The Carnot cycle efficiency is:

Known: $T_c = 318{,}81\ K$ and $T_h = 570{,}51\ K$

$$\eta_{Carnot} = 1 - \frac{318{,}81}{570{,}51} = 0.558$$

The heat extracted from the sunshine is calculable as:

$$\dot{Q}_{Srec} = \frac{25000}{0{,}558.0{,}85} = 52709{,}25\ kW \approx 52{,}7\ MW$$

Or the new net power retrieved is then:

$$\dot{W}_S = 73529{,}41.(0{,}85).(0.558) = 34874{,}99 \approx 34{,}8\ MW$$

The solar field contribution during sunshine hours will economize the consumption of natural gas.

The new gas flow rate $\dot{m}_{gtd}$is

$\dot{W}_{net} = 76077{,}8\ kW$, $\dot{W}_S = 34874{,}99\ kW$, $\eta_{ST} = 0{,}34$, $T_{g4} = 178{,}24$°C

$$\dot{m}_{gtd} = \frac{\frac{76077{,}8 - 34874{,}99}{0{,}34}}{1{,}105.(544 - 178{,}24)} = 299{,}84\ kg/s$$

We can see that this is actually lower than the exhaust gas flow rate of the gas turbines.

$$\frac{553{,}35 - 299{,}84}{553{,}35} = 0{,}458 \approx 45{,}8\%$$

So during sunny non-windy periods the average natural gas economy is:

$$(0{,}458).(161530{,}6) = 74003{,}11\ m^3/h$$

$$\frac{(0{,}458).6}{24} = 0.1145 \approx 11.45\%$$

III.4 Results and Discussion

III.4.1 Gas turbine analysis

The gas turbine calculations allowed us to obtain the following results that they are summarized in Table III.9

Table III.9 Siemens gas turbine SGT-800 parameters summarizing

Compressor Total Work $\dot{W}_C\ (kW)$	Turbine Total Work $\dot{W}_T\ (kW)$	Added Heat Flux $\dot{Q}_H\ (kW)$	Rejected Heat Flux $\dot{Q}_L\ (kW)$	Net Power $\dot{W}_{net}\ (kW)$	Thermal Efficiency η_{GT}
52878.78	101102.46	118054.12	69841.75	48223.68	40.8%

The net power is actually not far from the actual one given by the manufacturer of the gas turbine (SIEMENS), which was 47 MW. That's reasonable giving the fact that some additional losses were not considered in this study.

We can notice that the ratio of the compressor work to the turbine work (back work ratio) is $0{,}52$ which is remarkable, usually $55\ to\ 60\%$ of the turbine work is used to rotate the compressor, with that been said, this leaves 48% of the turbine work as net work.

For gas turbines a thermal efficiency of $40{,}8\%$ is quite high, which means that the SGT-800 is not only optimized, but also have a high thermal efficiency.

III.4.2 Steam turbine analysis

First we start with the obvious result, the increase in both the steam turbine net power and its efficiency, the results of the four cycles are shown in Table III.10.

Table III.10 Steam turbine net power and efficiency versus the condensation temperature

Temperature (^oC)	Steam Turbine Net Power $\dot{W}_{net}(kW)$	Steam Turbine Efficiency $\eta_{ST}(\%)$
64.97	67900	31.1
60.06	69963.47	31.9
53.97	72123.20	32.6
45.81	76077.80	34.0

In the *Figure III.8* we can see that the lower the condensation temperature, the higher steam turbine net power and efficiency. Also we can notice that they increase with different paces, the net power increases slightly faster than the thermal efficiency, the reason why is because the added heat to the Rankine cycle increases with lowering the condensation temperature which will slightly decelerate the increase in efficiency.

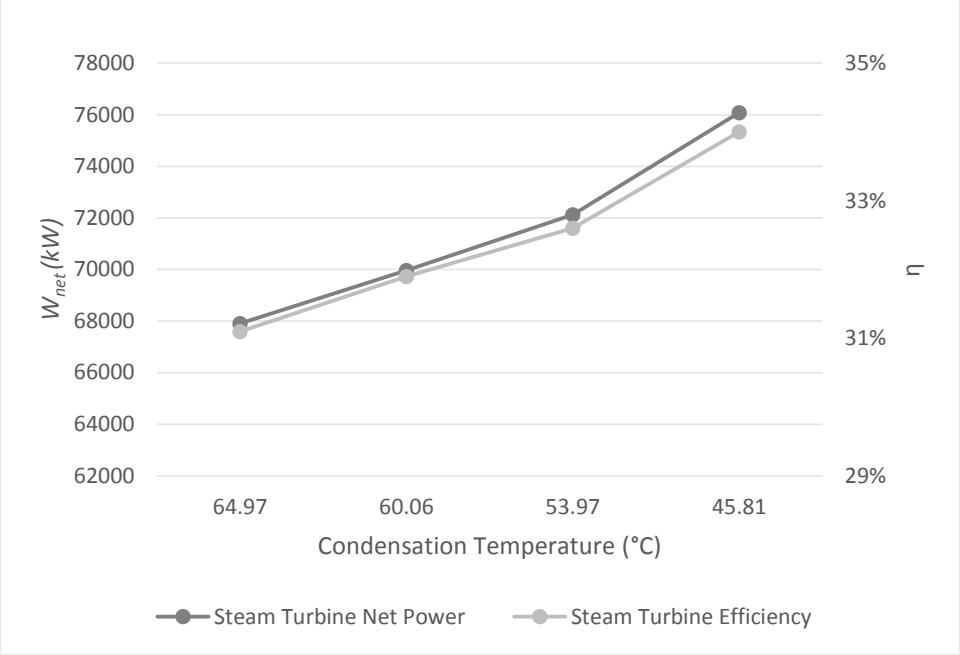

Figure III.8. Steam turbine net power and efficiency versus condensation temperature

Further analysis, all magnitudes of the four steam turbine cycles are represented in Table III.11 and the gain (or loss) of each parameter relative to each parameter of the first cycle.

Table III.11 Magnitudes at the four condensation temperatures and the gain (or loss) in each parameter

Temperature (°C)	Pump Work $w_p(kJ/kg)$	Turbine Work $w_T(kJ/kg)$	Added Heat $q_H(kJ/kg)$	Rejected Heat $q_L(kJ/kg)$	Net Power $w(kJ/kg)$	Efficiency $\eta_{ST}(\%)$	Quality x
64.97	10.55	980,07	3113.39	2133.33	969.52	31.1	0.914
60.06	10.52	1009.57	3133.93	2124.35	999.05	31.9	0.906
	-0.28%	3.01%	0.66%	-0.42%	3.05%	2.6%	-0.88%
53.97	10.50	1040.39	3159.43	2119.02	1029.89	32.6	0.897
	-0.47%	6.15%	1.48%	-0.67%	6.23%	4.82%	-1.86%
45.81	10.47	1096.83	3193.59	2096.72	1086.36	34.0	0.88
	-0.76%	11.91%	2.6%	-1.72%	12.05%	9.32%	-3.72%

III.4.2.1 The turbine and pump works

The turbine work and the pump work are what define the net work of the steam turbine.

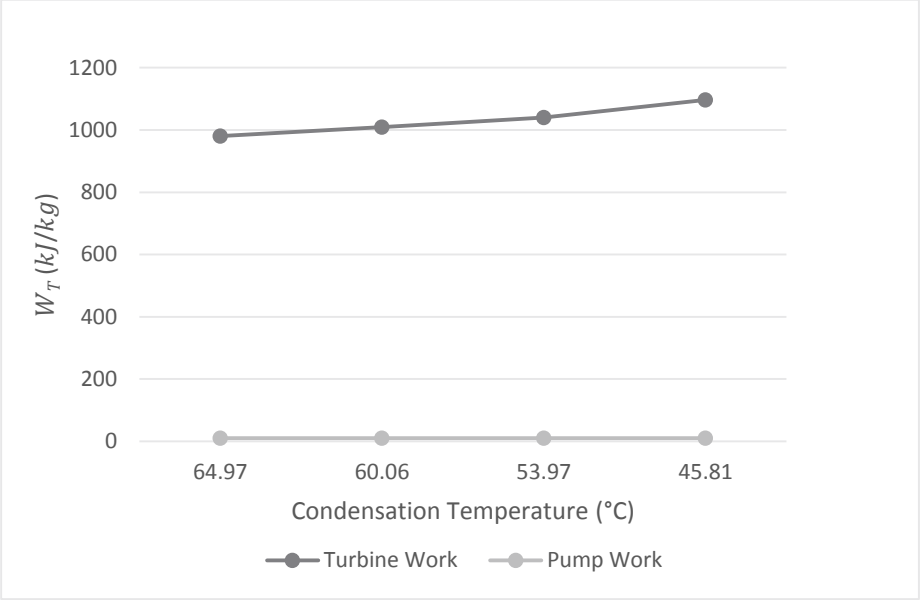

Figure III.9. Turbine work and pump work versus condensation temperature

Figure III.9 shows that the turbine work increases when the temperature of condensation decreases, this is due to the pressure difference between the inlet and exit points of the turbine. And again due to the pressure difference, one thinks that the pump work increases when lowering the condensation temperature, but the results show otherwise, this is because at low temperatures the specific volume of water shrinks which makes it easier for the pump to lift it up.

III.4.2.2. Added heat and rejected heat

The added heat is the heat recovered from the hot gases, and the rejected heat is the necessary heat rejected to the cold source to close the cycle.

As illustrated in *Figure III.10*, when decreasing the condensation temperature the added heat gets higher accordingly. This is due to the increase in the economizer duty (see *Figure III.16*). The rejected heat (heat sent to the Air-cooled condenser) decreases, because at low temperature the condensation process is easier.

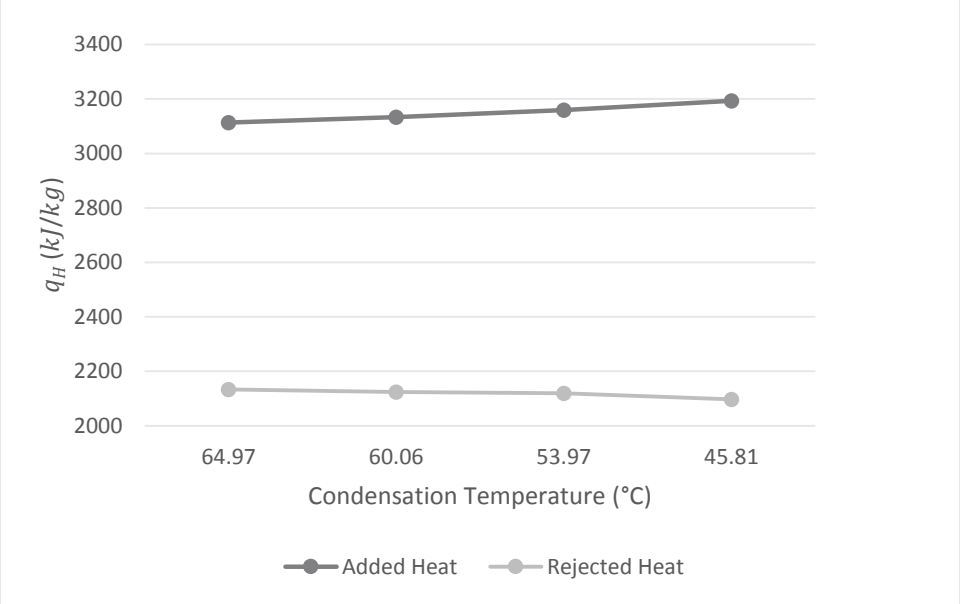

Figure III.10. Added heat and rejected heat versus condensation temperature

III.4.2.3. Efficiency and quality

Efficiency and quality versus the condensation temperature show the gain in efficiency and the ramification of this gain.

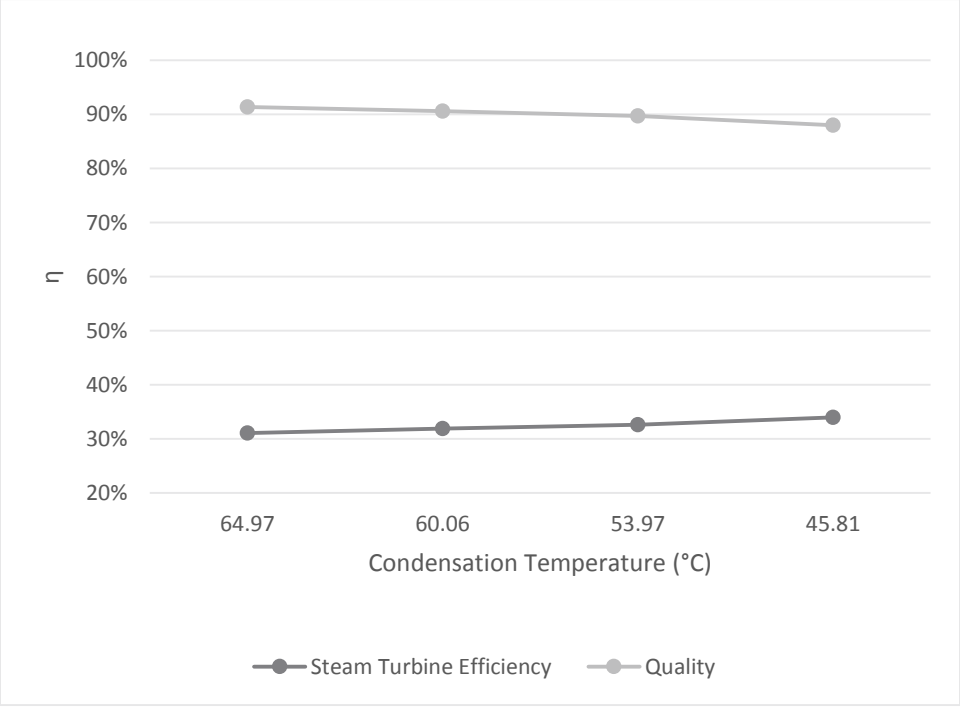

Figure III.11. Steam turbine efficiency versus quality versus condensation temperature

Figure III.11 shows the steam turbine efficiency versus the steam quality at the turbine exit point. Although the increase in the thermal efficiency, the steam quality gets poorer when lowering the condensation temperature. At low temperatures, the specific entropy of saturated vapor increases and since the expansion in the turbine is almost isentropic, the steam cannot be saturated at the turbine outlet if it's not superheated to high temperatures, which makes the superheater cost significantly more, also the temperature of superheated vapor is limited (585^{o}C for the SST-900[37] this is due to the characterization of the working fluid; see Chapter II.2.2).

The poorer the quality gets, the more it creates water droplets which at high velocity, they can be very destructive and damage the turbine blades. Also the fact that water in both gas and liquid forms pass through the turbine will create problems of two-phase flow such as vibration, noise …etc.

The decrease in vapor quality explains why the rejected heat in condenser decreases because a percentage of steam is already water.

Further analysis is represented in the following figure.

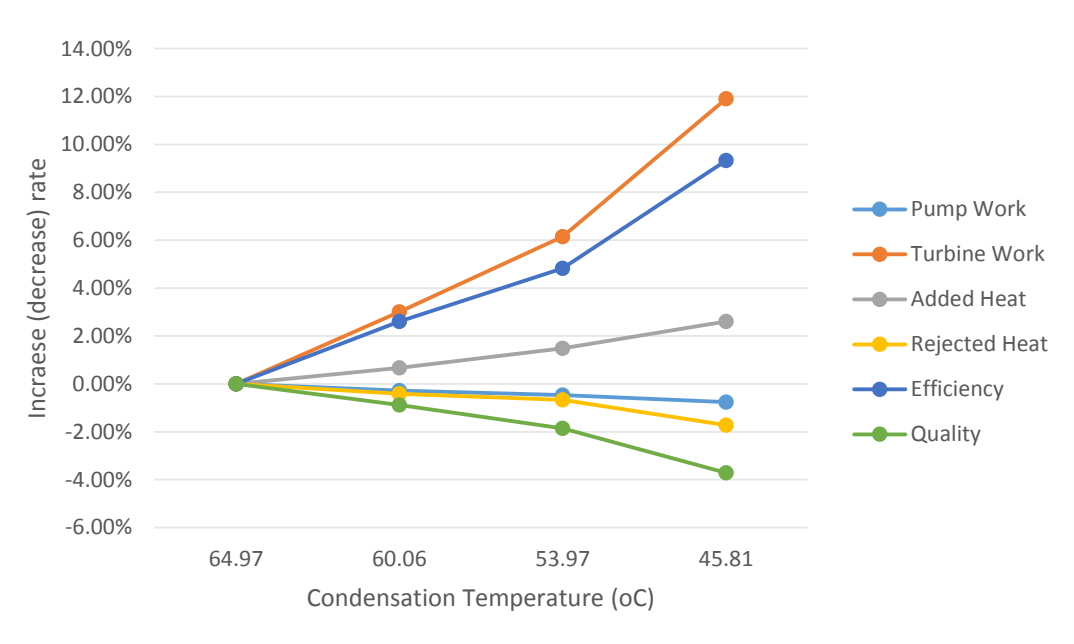

Figure III.12. Increase and decrease rates versus condensation temperature

Figure III.12 represent the rates at which the illustrated parameters increase (or decrease in cases of pump work, rejected heat, quality), so in this first analysis we see that the quality at the turbine exit is

the only disadvantage of lowering the condensation temperature. All remain parameters seem to behave in favor of increasing the net work.

We see that the rate the turbine work increases is higher than all the rates of other magnitudes, this is because the turbine exit state (state 5 in T-s Diagram) affect directly the turbine work.

III.4.3 Heat recovery steam generator

In the calculation section, we've seen the increase in the economizer duty at low temperature of condensation, the results are shown in Table III.12.

Table III.12 Stack temperatures and economizer heat fluxes

Condensation Temperature T_C(°C)	Stack Temperature T_{g4}(°C)	Economizer Heat Flux $\dot{Q}_{eco}(kW)$
64.97	187.42	73429.24
60.06	185.07	74866.15
53.97	182.15	76651.59
45.81	178.24	79042.37

We can see in *Figure III.13* that the lower the condensation temperature the lower stack temperature and the higher heat flux in the economizer.

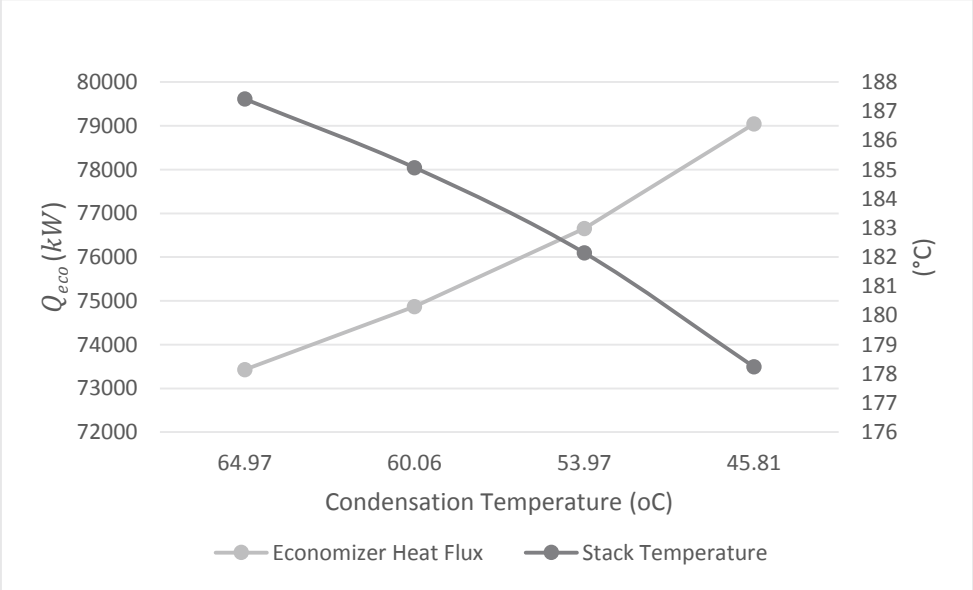

Figure III.13. Economizer heat flux and stack temperature versus condensation temperature

When the difference temperature between the hot gases and the temperature of feed water entering the economizer gets bigger, this allows more heat to be exchanged and improve the economizer duty which makes the hot gases stack temperature cooler. But this has a disadvantage that cannot be overlooked. Table III.13 represent the pinch point temperature difference versus the stack temperature versus the condensation temperature.

Table III.13 Stack temperatures and pinch point temperature differences

Condensation Temperature T_C(°C)	Stack Temperature T_{g4}(°C)	Pinch Point Temperature Difference ΔT_{PP}(°C)
64.97	187.42	10
60.06	185.07	8.44
53.97	182.15	6.52
45.81	178.24	3.93

This was expected, since the temperature of hot gases diagram is a linear function (all initial conditions remains the same such as hot gases flow rate, the exhaust gas temperature …etc.).

Now with the actual pinch point temperature differences one can determine the exact heat fluxes of each heat exchanger then the new steam flow rate.

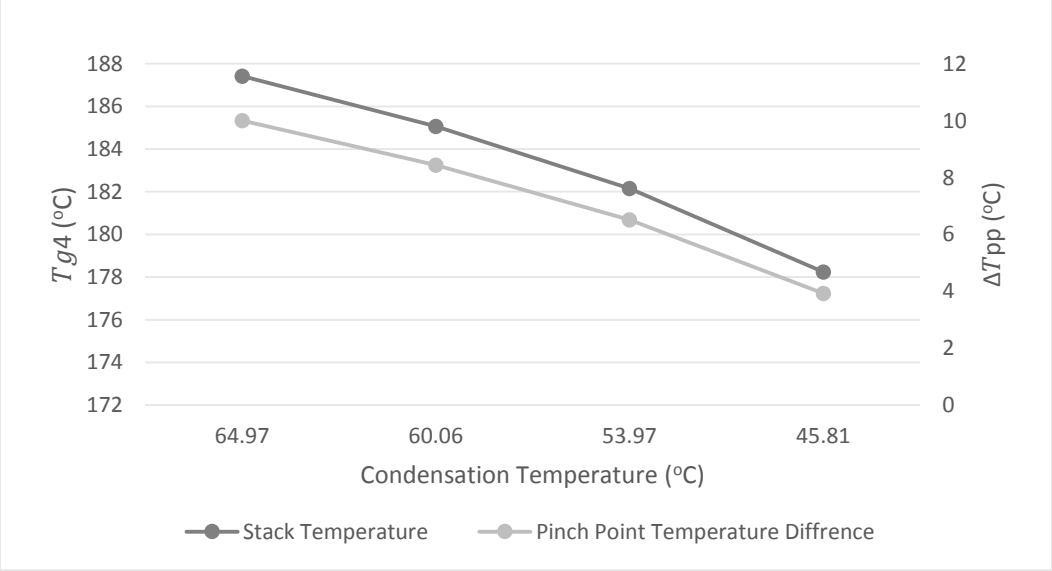

Figure III.14. Stack temperature and the pinch point temperature versus condensation temperature

When an 8.44°C and 6.52°C are acceptable pinch points temperature differences (still in the acceptance range), a 3.93°C is not, the range of pinch point temperature difference is between 5 and 15°C, a one lower will lead to a very expensive HRSG (if it is manageable), and one above will lead to a very poor performance in the HRSG.

III.4.4. Combined-cycle analysis

In this section will discuss the results of the combined-cycle calculation and compare them to those of the steam turbine.

Table III.14 CC Total net powers and their efficiencies

Temperature (°C)	Combined-Cycle Total Net Power $\dot{W}_{tot}(kW)$	Combined-Cycle Efficiency $\eta_{CC}(\%)$
64.97	164347.36	52.3
60.06	166410.83	52.7
53.97	168570.56	53.1
45.81	172525.16	53.9

First we can see that the combined cycle efficiency is much higher than both, the gas turbine and the steam turbine.

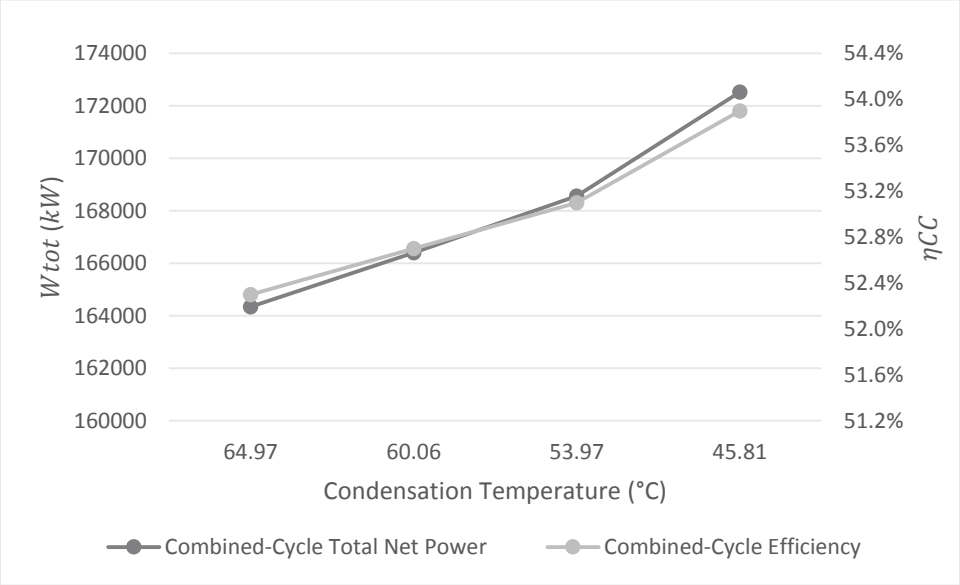

Figure III.15. Combined-cycle total net power and efficiency versus condensation temperature

Also in practical point of view, the efficiency of the combined is much higher; because the heat of the exhaust gases used to be referred at as “waste heat”.

It is noticeable that the two curves are one on the other almost like one curve, the combined-cycle total net power and its efficiency behaves the same way, in other words the rate they both increase with is the same. This was not the case with the steam turbine net power and efficiency (see *Figure III.8*).

Table III.15 Steam turbine and CC efficiencies

Temperature (^oC)	Steam Turbine Efficiency $\eta_{ST}(\%)$	Combined-Cycle Efficiency $\eta_{CC}(\%)$
64.97	31.1	52.3
60.06	31.9	52.7
53.97	32.6	53.1
45.81	34.0	53.9

Figure III.16 shows a comparison between the efficiency of the combined-cycle, and the efficiency of the steam turbine.

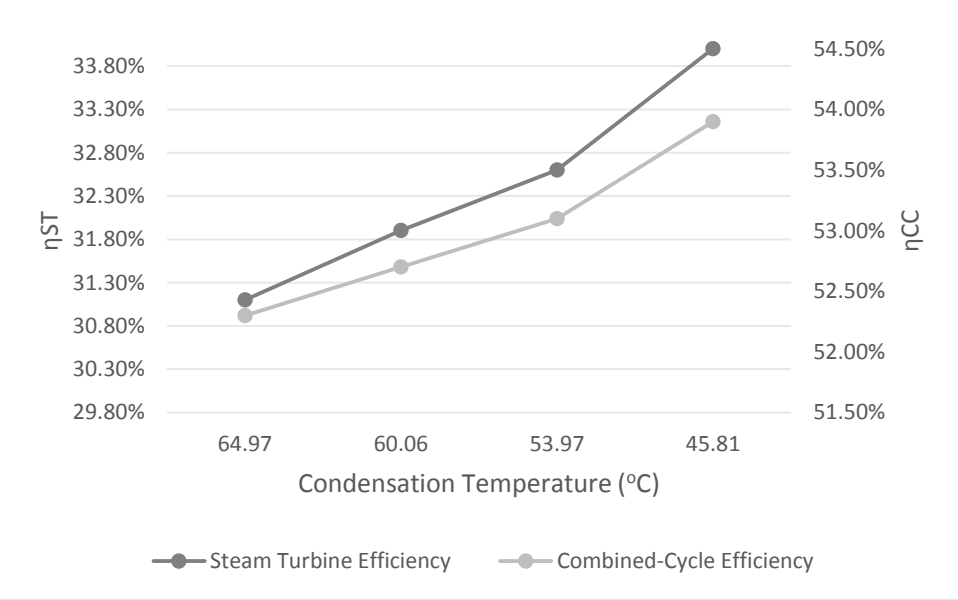

Figure III.16. Steam turbine efficiency versus the combined-cycle efficiency versus condensation temperature

Because of the same efficiency of the gas turbines in all four cycles, the combined cycle efficiency increase rate is not as fast as the steam turbine efficiency increase rate, also it is important to mention that the second burner decreases the combined-cycle efficiency.

III.4.5 Solar field analysis

The analysis of the solar field is required to tell whether the impact of the condensation temperature on the natural gas consumption is significant or insignificant.

In a first attempt we will fix the share of the solar field to $25\ MW$, and analyze the results. The second attempt will analyze the gain in the share of the solar field and its impact on the ISCC.

Table III.16 Heat fluxes of the solar field

Temperature (^oC)	64.97	60.06	53.97	45.81
Heat Extracted by the Solar Field $\dot{Q}_{Srec}(kW)$	73529.41	70701.35	68399.45	52709.25

We notice that the solar field needs less when lowering the condensation temperature to produce the $25\ MW$ net power, this means either decreasing the oil flow rate (HTF) which is not so interesting, since oil is recyclable and have a good lifetime, or using less collectors and eventually less land which can be very attractive in some regions (note that this solution does not improve the economization of natural gas).

Best solution is to leave the solar field as it is and use it to produce more power. This can be the best solution yet, because exploitation more energy from the sun will eventually economize a good amount of natural gas consumption which is the ultimate goal, as we all know fossil fuels are very expensive and pollutants. But since the gas flow of the gas turbine cannot be decreases, otherwise it will lower its performance (net power), this solution also can be very limited.

Table III.17 Economy of total gas flow rates

Temperature (°C)	Solar Net Power $\dot{W}_S(kW)$	Solar Efficiency $\eta_{Carnot}.\eta_T$ (%)	Total Gas Flow Rate $\dot{m}_{gtd}\ (kg/s)$	Economy of Total Gas Flow Rate (%)	Natural Gas Economy (m^3/h)
64.97	25000	0.346	350.1	36.7	59281.73
60.06	25999,99	0.354	347.48	37.2	60089.38
53.97	26874.99	0.366	347.13	37.3	60250.91
45.81	34874.99	0.47	299.84	45.8	74003.11

In Table III.17 if one looks at the total gas flow rate at the lowest temperature of condensation, it is not far from the gas flow rate already supplied by the gas turbines (exhaust gas flow rate), this means the second burner is meant to compensate the solar field contribution when there is none (night, non-sunny and windy periods). In other words, at night the second burner will supply the additional gas to the steam turbine to produce enough steam to attain the $67{,}9\ MW$, during the day when the solar field is capable of contributing , the second burner will be shutdown leading to an economy in consumption of natural gas.

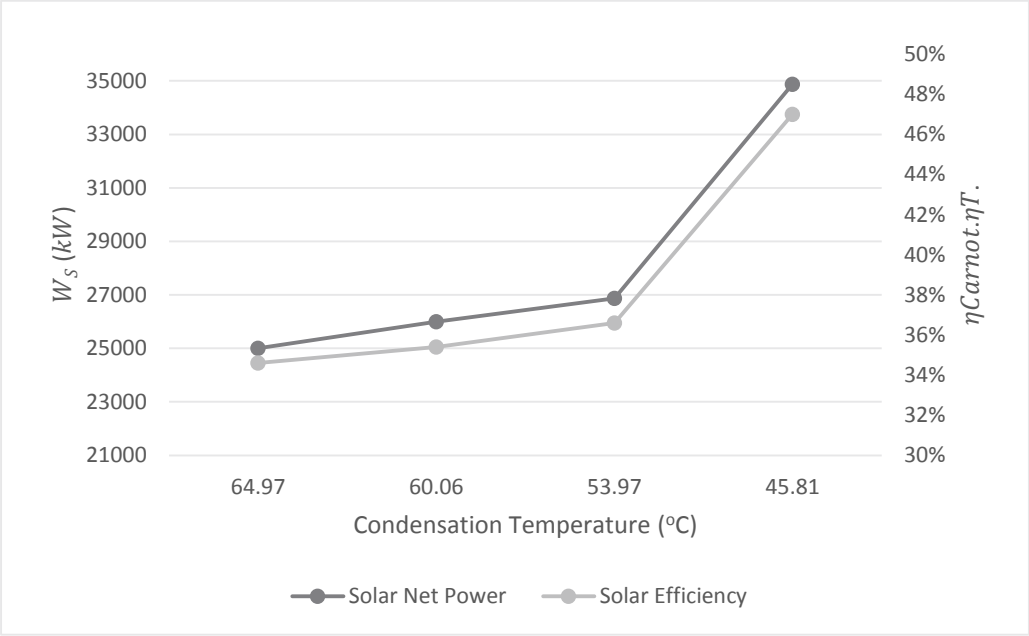

Figure III.17. Solar net power and efficiency versus condensation temperature

Figure III.17 represent the solar field net power and its efficiency versus the condensation temperature. The solar field net power and its efficiency also increase when lowering the condensation temperature, and because the solar field efficiency is direct function of difference between the hot temperature and the cold temperature (condensation temperature), we see that it increases greatly, especially at low temperatures. The solar field net power depends only on the solar field efficiency so it increases with the same pace as we see in *Figure III.17.*

With lowering the condensation temperature we gain in the net power produced by the solar field which will reduce the hot gases flow rate of the second burner as illustrated in *Figure III.18*, the more power the solar fields gains the more gas will be economized

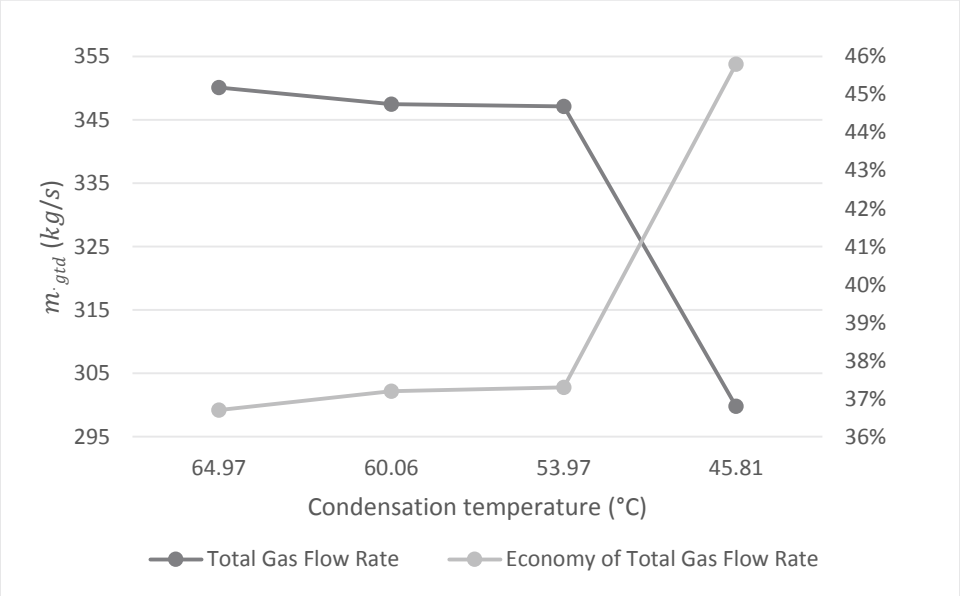

Figure III.18. Total gas flow rate and economy versus condensation temperature

Economy of natural gas per day is shown in Table III.

Table III.18 Economization of natural gas consumption

Temperature (°C)	64.97	60.06	53.97	45.81
Economization of Natural gas (%)	9.20	9.30	9.33	11.45

As said earlier, when the solar field is running, it does economize the consumption of natural gas almost by half, but only for six hours per day; the remaining hours the plant runs fully on natural gas, which will eventually reduce the daily economization. Considering TES, can significantly improve the economy of natural gas consumption.

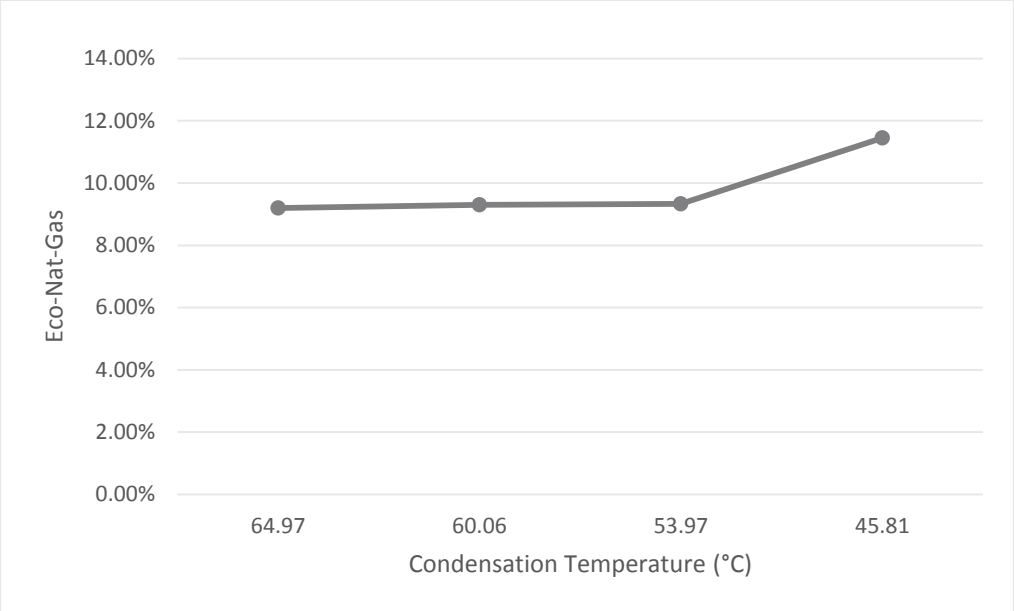

Figure III.19. Economy of daily natural gas consumption

In *Figure III.19*, we see that for the first two condensation temperatures, the economy of natural gas almost remains the same; however, the last temperature shows a good improvement. This is due to the low ratio of solar field working hours to the shutdown hours, which is $6/18$.

III.4.6 Integrated solar combined-cycle analysis

In a commercial point of view, the efficiency is what reflects the economics of the plant (the ratio of what you get to what you give). *Figure III.20* shows a comparison of the efficiencies of the steam turbine, the combined-cycle and the solar field.

At low temperatures of condensation the solar field efficiency increases even quicker which means the percentage that the solar field gains is much higher than the percentage that the combined-cycle and steam turbine gains. With that been said it seems that the solar field benefits from lowering the condensation temperature more than the steam turbine and as a result more than the combined cycle.

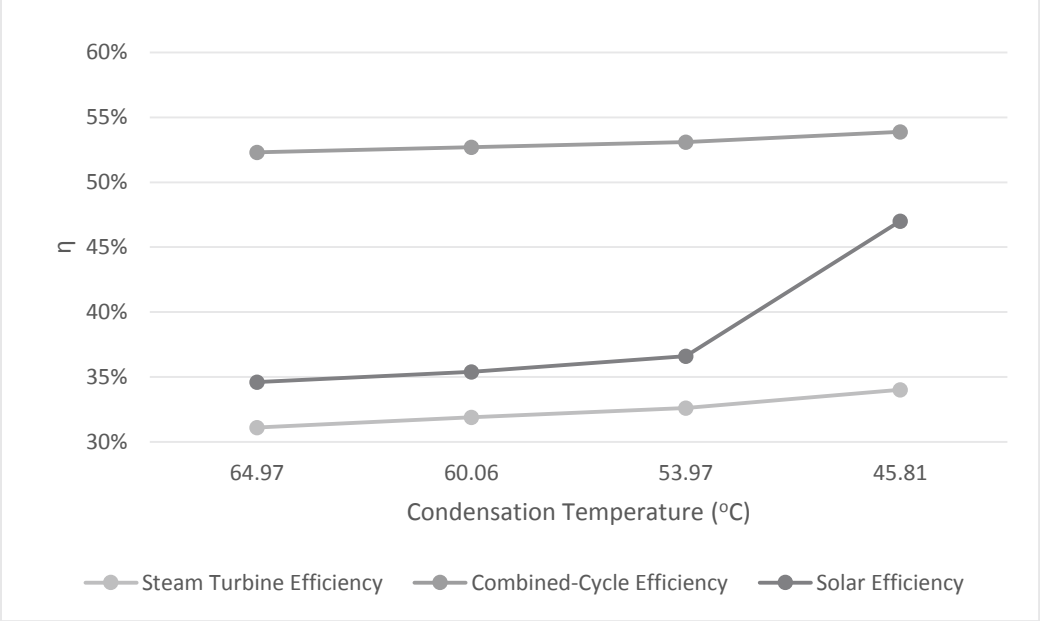

Figure III.20. Steam turbine and CC and the solar field efficiencies versus condensation temperature

III.4.7 Economic analysis

III.4.7.1 Natural gas consumption and annual savings

Table III.19 Economization of natural gas consumption and their annual savings

Scenario Case	Total Gas Flow Rate $\dot{m}_{gtd}\ (kg/h)$	Economy of Natural Gas Flow Rate (m^3/h)	Savings Per Day (MDA)	Annual Savings (BDA)
1 (64.97°C)	1260360	59281.73	27.743849	9.98778587
2 (60.06°C)	1250928	60089.38	28.121829	10.12385874
3 (53.97°C)	1249668	60250.91	28.197426	10.15107336
4 (45.81°C)*	1079424	74003.11	34.633455	12.46804397

- The annual cost of natural gas (without the solar field) : $108.858702\ BDA$
- * : Unpractical scenario case

With environmental point of the view, the most interest is the low emissions of CO_2, but with commercial point of view (SPP1 is commercial plant) the most attractive thing is the economy of consumption of natural gas which is money savings. In order to evaluate these savings one must know that the price of natural gas destined to electricity production is $780\ DA/1000\ m^3$ [38].

III.4.7.2 Electricity sales income and profits

We've seen that lowering the condensation temperature does increase the output power of the plant but this cannot be economically justified on energy value alone, some further evaluations are required. The evaluations would be on annual basis, also we take down 5 days from the year as non-operational days (maintenance and emergency shutdowns). The price of kWh are between $2\ DA/kWh$ and $3.20\ DA/kWh$ [31][32]. so if we consider that the price of the kWh is $2\ DA$ when the solar field is running which is 6 hours per day and when the solar field doesn't contribute; the price goes up to $3.20\ DA$, this gives an average price of $2.9\ DA/kWh$.

The following table gives a close idea of the actual electricity sales income and profits based on the calculations of our scenario cases.

Table III.20 Electricity sales incomes and annual profits

Total Net Power $\dot{W}_{tot}(kW)$	Power of Electricity (kWe)	(kWh) Per Day	Income Per Day (BDA)	Profits per Day (MDA)	Annual Profits (BDA)	Percentage of Annual Profits $(\%)$
164347.36	150000	3600000	1.0440000	/	/	/
166410.83	151933.09	3646394.16	1.0574543	13.4543	4.843548	1.29
168570.56	153904.92	3693718.11	1.0711782	27.1782	9.784152	2.60
172525.16*	157515.47*	3780371.28*	1.0963076*	52.3076*	18.830736*	5.01*

- The generators efficiency is $\eta_G = 0.913$ (The SPP1 total net power of electricity is $150\ MWe$)
- * : Unpractical scenario case

Lowering the condensation temperature can be done in two different ways; the first way is by humidifying the air blown into the air-cooled condensers, the second way is by increasing the blowing velocity of air-cooled condensers.

In order to humidify the air blown into the air-cooled condensers, one must have water resources. Due to the location of the SPP1; this solution does not seem very attractive. The second solution is by increasing the blowing velocity of air-cooled condensers; this can be done by some modifications (replacing the motors by more powerful ones) and what come with it, based on the calculations the heat exchangers also should be replaced or upgraded (if it is manageable).

Low condensation temperatures are hard to achieve in saharian weather. This can flip the situation, because in order to achieve such low condensation temperatures; the modifications cost can be high; and the profits behind these modifications does not cover it in short periods.

Table III.20 shows the annual costs of natural gas consumption, the annual incomes and percentage of annual profits in the four scenario cases.

Table III.21 Annual electricity sales incomes and percentages of annual profits

Annual Income of Electricity Sales (BDA)	Annual Savings of Natural Gas Cost (BDA)	Annual Cost of Natural Gas (BDA)	Annual Income (BDA)	Percentage of Annual Profit $(\%)$
375.840000	9.98778587	98.87091613	276.9690839	/
380.683548	10.12385874	98.73484326	281.9487047	1.8
385.624153	10.15107336	98.70762864	286.9165244	3.6
394.670736*	12.46804397*	96.39065803*	298.2800780	7.7

- The annual cost of natural gas (without the solar field) : $108.858702\ BDA$
- * : Unpractical scenario case

III.4.8. Closing thoughts and future of the SPP1

In “Solar Power Plant One”, the choice of the steam turbine SIEMENS SST-900 was clever since its output power is up to $250\ MW$ [28], and why use it if they are not willing to upgrade it to its full potential. Based on our calculations two gas turbines SIEMENS SGT-800 exhaust gases can deliver approximately $70\ MW$ to the steam turbine with additional firing, which means it takes about seven SGT-800 gas turbines to deliver $250\ MW$. But this not the case, because the steam turbine SST-900

maximum steam pressure can reach $165\ bars$ [28], which will improve the power at which the gas turbines deliver.

The installed solar field of the SPP1 is $183{,}860\ m^2$; a surface has been designed for a production of 17% solar without TES. SPP1 has high potential of solar thermal storage however the simulation showed that the possibility of storage is significant only if the area exceeds $300{,}000\ m^2$ [30].

Conclusion

The work presented in this paper allowed us to come out with several conclusions. We conclude that the combined-cycle does not only lower the emissions of CO_2 but also have high thermal efficiency that either gas or steam turbines cannot achieve alone.

Also, the calculations were nothing but a confirmation of the laws of thermodynamic, that is lowering the condensation temperature does increase the net power produced by the cycle and the thermal efficiency.

Furthermore, the analysis showed that all the magnitudes of the steam cycle behave in favor of increasing the net power of the cycle. For instance, even the pump work decreases at low temperature of condensation. Also the net work doesn't just depend on the temperature difference between the hot and the cold sources but depends more on low temperature of condensation. For example, two cycles working between 60° to 300°C, and 40° to 280°C, though the two cycles have the same temperature difference between the hot and the cold sources; the one with lower condensation temperature (cold source) will have the higher output power (this can be visible on T-s diagram).

In theory there is no disadvantage of lowering the condensation temperature, even the quality of steam is just a fraction if you don't relate it to technology.

In practice, our technology sets barriers to theory, which will create constraints to the space you can really play on; for instance water cannot be superheated to extreme high temperatures, physical and chemical characteristics of materials make the turbine blades damageable against water. Also materials cannot support extreme high pressures, those limitations make the gains in power fade when it comes to economics.

Nevertheless, the example of the SPP1 shows how relatively straightforward thermodynamics, along with the advances in the thermal properties of materials and clever design, can be used to significantly increase the efficiency of electricity generation. The ISCC electric generating plants have changed the landscape of electric power generation and will likely continue to do so in the near future.

References

[1] Fundamentals of Thermodynamics Sixth Edition (2003) Richard E.Sonntag, Claus Borgnakke, Gordan J. Van Wlyen. John Wiley & Sons.

[2] Combined-Cycle Gas & Steam Turbine Power Plants First Edition (1997) Rolf Kehlhofer. PennWell Publishing Company.

[3] Industrial Boilers and Heat Recovery Steam Generators (2003) Design, Applications, and Calculations, V. Ganapathy.

[4] Simplify heat recovery steam generator evaluation (1990) Insights, equations and examples illustrate a simpler method for predicting heat recovery steam generator V. Ganapathy**.**

[5] Boiler Calculations (2002) Sebastian Teir, Antto Kulla, Helsinki University of Technology Department of Mechanical Engineering.

[6] Brayton Cycle The Ideal Cycle for Gas-Turbine Engines In Relation to Power Plants, Denise Lane

[7] Fluid Mechanics Fundamentals and Applications (2006) Yunus A. Çengel, John M. Cimbala

[8] Conversion of Thermo-Mechanic Energy (2012) Courses of Prof. Ait Ali M.A .ENP

[9] Heat Transfer (2013) Courses of Prof. Arezki Smaili .ENP

[10] Fundamentals of Heat and Mass Transfer 7 Ed (2011) Theodore L.B, Adrienne S.L, Frank P.I, David P. D. John Wiley & Sons

[11] La Chaudière de Récupération, Elément de Base des Centrales Solaires à Cycle Combiné (2012) EL GHARBI Najla, CDER, Algiers.

[12] Advanced Engineering Thermodynamics 3Ed (2006) Adrian Bejan, John Willey & Sons, INC.

[13] Combined-Cycle Gas & Steam Turbine Power Plants Third Edition (2009) Rolf Kehlhofer.

[14] The Value of Concentrating Solar Power and Thermal Energy Storage (2010) Ramteen Sioshansi The Ohio State University, Paul Denholm National Renewable Energy Laboratory.

[15] Analysis of Solar Thermal Power Plants with Thermal Energy Storage and Solar-Hybrid Operation Strategy (2011), Stefano Giuliano, Reiner Buck and Santiago Eguiguren, German Aerospace Centre (DLR).

[16] Concentrating Solar Power for the Mediterranean Region (2005) German Aerospace Center (DLR), Institute of Technical Thermodynamics Section Systems Analysis and Technology Assessment.

[17] Advanced CSP Teaching Materials (2012), Chapter 5 Parabolic Trough Technology, Matthias Günther, Michael Joemann, Simon Csambor (DLR).

[18] Concentrating Solar Power Now (2006), Dr. Franz Trieb, German Aerospace Center (DLR).

[19] Spakovszky, Z.S. (2007), Combined Cycles in Stationary Gas Turbine for Power Production.

[20] Quaschning, V. (2003), Solar Thermal Power Plants, Renewable Energy World, Earthscan London Sterling. V.A.

[21] Solar Thermal Power Plants (2000), M. Becker, W. Meinecke, M. Geyer, F. Trieb, M. Blanco, M. Romero, Ferrière A.

[22] Greenpeace International (2003), Solar Thermal Power 2020 Exploiting the Heat from the Sun to Combat Climate Change.

[23] Two-tank Molten Salt Storage for Parabolic Trough Solar Power Plants (2004), Ulf Herrmann, Bruce Kelly , Henry Price.

[24] Hybrid Solar-Fossil Fuel Power Generation (2012), Elysia J. Sheu, Massachusetts Institute of Technology.

[25] Efficiency of Carnot Engine at Maximum Power Output (1974), F.L Curzon, B. Ahlborn, University of British Columbia.

[26] La Centrale Hybride de Hassi R'mel (2012) Extrait du Portail Algérien des ENERGIES RENOUVELABLES, EL GHARBI Najla, CDER, Algiers.

[27] SIEMENCE SGT-800 Industrial Gas Turbine brochure (2009), SIEMENCE energy sector, available at http://www.siemens.com/energy

[28] SIEMENCE SST-900 Industrial Steam Turbine brochure (2013), SIEMENCE energy sector, available at http://www.siemens.com/energy/steamturbines

[29] Décret exécutif n ° 05-128 du 15 Rabie El Aouel 1426 correspondant au 24 avril 2005 portant fixation des prix de cession interne du gaz naturel.

[30] Effect of wind speed on the efficiency of the integrated solar combined cycle power plants SPP I in Algeria (2013), A. Trad , Z. Belgroun, A.M Djebiret (UDES, CDER).

[31] Un sourire coûte moins cher que l'électricité, mais donne autant de lumière (2012) Pr Chems Eddine Chitour, Nationale School of Polytechnics.

[32] Centrale électrique hybride de Hassi'Rmel : L'Algérie entre dans l'ère des énergies propres (2012), El Wakab, A.A.

[33] Applied Thermodynamics and Engineering Fifth Edition (1993), T.D Eastop, A. Mcconkey, Pearson Education.

Appendix

Appendix-A Technical Specifications of SGT-800

Power generation	47.0 MWe	
Frequency	50/60 Hz	
Electrical efficiency	37.5%	
Heat rate	9,597 kJ/kWh	
Turbine speed	6.608 rpm	
Compressor pressure ratio	19	
Exhaust gas flow	131.5 kg/s	
Exhaust temperature	544° C	
NOx emissions: (with DLE corrected to 15 % O2 dry)	Natural gas: ≤15ppmV	
	Liquid fuel: ≤42ppmV	
Axial Compressor	15-stage axial-flow compressor 3-stages variable guide vanes	
	Electron-beam welded rotor	
	Cr-steel blades and vanes	
	Abradable seals	
	Controlled Diffusion Airfoils	
Combustion	30 dual-fuel Dry Low Emissions burners	
	Welded annular sheet metal design	
	Thermal-barrier-coated inner surface	
Turbine	Single-module high-efficiency 3-stage turbine	two first stages and stator flanges are air-cooled
		first stage of single-crystal material
		third stage with interlocking shrouds
Fuel System	Natural gas – Liquid fuel – Dual fuel	
	On-load fuel changeover capability	
	Load-rejection capability	
	Gas-supply pressure requirement: 27-30 bar	
Generator	Four-pole design	
	Rated voltage: 10.5 kV/11.0 kV/13.8 kV	
	50 Hz or 60 Hz	
	Protection IP54	
	PMG for excitation power supply	
	Complies with -IEC/EN 6034-1 standard	

Appendix-B Combustion Ratio of Air-Fuel

$$CH_4 + 2O_2 \rightarrow CO_2 + 2H_20$$

If we look up the atomic weights of the atoms that make up Methane and Oxygen, we get the following numbers:

Carbon: $C = 12{,}01\ g/mol$

Oxygen: $O = 16\ g/mol$

Hydrogen: $H = 1{,}008\ g/mol$

So one molecule of methane has a molecular weight of:

$$1(12{,}01) + 4(1{,}008) = 16{,}042\ g/mol$$

One Oxygen molecule weighs:

$$2\ (16) = 32\ g/mol$$

We need two Oxygen molecules for every molecule of Methane so the Oxygen-Fuel mass ratio is then:

$$r_{O/F} = \frac{2.\ (32)}{1.\ (16{,}042)} = 3{,}99$$

So we need $3.99\ kg$ of Oxygen for every $1\ kg$ of fuel

The Oxygen represent 23.2% of air, this gives:

$$r = 3{,}99.\frac{100}{23{,}2} = 17{,}2$$

So we need $17{,}2\ kg$ of air for every $1\ kg$ of Methane.